2001

A Study of the Applicability of Intrusion Technology for Evaluating Resilient Modulus of Subgrade Soil.

Ananda H. m. p. j Herath
Louisiana State University and Agricultural & Mechanical College

INFORMATION TO USERS

This manuscript has been reproduced from the microfilm master. UMI films the text directly from the original or copy submitted. Thus, some thesis and dissertation copies are in typewriter face, while others may be from any type of computer printer.

The quality of this reproduction is dependent upon the quality of the copy submitted. Broken or indistinct print, colored or poor quality illustrations and photographs, print bleedthrough, substandard margins, and improper alignment can adversely affect reproduction.

In the unlikely event that the author did not send UMI a complete manuscript and there are missing pages, these will be noted. Also, if unauthorized copyright material had to be removed, a note will indicate the deletion.

Oversize materials (e.g., maps, drawings, charts) are reproduced by sectioning the original, beginning at the upper left-hand corner and continuing from left to right in equal sections with small overlaps.

Photographs included in the original manuscript have been reproduced xerographically in this copy. Higher quality 6" x 9" black and white photographic prints are available for any photographs or illustrations appearing in this copy for an additional charge. Contact UMI directly to order.

ProQuest Information and Learning
300 North Zeeb Road, Ann Arbor, MI 48106-1346 USA
800-521-0600

A STUDY OF THE APPLICABILITY OF INTRUSION TECHNOLOGY FOR EVALUATING RESILIENT MODULUS OF SUBGRADE SOIL

A Dissertation

Submitted to the Graduate Faculty of the
Louisiana State University and
Agricultural and Mechanical College
in partial fulfillment of the
requirements for the degree of
Doctor of Philosophy

in

The Department of
Civil and Environmental Engineering

by
Ananda H.M.P.J. Herath
B.S., University of Peradeniya, Sri Lanka, 1983
M.S., University of Tokyo, Japan, 1988
August 2001

DEDICATION

This work is dedicated to my parents, late Mr. R.B.Herath, father, and Mrs. T.M.Herath, mother, for their invaluable sacrifice and constant inspiration throughout my education. This is also dedicated to my wife, Suba Herath, and my children.

ACKNOWLEDGMENTS

My deepest appreciation and sincere thanks to Dr. Louay N. Mohammad, my advisor, for his guidance and encouragement throughout the study. Without his support and constant inspiration, this study would not have been successful.

I wish to extend my appreciation to Dr. John B. Metcalf, my co-advisor, for his support and valuable direction in this study.

My sincere thanks to Dr. Mehmet T. Tumay, my minor professor, for providing the Continuous Intrusion Miniature Cone Penetration Test system and Research Vehicle for Geotechnical In-situ Testing and Support, which were developed by him. Without his dedication to the cone penetration test area during the last two decades, I would not have been able to do this research.

I would also express my appreciation to Dr. Hani H. Titi for his time and valuable advice throughout this research.

I am also very grateful to the other distinguished members of my committee, Dr. Lynn R. LaMotte, and Dr. Jim Chambers for their support and valuable suggestions in this study.

Special thanks are also offered to Mr. William T. Tierney for his efforts in conducting the cone penetration tests. I wish to acknowledge Amar Raghavendra for his help and encouragement with the laboratory tests. I would like to thank to Mark Morvant, Paul Brady, Melba Bounds, Kenneth Johnson, Jason Flory, Michael Cooper, David Wedlake, Robert Glen Graves, Willie Gueho, Greg Tullier, Baoshan Huang, and Dr. Khalid Farrag for their help with laboratory testing.

TABLE OF CONTENTS

LIST OF TABLES

LIST OF FIGURES

LIST OF ABBREVIATIONS

AASHTO	American Association of State Highway and Transportation Officials
ALF	Accelerated Load Facility
ASTM	American Society for Testing and Materials
BH	Borehole
c	Cohesion intercept
CBR	California Bearing Ratio
CICU	Isotropically Consolidated Undrained Triaxial Compression Test
COV	Coefficient of Variation
CPT	Cone Penetration Test
CIMCPT	Continous Intrusion Miniature Cone Penetrometer Test
E	Modulus of Elasticity (Young's modulus)
ESAL	Equivalent Single Axial Loading
EMCRF	Engineering Materials Characterization Research Facility
FHWA	Federal Highway Administration
FWD	Falling Weight Deflectometer
f_s	Sleeve friction
G	Shear modulus
G_s	Specific gravity
k_o	Coefficient of lateral earth pressure at rest
LA DOTD	Louisiana Department of Transportation and Development
LCD	Liquid Crystal Display
LL	Liquid Limit
LTRC	Louisiana Transportation Research Center
LVDT	Linear Variable Differential Transducer
MTS	Material Testing System
M_r	Resilient modulus
MCPT	Miniature Cone Penetrometer Test
NA	Not available
NDT	Nondestructive Test
NP	Non plastic
PCPT	Piezocone penetration test
PI	Plasticity Index
PL	Plasticity Limit
PRF	Pavement Research Facility
q_c	Cone tip resistance
R	Reliability
R^2	Coefficient of multiple determination
REVEGITS	Research Vehicle for Geotechnical In-situ Testing and Support
RMSE	Root Mean Squared Error
R_f	Friction ratio
SAS	Statistical Analysis System
SHRP	Strategic Highway Research Program
SN	Structural number

S_o	Combined standard error of the traffic prediction and performance prediction
SSV	Soil Support Value
STD	Standard deviation
S_u	Undrained shear strength
TRB	Transportation Research Board
USCS	Unified Soil Classification System
UU	Unconsolidated Undrained Triaxial Compression Test
U_r	Relative damage
w	water content
w_{opt}	Optimum water content
W_{18}	Predicted number of 18-kip equivalent single axle load
Z_R	Standard normal deviation
γ_d	Dry unit weight
γ_{dmax}	Maximum dry unit weight
γ_w	Unit weight of water
ε_r	Axial strain
υ	Poisson's ratio
σ_1	Major principal stress
σ_3	Minor principal stress
σ_c	Confining stress
σ_d	Deviator stress
σ_h	Horizontal stress
σ_v	Vertical stress
ϕ	Angle of internal friction
ΔPSI	Difference between the initial design serviceability index and the design terminal serviceability index.

ABSTRACT

The cone penetration test may be applied for estimation of the resilient modulus of subgrade soil. The main objectives of this study were to assess the applicability of the intrusion technology in evaluating the resilient characteristics of subgrade soil, develop models among the cone penetration test parameters, resilient modulus, soil properties, and stresses of subgrade soil, and to validate these models.

Field cone penetration and laboratory tests were performed on different soil types. Disturbed and undisturbed soil samples were obtained close to the cone penetration test locations. Laboratory tests were also performed to obtain the resilient modulus, strength parameters, compaction characteristics, and physical properties of subgrade soil. The results of the laboratory soil properties, resilient modulus, and eight field cone penetration tests are presented.

The models, among the cone penetration parameters, resilient modulus, moisture content, dry unit weight, and stress levels, were developed. Both in-situ stresses and induced traffic stresses were considered. Four models were developed for fine-grained and coarse-grained soil with in-situ and traffic stress conditions. These models were calibrated using the field test results of two soil types and used to predict the resilient modulus of different soil types.

The cone penetration, resilient modulus, and soil property tests were also performed on the laboratory compacted soil samples to investigate the effects of the variation in the moisture content and unit weight on the resilient modulus as well as to validate the proposed models. Special test equipment and a miniature cone with a straight push rod were developed for the laboratory cone testing. Four soil types and

three levels of moisture contents, such as dry side, optimum, and wet side, were selected for this testing. The results of the laboratory soil property, resilient modulus, and twelve laboratory cone penetration tests are presented. Simplified design charts, based on the cone penetration parameters and resilient modulus, were also developed. The proposed models were implemented in the selected road rehabilitation projects.

CHAPTER 1

INTRODUCTION

This dissertation presents the research effort and conclusions of the assessment of the applicability of the intrusion technology for evaluating resilient modulus of subgrade soil. Chapter1 includes the introduction and the problem statement. Chapter 2 presents background, limitation, objectives, and scope of the study. Chapter 3 describes the laboratory and field testing program that includes a brief description of the field and laboratory testing equipment and testing procedures. Chapter 3 also presents the laboratory cone penetration testing (controlled testing) program. Chapter 4 presents the analysis of results. Chapter 5 includes the field application of the proposed correlations in the selected rehabilitation projects. Chapter 6 presents the summary and conclusions.

1.1 Problem Statement

Flexible and rigid pavements are the major pavement types used in roadways. Figure 1.1 depicts the typical structural layers of each pavement type. Figure 1.1 (a) shows a rigid pavement that consists of a Portland cement concrete slab, base or subbase, and subgrade. The pavement slab consists of Portland cement concrete, reinforcing steel, load transfer devices, joints, and sealing materials.

Figure 1.1 (b) presents a flexible pavement that consists of a surface course (asphalt concrete wearing and binder course layers), base, subbase, and subgrade. The base is located immediately below the surface course. It consists of crushed stone, crushed gravel and sand, or crushed slag. Subbase is located between the subgrade and base. It consists of a compacted layer of granular materials or a layer of treated soil. Subgrade is a compacted in-situ soil or borrow material.

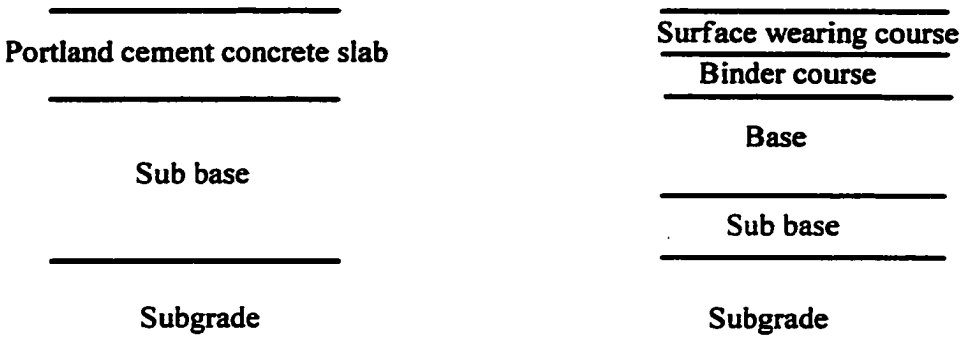

(a) A rigid pavement (b) A flexible pavement

Figure 1.1 Typical pavement sections

Static properties, such as California Bearing Ratio (CBR) and soil support value (SSV), used for flexible pavement design and subgrade soil characterization, do not take into account the dynamic response of the moving vehicles. In order to incorporate this dynamic behavior, the resilient modulus was introduced in the mechanistic design of pavements by the American Association of State Highway and Transportation Officials (AASHTO) guide for design of pavement structures (1986,1993, and the proposed 2002). After its introduction, the resilient modulus gained popularity in the pavement design. The resilient modulus is the definitive material property used to characterize subgrade soil in pavement structures. The subgrade soil charaterization, based on the resilient modulus, is a realistic way to analyze the moving vehicle loads on a pavement. The resilient modulus represents the dynamic stiffness of pavement materials under repeated loading of the moving vehicles.

In flexible pavement design, the resilient modulus is a direct input parameter. The AASHTO design equation, as presented in Section 4.6, Chapter 4, includes the subgrade resilient modulus along with other parameters, such as traffic loading, change in Present

Serviceability Index (PSI), reliability, and standard deviation. This design equation estimates the structural number (SN) and then it estimates the pavement thickness using the structural coefficients of each layer. In rigid pavement design, the subgrade resilient modulus is to be converted to a modulus of subgrade reaction (k-value).

The resilient modulus denotes a basic constitutive relationship between stress and deformation of materials. The resilient modulus (M_r) is the ratio of the deviator axial stress (σ_d) to the recoverable (resilient) axial strain (ε_r). Figure 1.2 illustrates the definition of the resilient modulus.

$$M_r = \frac{\sigma_d}{\varepsilon_r} \tag{1}$$

The resilient modulus can be estimated from the empirical correlations, in-situ nondestructive testing, and laboratory testing on soil samples. Several empirical correlations have been reported (Uzan 1985; AASHTO, 1986; Pezo et al., 1994; Allen, 1996; Mohammad et al., 1998, 1999, and 2000) which can be used to estimate resilient modulus from soil support value, CBR, stress levels, and soil properties. Laboratory test methods and in-situ nondestructive test methods (NDT) are also used to evaluate the resilient modulus. The laboratory tests require sophisticated equipment and skilled technicians. Also, laboratory test methods are considered laborious, time consuming, and expensive. On the other hand, the backcalculated resilient modulus from in-situ nondestructive test results may have low repeatability. The resilient modulus values from the NDT were greater than those from the laboratory tests (AASHTO guide for design of pavement structures, 1993) and they must be adjusted before use in the design of flexible

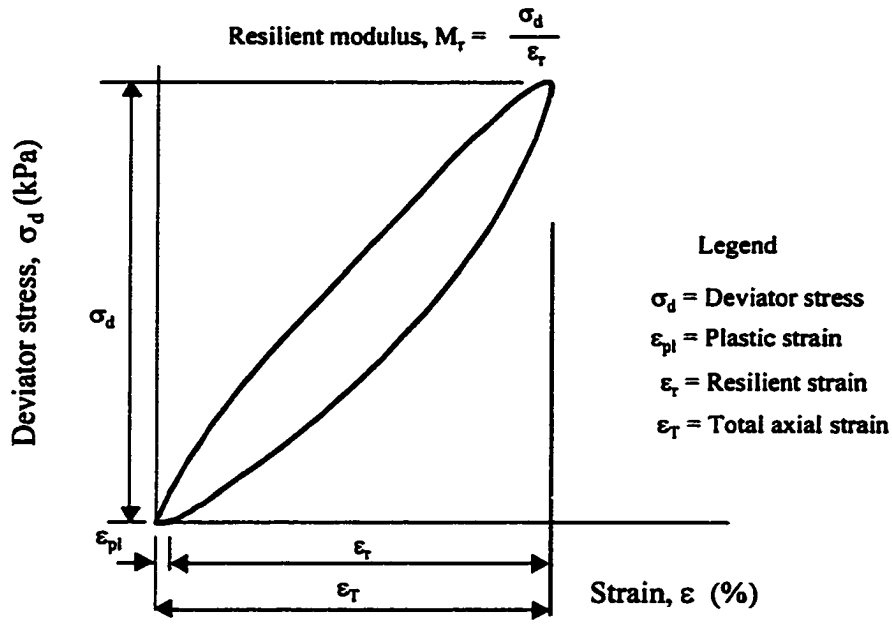

Figure 1.2 The definition of the resilient modulus

pavements. If not, it will result in an under designed pavement structural layer. The design resilient modulus value has an effect on the design structural number and hence on the overlay thickness in the pavement. The higher the resilient modulus value, the thinner the overlay thickness in the pavement.

The above mentioned limitations of the laboratory test and NDT methods imply a necessity of an alternative in-situ test method to evaluate the resilient properties of subgrade soil. Because of its rapidity and simplicity, the cone penetration testing (CPT) has become a popular in-situ test method. Also, the CPT results are repeatable and reliable (Campanella and Robertson, 1981; Tumay, 1981). The CPT data has successfully been used to evaluate soil classification, soil stratigraphy, shear strength, and deformation properties of soil, such as Young's modulus (E) and shear modulus (G) (Schmertmann, 1978; Campanella and Robertson, 1981; Robertson and Campanella, 1983). These interpretation methods are based on empirical correlations, theoretical and analytical approaches. It is expected that the CPT method may also be applied for evaluating the resilient modulus of subgrade soil.

An experimental program was performed to study the application of the CPT in evaluating the resilient modulus of subgrade soil. To accomplish this objective, different subgrade soil sites in Louisiana were selected for the field cone penetration and laboratory testing. The soil types included fine-grained and coarse-grained soil. The field cone penetration tests included 15 cm^2 friction cone penetrometer tests and 2 cm^2 continuous intrusion miniature cone penetration tests. Disturbed and undisturbed soil samples were obtained close to the cone penetration test locations. The laboratory tests were also performed to obtain the resilient modulus, strength parameters, compaction

characteristics, and physical properties of subgrade soil. The implementation of the miniature cone penetration test was verified. Statistical models were developed to correlate the resilient modulus, the cone penetration test parameters, stress levels (in-situ or traffic), moisture content, and unit weight. The resilient moduli were evaluated for both the in-situ and traffic loading conditions. These models were developed, based on the results of two field soil types, and used to evaluate the resilient modulus of other soils. The proposed models were validated by the test results of the rest of the field tests. The measured and predicted resilient modulus values were not significantly different. The laboratory cone penetration tests were also performed on the compacted soil samples of four soil types at three different moisture content levels, such as dry side, optimum, and wet side, to study the effects of variation in the moisture content on the resilient modulus, establish preliminary design charts, and validate the models. Insufficient data was available to verify the preliminary design charts. The use of the preliminary design charts or proposed models, to compute an effective subgrade soil resilient modulus, was illustrated.

The proposed models were successfully implemented in the road rehabilitation projects, such as LA-482, LA-513, and Henderson levee road. A quick and effective assessment of pavement subgrade soil resilient properties with the cone penetration test will provide a cost-effective input to pavement design.

CHAPTER 2

BACKGROUND

2.1 Introduction

This chapter presents the literature review of the resilient modulus and cone penetration tests, limitations, objectives, and scope of the study.

2.2 Resilient Modulus

The resilient modulus is estimated from the backcalculation of the NDT deflection results, laboratory triaxial testing on soil samples, and correlations with soil properties, CBR, and soil support values. The Dynaflect, Road Rater, and Falling Weight Deflectometer (FWD) are the devices used for NDT test methods. These NDT methods measure the deflection of the pavement under a loading. These deflections are used in backcalculation subroutines to evaluate the resilient modulus. Backcalculated modulus depends on many factors, such as loading condition and stiffness in layers (Sebaaly et al., 1992; Lee et al., 1994).

There are many laboratory testing devices used for determining the resilient modulus of subgrade soil. The devices used for laboratory testings are triaxial cell, resonant column, simple shear device, torsional apparatus, hollow cylinder and true triaxial cell. Because of its simplicity, repeatability and accuracy, the triaxial cell is the most popular laboratory testing device. But these laboratory tests are laborious, time consuming, and expensive.

In 1986, AASHTO recommended the testing procedure, T 274-82, to determine the resilient modulus of subgrade soil. Inadequate conditioning steps and over stressing the sample were reported in this test procedure (Mohammad et al., 1993; Nazarian, 1993).

The major drawback of the T 274-82 was that the stresses were so high that the specimen may be damaged in the preconditioning stage. The AASHTO T 274-82 test procedure was modified and replaced by an interim AASHTO procedure T 292-91I. Then in 1992, AASHTO adopted the Strategic Highway Research Program (SHRP) Protocol 46 (AASHTO T 294-92I). After including the previous developments in the test procedure for determination of the resilient modulus of subgrade soil, the current test procedure, T 294-94, was introduced. This procedure requires a test system that includes a triaxial cell, a closed loop electro-hydraulic repeated loading system, load and specimen response control system, and measurement and recording system. Figure 2.1 shows the load pulse used in this test method. In order to simulate traffic loadings, AASHTO T 294-94 recommends the haversine-shaped load pulse with a 0.1 second load followed by a 0.9 second rest period.

Resilient modulus is influenced by many factors. Many investigators (Rada et al., 1981; Kamal et al., 1993; Mohammad et al., 1994) observed an increase in resilient modulus of granular materials with increase in confining pressure. This is due to the fact that increase in stiffness and decrease in dilational properties of granular soil. The resilient modulus of cohesive soil decreases as deviator stress increases (Fredlund et al., 1977). The same observations were made by Mohammad et al., (1998 and 1999) for cohesive soils. These observations confirm the stress and dilational property dependent nature of the resilient modulus of subgrade soil. Many researchers have studied the effect of moisture content on resilient modulus of soil (Allen, 1989; McGee, 1989; Monismith, 1989; Mohammad et al., 1995; Drumm et al., 1997; Mohammad et al., 2000). They reported that resilient modulus of cohesive soil decreases as the moisture content

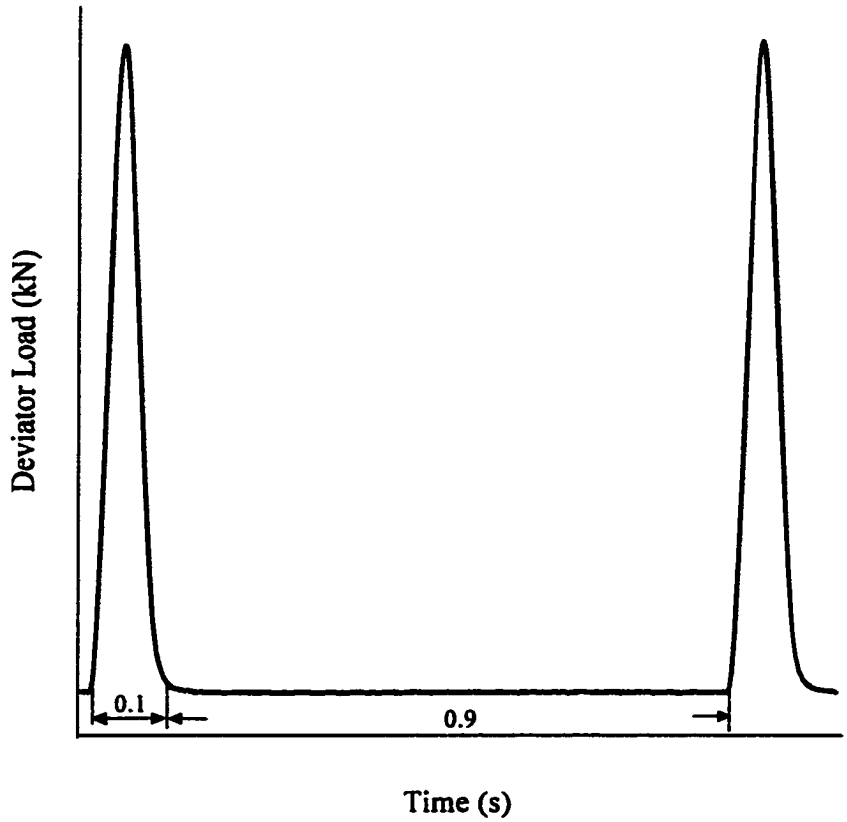

Figure 2.1 Load pulse used in the AASHTO T- 294 testing procedure

increases. The resilient modulus can be influenced by the seasonal variation of moisture in soil, such as repeated freeze-thaw cycle. Several investigators (Nataatmadja et al., 1989; Mohammad et al., 1994) reported that the resilient modulus can also be influenced by dry unit weight, size of the specimen, stress pulse shape, duration, frequency and sequence of stress levels, testing equipment, and specimen preparation as well as conditioning methods.

When the load is repeated thousands of times, the nonlinear behavior of subgrade soil is reduced. After thousands of times application of the load, plastic deformation is virtually completed. Then the soil sample response is virtually elastic and linear

(AASHTO, 1992). Based on this, AASHTO T 294-94 recommends using one thousand cycles of preconditioning load to the specimen. At each stress level during the testing, T 294-94 test procedure requires 100 cycles of loadings to the specimen. Resilient modulus is determined by taking the average of the last five cycles.

Several empirical correlations have been developed to predict the results of the resilient modulus test (Uzan 1985; AASHTO, 1986; Pezo et al., 1994; Allen, 1996; Mohammad et al., 1998, 1999, and 2000). For granular materials, the relationship given below may be used as recommended by the AASHTO.

$$M_r = k_1 \theta^{k_2} \qquad (2.1)$$

This is known as the bulk stress model. The AASHTO recommended the deviator stress model for cohesive soil. It is given by,

$$M_r = k_3 \sigma_d^{k_4} \qquad (2.2)$$

where ,

M_r - resilient modulus,

k_1, k_2, k_3,and k_4 - material constants,

σ_d - deviator stress = $\sigma_1 - \sigma_3$,

σ_1– major principal stress, σ_2– intermediate principal stresses, and σ_3 -minor principal stress, and

θ - bulk stress $=\sigma_1 + \sigma_2 + \sigma_3$.

The bulk stress model is very simple. However, the disadvantages those are the bulk stress model does not show individual effects of the deviator and confining stresses

while the deviator stress model does not show the significance of the confining stress on cohesive soil (Ullidtz, 1987; Nataatmadja et al., 1989).

Mohammad et al. (1999, 2000) proposed an octahedral stress model to over come some of the limitations discussed above. This model takes into account the effects of shear and influence of the stress state. This model can be used for both fine-grained and coarse-grained soils. The model considers the octahedral shear and normal stresses. The octahedral model is given as follows,

$$\frac{M_r}{\sigma_{atm}} = k_1\left(\frac{\sigma_{oct}}{\sigma_{atm}}\right)^{k_2}\left(\frac{\tau_{oct}}{\sigma_{atm}}\right)^{k_3} \qquad (2.3)$$

where , M_r is the resilient modulus, k_1 , k_2, and k_3 are material constants, σ_{oct} is the octahedral normal stress, τ_{oct} is the octahedral shear stress, and σ_{atm} is the atmospheric pressure (σ_{atm}=101.35 kPa). Many researchers correlated resilient modulus with strength and physical properties of soil such as California Bearing Ratio, moisture content, plasticity index, confining pressure and deviator stress (AASHTO, 1986; Allen, 1986; Carmichael III et al., 1986; Mohammad et al., 1999; Puppala et al., 1999; Mohammad et al., 2000). But these models have to be calibrated and validated for local conditions. This requires a significant effort and experimental work. Therefore use of these models are considered time consuming, laborious, and expensive.

2.3 Cone Penetration Test

The cone penetration test provides a rapid , continuous reading of tip resistance (q_c) and sleeve friction (f_s) as the cone penetrates into the ground. As shown in Figure 2.2, the CPT consists of a series of cylindrical push rods with a cone at the bottom.

The penetration resistance is related to the strength of the soil. The tip resistance depends on the size of the cone tip, rate of penetration, types of soil, density and moisture content (Schmertmann, 1978). The standard cone has a projected tip area of 10 cm^2 and an apex angle of 60 degrees.

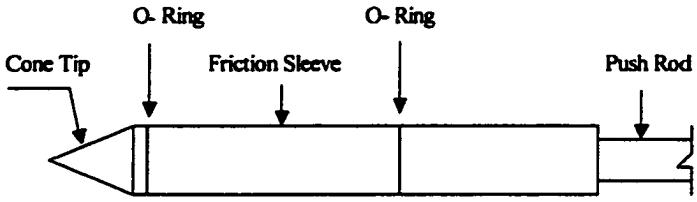

Figure 2.2 A typical friction cone penetrometer

A typical friction sleeve, located immediately above the tip, has 150 cm^2 surface area for the 10 cm^2 cones and 200 cm^2 for the 15 cm^2 cones. A 20 mm/ sec penetration rate is normally used in the standard tests. The CPT and piezocone penetration tests (with pore water pressure measurements) (PCPT) have been used to determine soil properties such as soil classification, shear modulus, friction angle, in-situ stress state, constrained modulus, stress history or over consolidation ratio, sensitivity, undrained strength, hydraulic conductivity, coefficient of consolidation, unit weight, and cohesion intercept (Wissa et al., 1975; Robertson and Campanella, 1983).

The cone penetration test has gained the popularity among other in-situ tests in the geotechnical area. This is due to the fact that cone penetration test is simple, economical, rapid, and its results are repeatable and reliable. The cone penetration test may be a replacement for the current resilient modulus evaluating methods. In this study, the miniature cone penetration test was used to evaluate the resilient modulus of subgrade soil in pavements.

2.4 Limitation

The background review shows that most of the resilient modulus prediction models need a significant amount of experimental data to calibrate them. Some of the models need to be calibrated for each type of soil. Therefore, use of these models are considered to be time consuming and expensive. Some of these models were based on static properties, such as CBR.

Most of these models were developed to predict the resilient modulus only under in-situ conditions. They do not take into account the traffic loading condition. Further, these prediction models may not predict the resilient modulus of subgrade soil accurately under both in-situ and traffic loading conditions.

The cone penetration test is a quasi-static test whereas, the resilient modulus test is a dynamic test. The difference in the testing modes may have a limitation on the use of the cone penetration test method to determine the resilient modulus of subgrade soil. However, the potential of the application of the CPT method in evaluating low strain dynamic shear modulus and liquefaction of soil were reported in the literature (Campanella, et al., 1983; Tumay, 1985; Puppala et al., 1995). The resilient modulus has similarities and relations to the shear modulus. Since the cone penetration and resilient modulus tests were performed under the same in-situ conditions, these test parameters depend on the same soil variables. Under the same in-situ conditions, it is expected that cone test parameters and resilient modulus may be less influenced by the testing modes. The same in-situ condition may be obtained by maintaining the same field moisture content and unit weight in the soil samples, used for the laboratory resilient modulus and soil property tests

2.5 Objectives

The objectives of this study are as follows.

- To assess the applicability of the intrusion technology in evaluating the resilient characteristics of subgrade soil.
- To develop models among the cone penetration test parameters, resilient modulus, soil properties, and stresses of subgrade soil.
- To validate these models.

2.6 Scope of the Study

Field cone penetration testing with the 2 cm^2 and 15 cm^2 cone penetrometrs were conducted at eight locations covering common soil types in Louisiana. Six of them were fine-grained soils and two of them were coarse-grained soils. The laboratory resilient modulus tests were performed on the undisturbed soil samples taken close to the cone test locations. Effects of variation in moisture contents on the resilient modulus and cone penetration parameters were also studied by conducting the resilient modulus and laboratory cone penetration tests on the compacted soil samples, in the laboratory, of four soil types with three moisture levels, such as dry side, optimum, and wet side.

CHAPTER 3

LABORATORY AND FIELD TESTING PROGRAMS

3.1 Introduction

This chapter presents the methodology used in the field and laboratory testing program. The cone penetration test systems and the resilient modulus test system are described. Brief descriptions of the experimental soil sites are also presented. The laboratory cone penetration testing procedure is described.

3.2 Laboratory Testing Program

Figure 3.1 shows the location of field sites. Tables 3.1 and 3.2 show the testing programs used in this study.

3.2.1 Equipment for the Resilient Modulus Testing

Mohammad et al. (1994) developed a resilient modulus testing system at Louisiana Transportation Research Center. Figure 3.2 depicts the Dynamic Material Test System (MTS) used for resilient modulus testing. This system consists of an MTS810 closed-loop servo-controlled hydraulic loading system, a digital controller, a load unit controller, a computer, and a data acquisition package, TestStarII. A pressure chamber is used to accommodate the soil specimen during the resilient modulus testing.

3.2.2 Loading System

A hydraulic actuator and a load frame are the main features of the loading system. A maximum dynamic force of 100 kN (22 kips) can be applied with this loading system.

3.2.3 Digital Controller

The digital controller is the interface between the computer and the MTS system. This controls the MTS system in either displacement or force mode, conditions sensors,

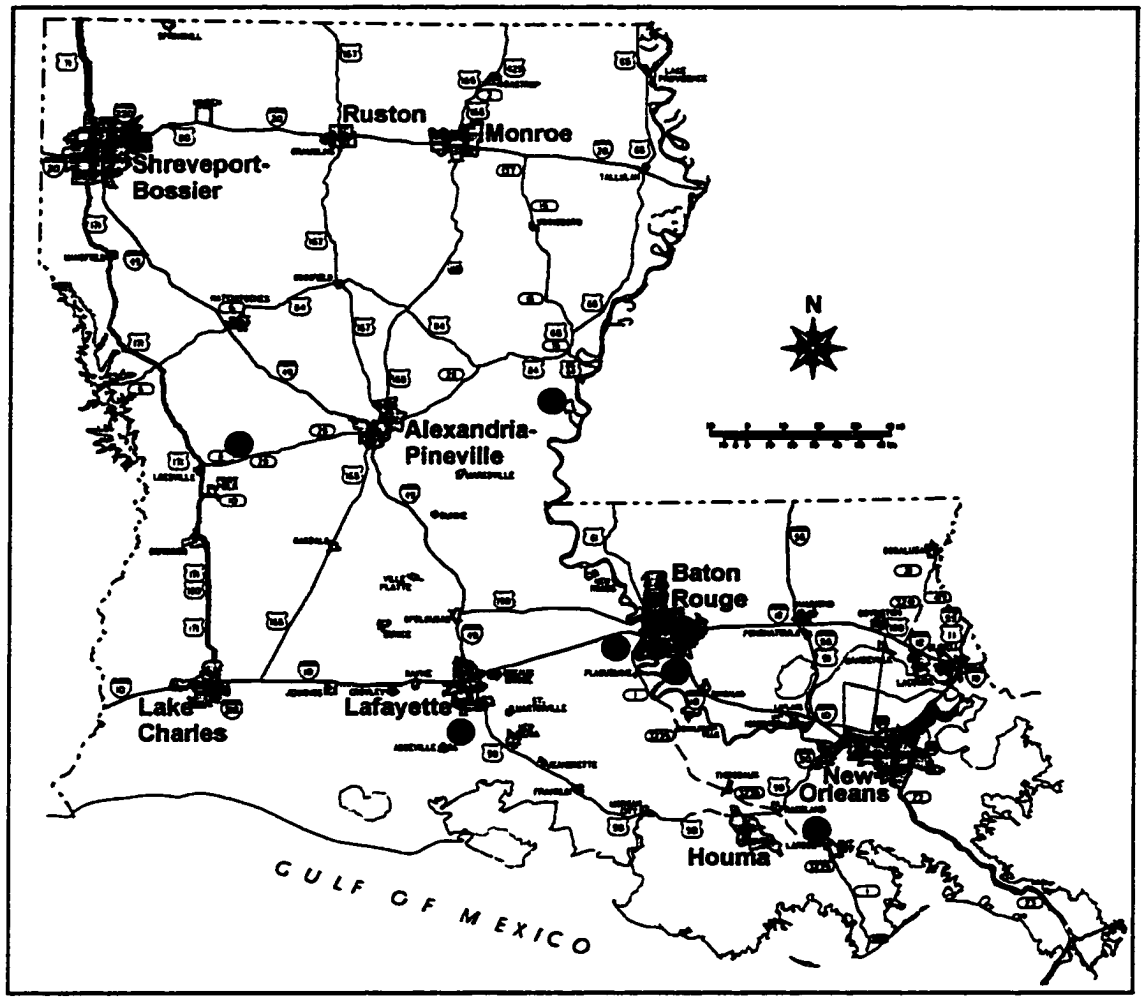

● - test locations

Figure 3.1 Locations of the field testing sites

Table 3.1 Laboratory program for soil testing

Tests \ Soils	PRF-Silty clay	PRF-Heavy clay	I-10/ LA-42 Clay	LA-15 Clay	LA-28 Sand	LA-89 Silty clay loam	Siegen Lane Clay
AASHTO T 294 Resilient modulus	✓	✓	✓	✓	✓	✓	✓
LA DOTD TR 407-89 Mechanical analysis of soils	✓	✓	✓	✓	✓	✓	✓
LA DOTD TR 403-92 Determination of moisture content	✓	✓	✓	✓	✓	✓	✓
LA DOTD TR 413-71 Organic material in soil	✓	✓	✓	-	-	-	-
LA DOTD TR 428-67 Determining the Atterberg limits of soils	✓	✓	✓	✓	-	✓	✓
ASTM D854-92 Test method for specific gravity of soils	✓	✓	✓	✓	✓	✓	✓
ASTM D4767-88 Test method for consolidated undrained triaxial compression test on cohesive soils	*	*	*	✓	-	✓	✓
LA DOTD TR 418-93 Moisture-density relationships (standard Proctor test)	*	*	✓	✓	✓	-	✓
ASTM D2487-93 Test method for classification of soil for engineering purposes (unified soil classification system)	✓	✓	✓	✓	✓	✓	✓
LA DOTD TR423-89 Classification of soil and soil-aggregate mixtures for highway construction purposes	✓	✓	✓	✓	✓	✓	✓

Legend: ✓- test done and *- obtained from previous studies, LA DOTD-Louisiana Dept. of Transportation and Development, ASTM- American Society for Testing and Materials, AASHTO- American Association of State Highway and Transportation Officials

Table 3.2 Field testing program

Soils	Field testing method	Number of tests within test sets			
		Test set 1	Test set 2	Test set 3	Test set 4
PRF-Silty clay	CIMCPT:	4	4	4	-
	CPT:	1	1	1	-
	Soil sampling:	1	1	1	-
PRF-Heavy clay	CIMCPT:	3	2	2	-
	CPT:	1	2	1	-
	Soil sampling:	1	1	1	-
I-10/LA-42 clay	CIMCPT:	2	4	2	4
	CPT:	2	2	2	2
	Soil sampling:	1	1	1	1
LA-15 clay	CIMCPT:	4	4	4	-
	CPT:	2	2	2	-
	Soil sampling:	1	1	1	-
LA-28 sand	CIMCPT:	4	4	4	-
	CPT:	2	2	2	-
	Soil sampling:	1	1	1	-
LA-89 clay	CIMCPT:	4	4	4	-
	CPT:	2	2	2	-
	Soil sampling:	1	1	1	-
Siegen Lane clay	CIMCPT:	4	4	4	-
	CPT:	2	2	2	-
	Soil sampling:	1	1	1	-

Legend: CIMCPT- Continuous Intrusion Miniature Cone Penetration Test , CPT- Cone Penetration Test, Soil sampling- Soil retrieved from the boreholes by the shelby tubes

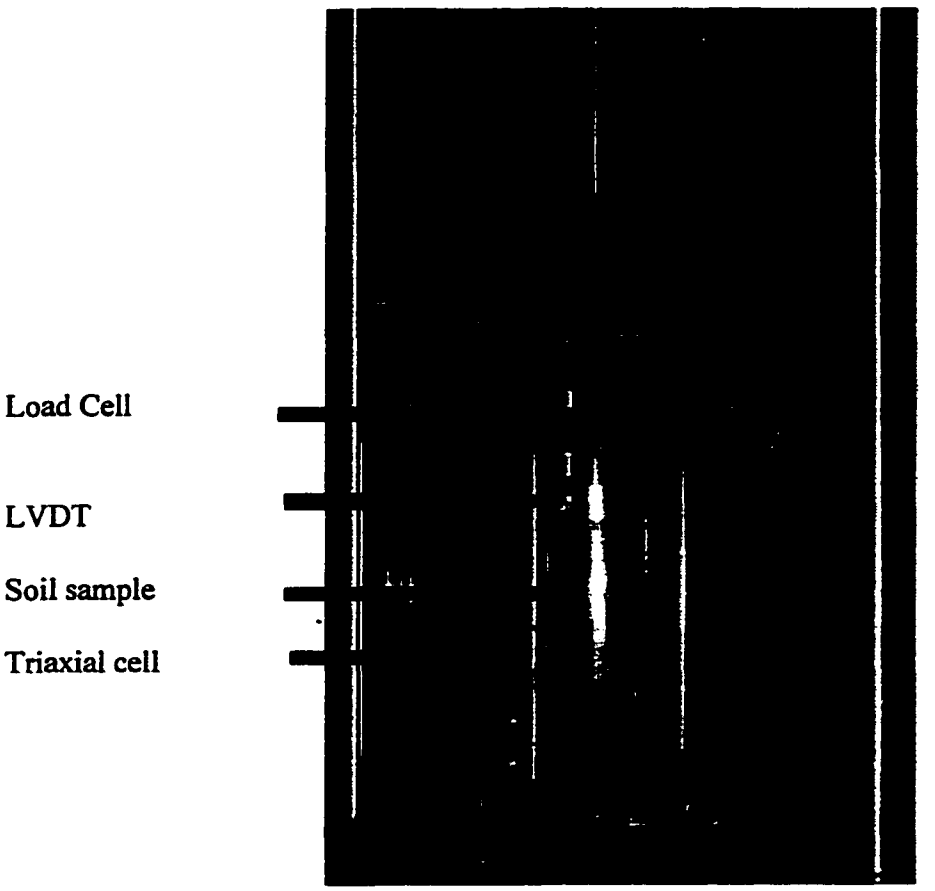

Figure 3.2 The MTS system

and provides connections for external equipment. It also controls the hydraulic power supply to the MTS machine. It has 16 channels for analog inputs and outputs. With the data acquisition package, TestStarII, the computer downloads the program code to the digital controller and it controls the MTS system.

A closed loop control system, as shown in Figure 3.3, is employed in the MTS testing system. When the control signal requests a specified force, the force sensor sends a feedback signal. When the control signal requests a specified displacement, the LVDT sends a feedback signal.

3.2.4 Load Unit Control Panel

This panel can be used by the user to control the load hydraulics while handling the sample for test preperation. The machine status and custom messages are shown on the panel's display. This panel can be used to control the program start, stop, hold, and resume operations.

3.2.5 Triaxial Cell

A plexiglas triaxial cell, diameter of 203 mm (8 in.) and a height of 330 mm (13 in.), is used in this system. Compressed air is used to apply the confining pressure inside the cell to a maximum of 700 kPa (98 psi).

3.2.6 Pressure Control Panel

This applies and controls the confining pressure inside the triaxial cell. A minimum pressure of 0.35 kPa (0.05 psi) can be applied with this panel.

3.2.7 LVDTs and Load Cell

Two vertical LVDTs are symmetrically placed on the top of the sample to measure the displacements. These LVDTs have a full scale stroke of ±6.35mm.

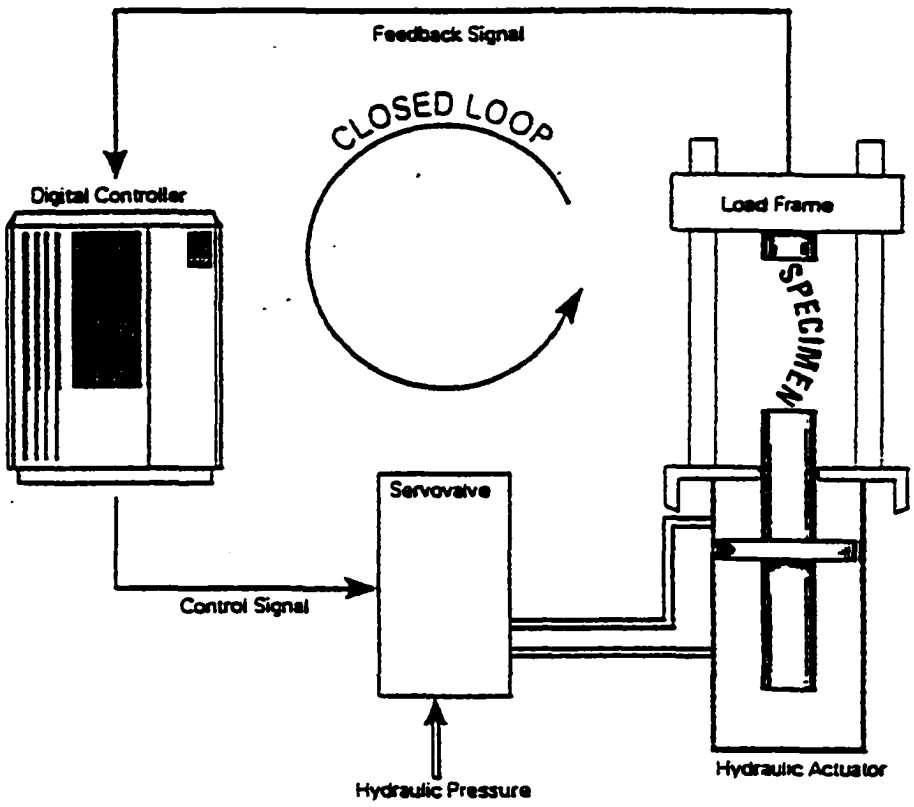

Figure 3.3 Closed loop control system in the MTS

A load cell of capacity of 2.72 kN (600 lbs) is installed in the loading unit inside the triaxial cell.

3.2.8 Data Acquisition and Equipment Control

A signal conditioner, data acquisition board, and a software for equipment control, data reduction and analysis are used in the data aquisition system. All the sensors have a ± 5 Volt range. The load cells have a fixed output level of ± 10 Volts for ± 2.72 kN (600 lbs).

3.2.9 Laboratory Resilient Modulus Testing Procedure

Undisturbed soil samples, 142 mm (5.6 in) in height and 71 mm (2.8 in) in diameter, were trimmed and prepared for the laboratory resilient modulus testings. Moisture content and dry unit weight were determined. According to the AASHTO T- 294 procedure, repeated loading triaxial tests were conducted to determine the resilient modulus of the subgrade soils. In order to minimize the imperfect contacts between the specimen ends, conditioning cycles were first performed on the soil samples. This also minimizes errors due to misalignment of the specimen. Tests were performed at different combinations of confining and deviator stress sequences. These stress sequences cover the expected in-service traffic loading range. The AASHTO T- 294 provides the magnitudes of the confining and deviator stresses and the number of cycles for the soil testing.

3.3 Field Testing Program

The field testing program consisted of the cone penetration testing and soil sampling. The program was aimed to cover common soil types in Louisiana. They include heavy clay, silty clay, overconsolidated clay, and sand.

3.3.1 Description of the Test Sites

Field cone penetration tests were performed at seven test sites which comprise common soil types in Louisiana. Cone penetration tests were performed at the Pavement Research Facility (PRF), Port Allen, the intersection of interstate I-10 and state highway LA-42 (Highland Road), state route LA-15, LA-1, LA-28, LA-89, and Siegen lane. The PRF site has heavy clay and silty clay locations. Six of the tested soils are fine-grained and two are coarse-grained. In the silty clay, three sets of tests were conducted. Each set consisted of four miniature cone penetration tests, one CPT test, and undisturbed soil sampling. The cone tip resistance and sleeve friction were recorded continuously from the surface to 2 or 3 m depth. The cone penetration tests consisted of three sets at each site. Each set consisted of four miniature cone penetration tests and one or two CPTs.

3.3.2 Research Vehicle for Geotechnical In-situ Testing and Support (REVEGITS)

The research vehicle for geotechnical in-situ testing and support, sponsored by the National Science Foundation, is an in-situ testing and support system mounted on a twenty-ton truck powered by a caterpillar 210 HP diesel engine. This system is equipped with several types of cone penetration test equipment such as standard cone penetration tests, piezocone penetration tests, siesmic cone penetration tests, conductivity cone penetration test, self boring pressuremeter tests, and dilatometer tests (Tumay 1994; Tumay et al., 1997). Tumay et al. (1992) reported that the results of the 10 and 15 cm^2 cone penetrometers were not significantly different. As a reference cone the 15 cm^2 cone penetrometer was used since its results are not significantly different from the 10 cm^2 cone penetrometer. Figure 3.4 depicts the inside of the REVEGITS. It shows the hydraulic pushing system, segmental push rods and other features of the REVEGITS.

Figure 3.4 The REVEGITS system (after Tumay, 1994)

3.3.3 Continuous Intrusion Miniature Cone Penetration Test (CIMCPT or MCPT)

Tumay et al. (1997 and 1998) developed the CIMCPT system, sponsored by the Priority Technology Program of the Federal Highway Administration, for site characterization of subgrade soil, construction control of embankments, assessment of the effectiveness of ground modification, and other shallow depth (upper 5 to 10 m) applications. It is equipped with a miniature cone penetrometer test equipment. The miniature cone penetrometer used in this study has a cross sectional area of 2 cm^2, friction sleeve area of 40 cm^2, and a cone apex angle of 60 degrees. The miniature cone is attached to a coiled push rod which replaces the segmental push rods in the standard cones. A 20 mm/sec penetration rate was used. Figure 3.5 shows the continuous push device and coiled thrust rod. The CIMCPT provides a finer soil profile as compared to the *CPT*. Due to the scale effects, the miniature cone records a slightly higher tip resistance and lower sleeve friction than the 15 cm^2 cone does (Tumay et al., 1997; Kurup and Tumay, 1999; Mohammad et al., 2000; Titi et al., 2000). Figure 3.6 compares the cone penetrometers used in this study.

3.3.4 Procedure

Two types of cone penetrometers were employed for the field cone penetration testing. Most of the tests were conducted with a miniature friction cone penetrometer. In order to calibrate the miniature cone, the 15 cm^2 cone was also used. In order to minimize the disturbance, the miniature cone tests were first performed. Then the 15 cm^2 friction cone tests were performed. The cone tip resistance and the sleeve friction were recorded continuously. At each site, a cone penetration test plan were prepared to evaluate the reliability and repeatability of the miniature cone penetration tests. As

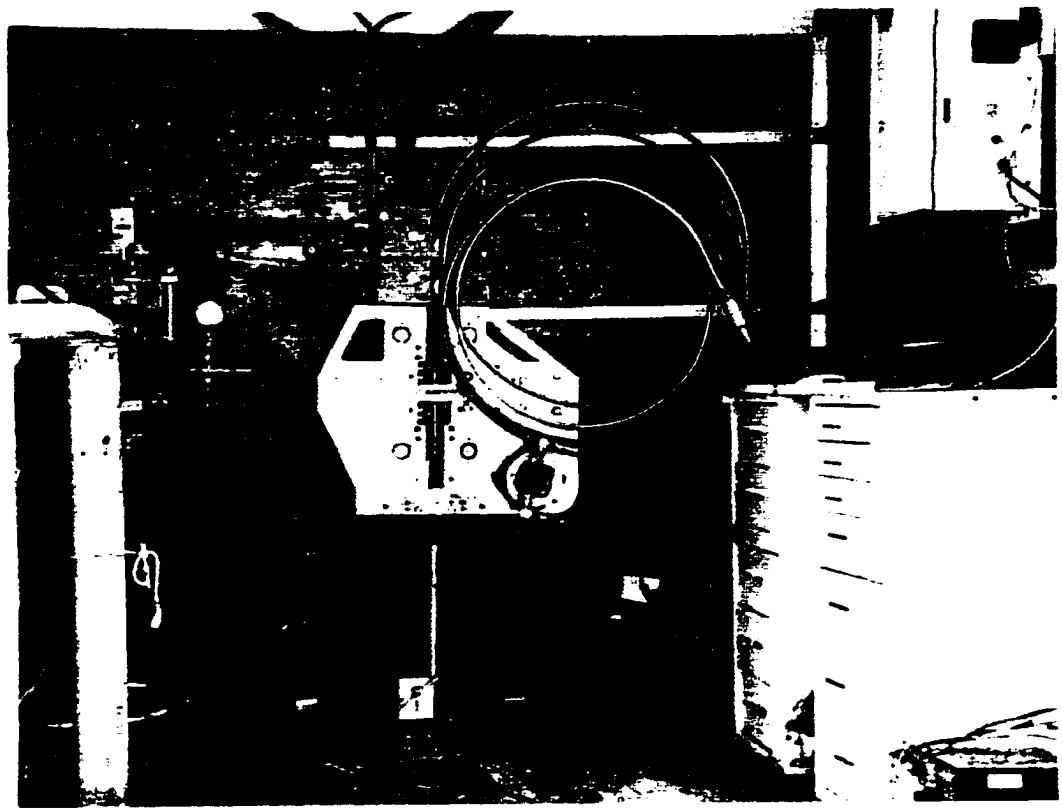

Figure 3.5 The CIMCPT system (after Tumay, 1997)

Figure 3.6 The 15 cm^2 cone, 2 cm^2 miniature cone, and a ball point pen (after Tumay)

shown in Figure 3.7, a typical cone penetration test consists of three sets at each site. Undisturbed soil samples were collected using shelby tubes at different depths (up to top 3 m from the surface). Two or three shelbytube samples were retrieved from a borehole. After the samples being retrieved, both ends of the shelby tubes were sealed with polyethylene covers. Then soil samples were extracted from the shelby tubes, they were sealed and stored in a constant humidity room for laboratory testing. This procedure ensures the same in-situ moisture content in the samples during their transportation and handling. Both soil sampling and cone penetration tests were performed in the same day to ensure similar conditions. This procedure minimizes the difference between field and laboratory testing parameters in terms of moisture content and unit weight.

3.3.5 Laboratory Soil Property Testing

Particle size distribution, Atterberg limits, water content, specific gravity, and standard Proctor compaction tests were performed. At different confining pressures, drained and undrained triaxial tests were performed. These tests are used to obtain the shear strength parameters, cohesion intercept and effective friction angle.

3.4 Laboratory Cone Penetration Testing

This section presents the methodology used in the laboratory cone testing program. The details of the equipment used in this study are also described. The equipment includes the cone penetration test system used for the laboratory cone testing program.

3.4.1 Introduction

The AASHTO guide for design of pavement structures (1993) stipulates that laboratory resilient modulus tests be performed on representative subgrade soil samples

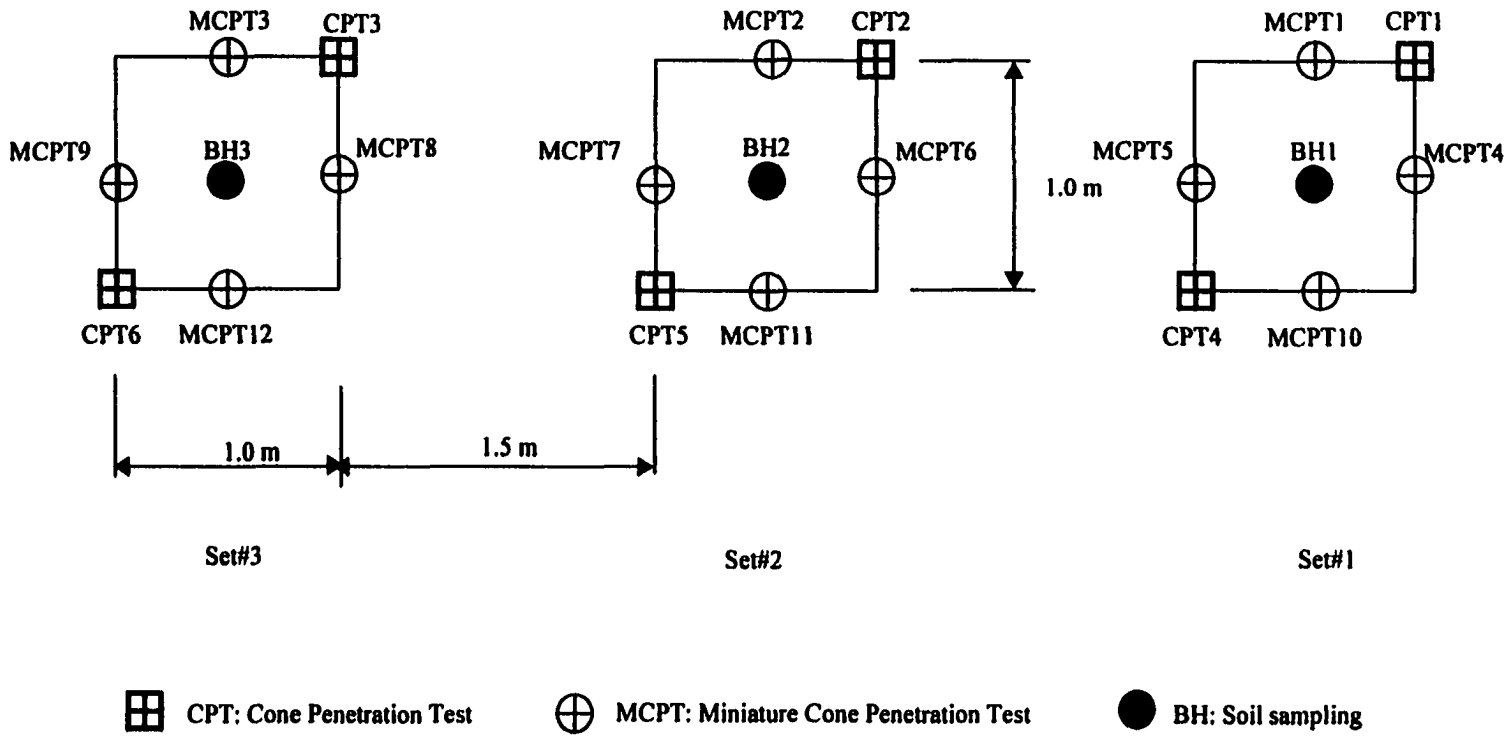

Figure 3.7 A typical layout for the field cone penetration tests at a site

in different moisture seasons in a year, such as rainy and dry, to estimate the seasonal resilient modulus values. This procedure quantifies the relative damage in a pavement during each moisture season in a year. The relative damage is taken into account in the pavement design. From the relative damage, an effective design resilient modulus value is estimated. In addition to estimating the seasonal modulus values, the AASHTO guide for design of pavement structures states that a year be divided into different time intervals during which the estimated seasonal resilient modulus values are effective. The minimum time interval might not be less than one-half month for any season. In this procedure, the seasonal resilient modulus values are assigned in their corresponding time periods. Then the seasonal resilient modulus values must be converted to the effective design resilient modulus value with the aid of the charts or equations given in the AASHTO guide for design of pavement structures. For rigid pavements, the resilient modulus of subgrade must be converted into an effective modulus of subgrade reaction (k-value) with the aid of the charts or equations given in the AASHTO guide for design of pavement structures.

In the field, a subgrade soil encounters wetting and drying cycles. The subgrade resilient modulus increases as soil dries out in the field. In the field, the resilient modulus is expected to decrease in a wet period. Therefore, the laboratory resilient modulus test should be performed on samples taken in wet seasons and dry seasons since they change the subgrade soil resilient modulus. Both the resilient modulus and cone penetration test parameters are affected by the moisture content and unit weight of soils. Due to these facts, duplicating the moisture cycle is important. As given in Table 3.3, a laboratory cone penetration testing program was performed to study the effect of moisture content

Table 3.3 The moisture-unit weight combinations used in the tests

Soil type \ Moisture level		Moisture content, w (%)	Dry unit weight, γ_d (kN/m^3)
Silty clay	dry	14.4	16.1
	optimum	18.0	16.7
	wet	21.8	16.1
Heavy clay	dry	26.4	13.1
	optimum	31.4	13.6
	wet	36.4	12.8
Silt	dry	10.7	16.4
	optimum	15.2	17.2
	wet	20.4	15.9
Sand	dry	5.0	16.1
	optimum	8.1	16.4
	wet	11.0	15.7

and unit weight on the resilient modulus and cone penetration test parameters. Laboratory cone penetration tests were performed on four soil types, silty clay, heavy clay, silt, and sand, with three different moisture-unit weight combinations: dry side (3 to 5 % below optimum), optimum, and wet side (3 to 5 % above optimum). This study presents twelve laboratory cone penetration tests on four soil types with different moisture-unit weight combinations. In addition to these, resilient modulus, soil classification, specific gravity, triaxial, Atterberg limit, moisture content, and unit weight tests were performed. Laboratory cone and resilient modulus test results were interpreted by the models developed in the field testing program. Simplified design charts, developed using these test results, may be utilized in evaluating the resilient modulus from the cone penetration test results. A design example is presented in Section 4.5.8.2, Chapter 4, to illustrate the use of the simplified design charts.

3.4.2 Objectives

- The main objective in this study was to evaluate the effect of variation in the moisture and unit weight on the predicted resilient modulus from the cone parameters.
- Verify the models which were developed using the field cone penetration and corresponding resilient modulus testing results.
- Develop simplified design charts to evaluate resilient modulus from the cone penetration test results.

3.4.3 Methodology

In order to achieve the objectives, an experimental setup was constructed at Louisiana Transportation Research Center (LTRC) to perform the laboratory cone penetration tests. Effects of moisture content, dry unit weight, and soil type were studied. During the cone penetration tip resistance, sleeve friction, and penetration depth were recorded continuously by the data acquisition system.

3.4.4 Equipment for the Laboratory Cone Test

As shown in Figure 3.8, this experimental setup consists of a 55 gallon metal rigid wall container, 572 mm in diameter and 864 mm in height, reaction frame of 1130 mm in height and 1525 mm in width, loading frame, hydraulic loading system, 2 cm^2 miniature cone penetrometer, depth encoder system, cone pushing and grabbing system, control box, computer, and data acquisition system. Special straight push rod with a length of 1800 mm was made for this purpose and attached to the 2 cm^2 miniature cone for continuous intrusion. The hydraulic pushing system, mounted on a metal frame above the soil sample, consists of dual piston, double acting hydraulic jacks on a

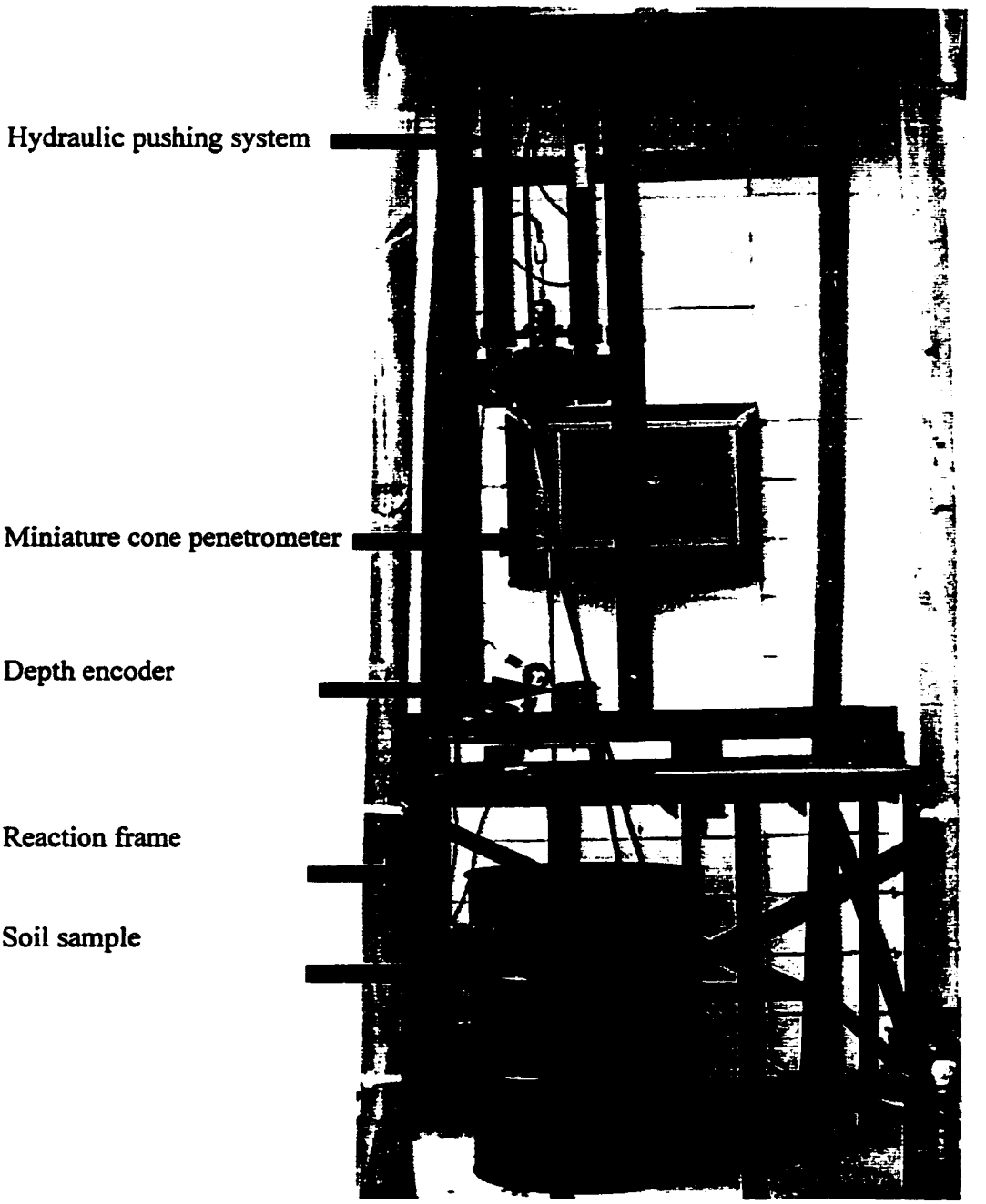

Figure 3.8 The laboratory cone test setup

collapsible frame. A single stroke of the pushing system is 640 mm. This stroke is enough to penetrate a soil sample, used in this study, continuously at a rate of 20 mm/sec,. An electronic analog to digital converter depth decoding system is employed to measure the depth at 4 mm intervals.

3.4.5 Data Acquisition System

The data acquisition system (Tumay, 1997) is depicted in Figure 3.9. The data acquisition system consists of a Pentium II computer collecting data from the cone penetrometer through the DGH modules, made by the DGH corporation, Manchester, New Hampshire. All of the DGH modules are connected to a conversion box via RS485. The conversion box allows output of RS232 for serial line communication with the computer. The DGH modules are connected to different channels in the cone penetration system, such as depth encoder and strain gauges of tip and sleeve. The first DGH module, D1622, is a pulse counter which is connected to the depth encoder. Other two channels are DGH modules D1102 which measure voltage with a precision of ±10 mV. These two are connected to the strain gauges of the tip and sleeve.

3.4.6 Testing Program

3.4.6.1 Soil Compaction

Disturbed soils of heavy clay, silty clay, and silt, and sand, were collected by digging the corresponding soil sites and they were dried in the oven. Soil property tests, such as moisture unit weight relationship, hydrometer, soil classification, specific gravity, Atterberg limit tests, and triaxial, were performed on these soils to characterize them. The standard Proctor test was performed to establish the moisture content-density relationship for each soil. The optimum moisture content and maximum dry unit weight,

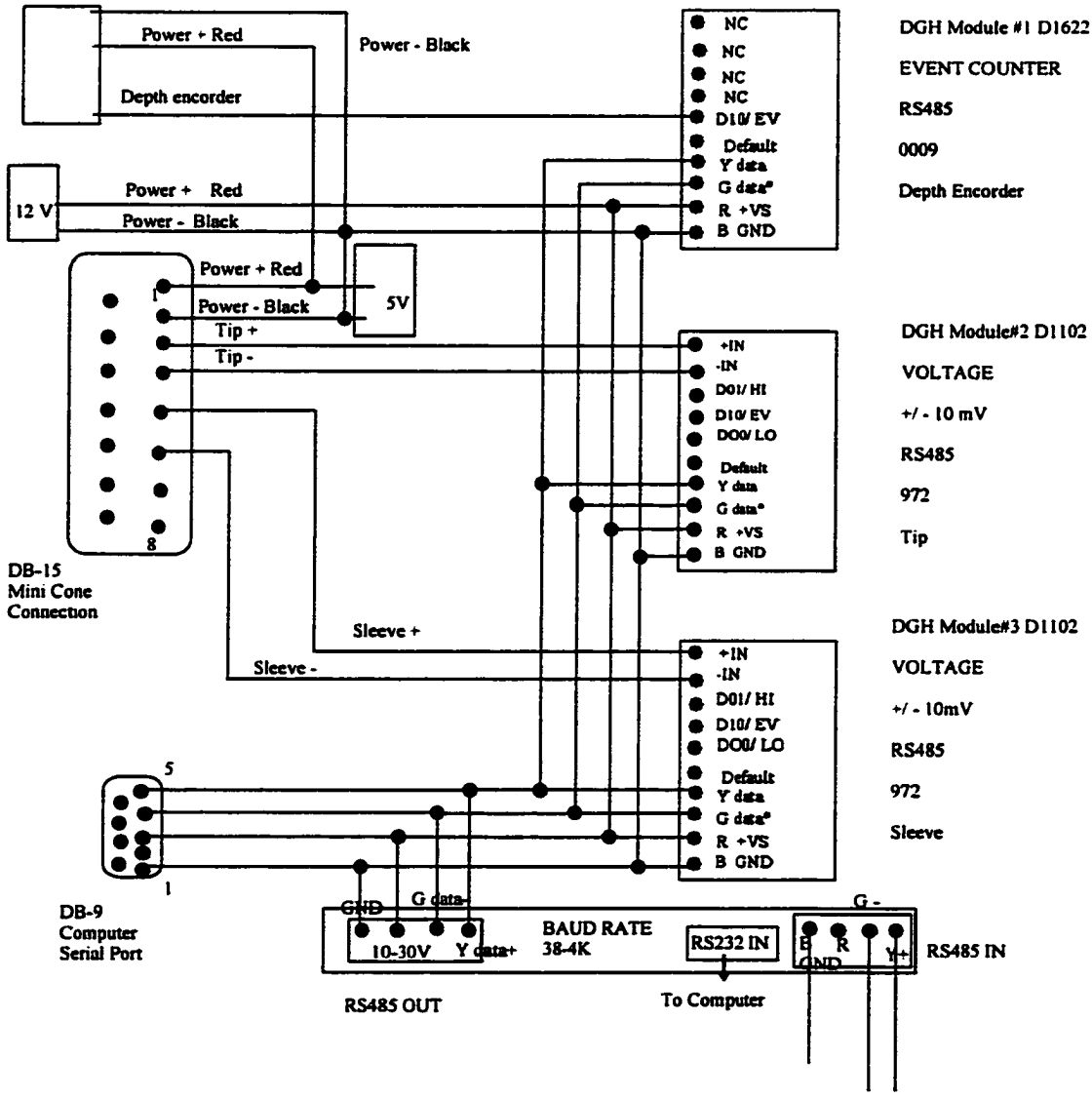

Figure 3.9 The data acquisition system for the miniature cone penetration (after Tumay, 1997)

obtained from the standard Proctor tests, of each soil type are given in Chapter 4, Tables 4.1 and 4.8. For the soil compaction in this testing, three moisture content-unit weight levels of the moisture- unit weight curve were selected. These are dry side (about 3 to 5 % below the optimum), optimum, and wet side (about 3 to 5 % above the optimum). The selected moisture content-unit weight levels are given in Table 3.3. First, dry soils were pulverized and sieved through No. 4 (4.75 mm) sieve. Second, the weight of the soil, passing No. 4 sieve, at the required water content, to be compacted into the volume of the container to obtain the required density, was calculated. After establishing the number of layers to be compacted in the container, soil was mixed with the required amount of water in a mixing pan. After placing the required amount of wet soil for the first layer in the container, it was compacted until the required height was achieved. Fine-grained soil was compacted using an electric jack hammer, whereas coarse-grained soil was compacted using an electric vibrator. A certain selected pattern of compaction was followed. While the compactor compacting, it moved on the soil surface very closely in a circular path starting from the center of the soil sample so that every where in the soil surface was compacted uniformly. Then the compactor moved to the adjacent circular path and compacted the soil. This procedure continued until the compactor reached the rigid wall of the container. This path was reversed and this procedure was repeated until the required height was achieved. In this way, a uniform compaction effort was applied on the soil layer.

In order to determine the layer thickness, several compaction trials were performed with different layer depths. The results varied between 100 mm to 150 mm. After these compaction trials, each layer thickness in compaction was maintained at

125 mm. At least six layers were used for soil compaction. After compacting each layer, the top of the surface was scarified. This compaction procedure was repeated for the other layers.

3.4.6.2 Cone testing

After compacting soil in the container, the cone penetration test was performed with the miniature cone penetrometer. The test layout, as shown in Figure 3.10, was used in the laboratory cone test. Table 3.4 presents the summary of the testing program. Since the diameter of the miniature cone penetromer, used in this test, is 15.88 mm, this test layout allows to maintain a diameter ratio larger than 15 as explained in Section 4.5.2 in Chapter 4. This test layout was selected to avoid the boundary effects. Cone penetration tests were performed continuously using a 2 cm^2 miniature cone penetrometer.

3.4.6.3 Soil testing

After the cone penetration test, soil samples were collected at different depths of the container for the laboratory resilient modulus and soil property tests. For silty clay, heavy clay, and silt, sand cone tests, LADOTD TR 401-95, were performed at different depths to obtain the unit weight of soil. First the metal cone was calibrated with clean, dry, fine sand passing the No. 10 (2 mm) sieve and retained on the No. 50 (0.3 mm) sieve. In the calibration process of the metal cone, unit weight and weight of fine sand which filled the metal cone were obtained. The sand cone jar was filled with clean dry fine sand and weighed. At the selected depths in the soil sample, a leveled surface was prepared for the sand cone testing. Then the sand cone jar with valve closed was inverted and placed on the prepared surface. After placing the sand cone firmly against the prepared surface, opened the valve and let fine sand flow to a stop. Then closed the valve

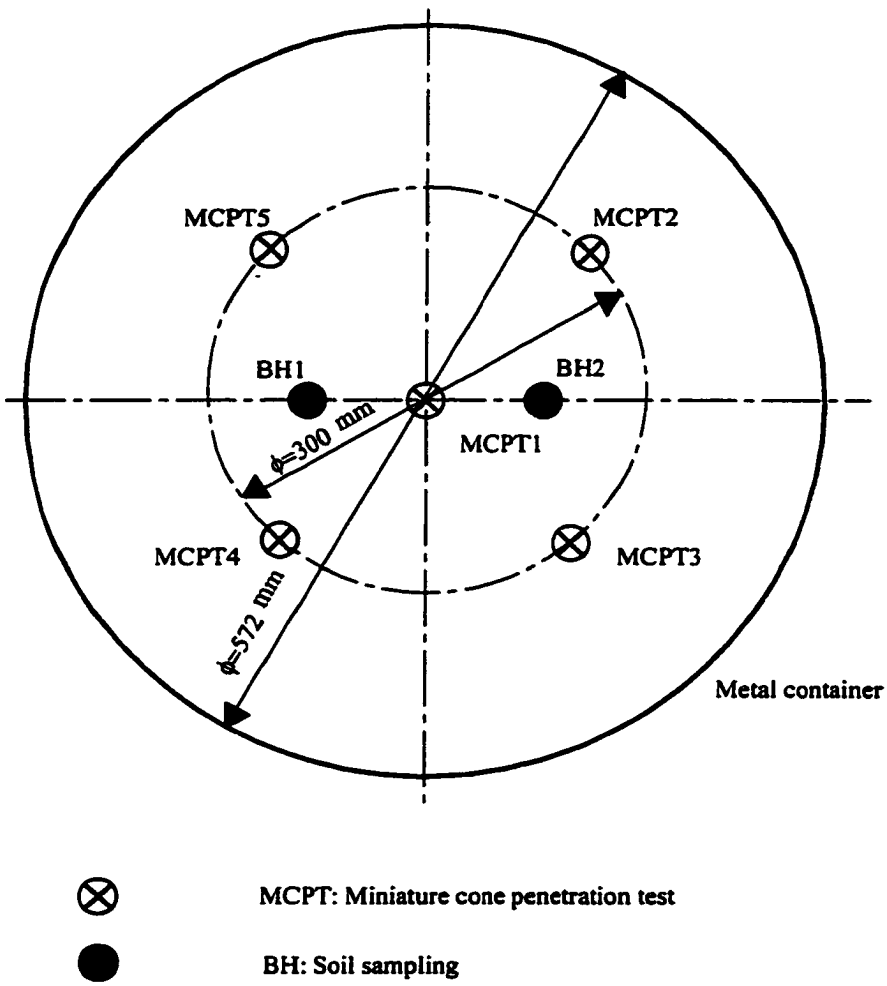

Figure 3.10 A typical layout for the laboratory cone test of the compacted soil samples

Table 3.4 Laboratory cone testing program

Soil type	Tests	No. of tests
PRF-silty clay	CIMCPT:	5
	Soil sampling:	2
PRF-heavy clay	CIMCPT:	5
	Soil sampling:	2
PRF-silt	CIMCPT:	5
	Soil sampling:	2
Sand	CIMCPT:	5
	Soil sampling:	2

Legend: CIMCPT- Continuous Intrusion Miniature Cone Penetration Test ,

Soil sampling- Soil samples retrieved from the boreholes

and weighed the sand cone jar. Then the weight of fine sand in the metal cone was estimated. After removing all fine sand from the prepared surface, a small hole was prepared in the center of the original position of the sand cone by excavating soil. The excavated soils were carefully collected without losing any part of them. The weight of the excavated soil was measured. Then the sand cone jar with valve closed was inverted and placed on the prepared hole such that the metal cone covered the open area of the hole. After placing the sand cone firmly against the prepared surface, opened the valve and let fine sand flow to a stop. The valve was closed and the sand cone jar was weighed. The weight of the fine sand, filled the excavated hole, was estimated. Then the volume of the excavated hole was estimated. The excavated soil was dried and weighed. Next, the unit weight of the excavated soil was estimated. The excavated soil was subjected to the moisture content evaluation. This procedure was repeated at each selected location in the soil sample. In this way, moisture and unit weight profile of the compacted soil in the container was established. Due to the relatively small dimensions of the compacted soil sample, the nuclear density test may not be suitable in this study. Unfortunately, the balloon test was not available for this study.

3.4.6.4 Resilient Modulus Testing

Resilient modulus tests were also performed on the compacted soil samples. These resilient modulus tests represent the corresponding moisture-unit weight combination at the cone penetration tests. According to the AASHTO T-294 test procedure, laboratory compacted soil samples, at the corresponding moisture unit weight combination of the cone penetration tests, were used for the resilient modulus testing. The laboratory cone test results were used to validate the proposed models.

CHAPTER 4

ANALYSIS OF RESULTS

This chapter presents the results of the field and laboratory tests. Soil characterization of the tested soils is described. The repeatability of the continuous intrusion miniature cone penetration test results is analyzed. The cone and resilient modulus test results are analyzed. The models to predict the resilient modulus from the cone penetration test results are developed. Preliminary design charts are proposed but not verified due to lack of data. Sensitivity of the pavement design equation is analyzed.

4.1 Soil Characterization

Both the resilient modulus and the cone penetration test results depend on the soil type and its properties. Therefore, soil characterization is also performed to identify the soil variables which are important for both testing. Tables 4.1 and 4.2 present the properties of the soils used in this research.

4.1.1 Pavement Research Facility

The Pavement Research Facility (PRF) is located at Port Allen, Louisiana. This is the experimentation test site for the Louisiana Transportation Research Center. The PRF site was selected for the field testing due to the availability of two types of cohesive soils, heavy clay and silty clay. This site comprises a natural soil deposit of heavy clay (CH) with 84 percent clay and 14 percent silt. A 1.52 m thick silty clay embankment was constructed at this site. The PRF-silty clay is classified as CL-ML (silty clay) in the unified soil classification system, USCS, and A-4 (silty soil) in the AASHTO classification system. To separate the heavy clay subgrade, a soft soil, and silty clay embankment, a geotextile fabric was installed.

Table 4.1 Properties of fine-grained soils used in the investigation

Property \ Soil site	PRF-Silty clay	PRF-Heavy clay	I-10/ LA-42 Clay	LA-15 Clay	LA-89 Silty clay loam	Siegen Lane Clay
Passing sieve #200 (%)	93	98	90	98	91	98
Clay (%)	23	84	42	44	26	33
Silt (%)	70	14	48	54	65	65
Organic content (%)	4.7	9.2	8	NA	NA	NA
Liquid limit (LL) (%)	28	93	50	52	34	35
Plastic limit (PL) (%)	22	27	16	25	23	23
Plasticity index (PI)	6	66	34	27	11	12
Specific gravity (G_s)	2.67	2.68	2.69	2.70	2.69	2.69
Angle of friction (ϕ) (^{0})	22.0	14.0	28.5	14.0	17.0	19.2
Optimum water content (w_{opt}) (%)	18.0	31.4	18.1	28.1	20.2	17.5
Maximum dry unit weight (γ_{dmax}) (kN/m^3)	16.7	13.6	16.8	15.1	16.5	17.0
Soil classification (USCS)	CL-ML (Silty clay)	CH (Fat clay)	CH (Fat clay)	CH (Fat clay)	CL (Lean clay)	CL (Lean clay)
Soil classification (AASHTO)	A-4 (Silty soil)	A-7-6 (Clayey soil)	A-7-6 (Clayey soil)	A-7-6 (Clayey soil)	A-6 (Silty clay loam)	A-6 (Silty clay)

Table 4.2 Properties of coarse-grained soil used in the investigation

Property \ Soil site	LA-1 Sand	LA-28 Sand
Passing sieve #200 (%)	5	30
Clay (%)	5	12
Silt (%)	0	18
Organic content (%)	NA	NA
Liquid limit (LL) (%)	NA	NA
Plastic limit (PL) (%)	NA	NA
Plasticity index (PI)	NA	NA
Specific gravity (G_s)	2.69	2.68
Angle of friction (ϕ) (^{0})	28	28
Optimum water content (w_{opt}) (%)	14.4	11.4
Maximum dry unit weight (γ_{dmax}) (kN/m^3)	16.3	18.3
Soil classification (USCS)	SP-SM (Poorly graded sand with silt)	SM (Silty sand)
Soil classification (AASHTO)	A-3 (fine sand)	A-2-4 (Silty sand)

The PRF-heavy clay is a very soft material. According to soil tests, this clay consists of medium gray soft normally consolidated clay with traces of organic materials and iron oxide. The PRF-heavy clay is classified as CH (fat clay) in the USCS and A-7-6 (clay) in the AASHTO classification system.

4.1.2 State Route LA-42 (Highland Road) at I-10

This site is located at the intersection of the State Route LA-42 (Highland Road) and the Interstate I-10, Baton Rouge, Louisiana. The laboratory soil test results showed that this soil consists of the brownish gray fissured stiff overconsolidated clay. Chen and Mayne (1994) performed a detailed soil sampling and cone penetration testing at this site up to 34 m. The soil is classified as CH (fat clay) in the USCS and A-7-6 (clay) in the AASHTO classification system.

4.1.3 State Route LA-15

The LA-15 test site is located in Concordia Parish about 15 miles south of Vidalia. The site is a part of the Mississippi River Levee. This is also located at the up slope of the LA-15. The soil is classified as the A-7-6 (clayey soil) using the AASHTO classification.

4.1.4 State Route LA-89/ New Iberia

The LA-89 site is located in New Iberia. The site consists of lime treated recycled soil-cement base. The subgrade soil is classified as CL (lean clay) in the USCS classification and A-6 (silty clay loam) in the AASHTO classification system.

4.1.5 Siegen Lane/ Baton Rouge

The Siegen Lane test site soil is classified as CL (lean clay) in the USCS classification and A-6 (silty clay) in the AASHTO classification system.

4.1.6 State Route LA-28/ Simpson

The LA-28 site is located in Simpson, Vernon Parish. This site is used as a borrow pit for the roadway embankment construction by the Louisiana Department of Transportation and Development. The soil at this site is coarse-grained soil. The soil is classified as SM (silty sand) in the USCS classification and A-2-4 (silty sand) in the AASHTO classification system. Shear strength parameters for this soil was estimated from Das (1983).

4.1.7 State Route LA-1/ Larose

This site is located on LA-1 in Larose, Lafourche Parish. This is an embankment. The soil at this site is coarse-grained soil. SP-SM (poorly graded sand with silt) in the USCS classification and A-3 (fine sand) in the AASHTO classification system. Shear strength parameters for this soil was also estimated from Das (1983).

4.2 Cone Test Results

The CIMCPT is a newly developed system. The miniature friction cone is to be calibrated with respect to the 15 cm^2 cone in different soil types. Cone penetration tests were performed according to Table 3.2 in Chapter 3 in order to ensure the reliability and repeatability of the miniature cone penetration test data.

The field testing layout for the PRF-silty clay is given in Figure 4.1. Twelve CIMCPTs and three CPTs were performed. Soil samples were also obtained for the laboratory testing, as described in Section 3.3.4. The field tests were performed in three sets. The cone penetrated to a depth of 2 m. Figure 4.2 depicts the cone penetration test results for the PRF-silty clay for field test set 1. According to Figure 4.2, in the 0.3 m limestone base, the tip resistance of the miniature cone penetrometer fluctuates due to its

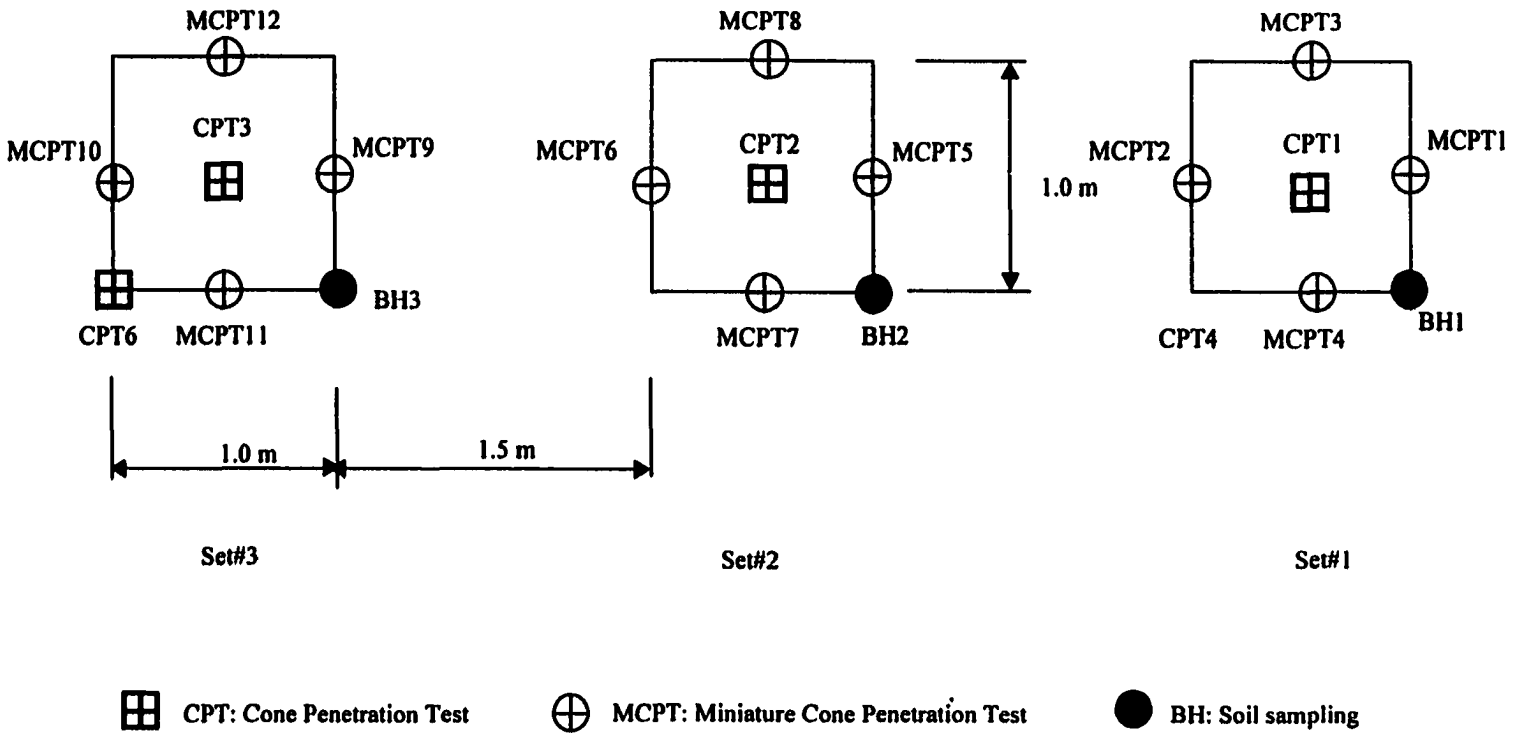

Figure 4.1 Field test layout for the PRF-Silty clay site

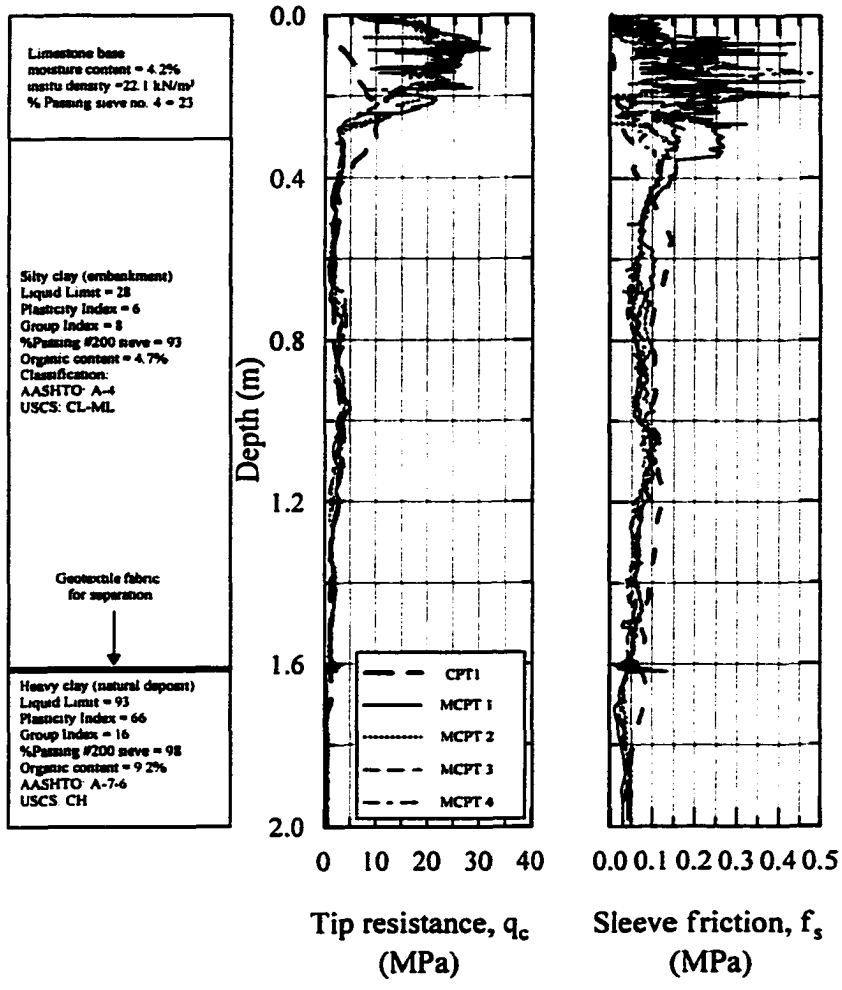

Figure 4.2 Cone penetration test results of the PRF-silty clay (set #1)

high sensitivity. In this layer, the tip resistance recorded by the miniature cone is higher than that of the CPT. In general, the tip resistance of the miniature cone penetration test is slightly higher than that of CPT (Tumay et al., 1997 and 1998). But the sleeve friction of the miniature cone penetration test is slightly lower than that of CPT. This observation was also made by Tumay et al., (1997 and 1998). This is attributed to the scale effect of the miniature cone penetrometer (de Lima and Tumay,1991 and Tumay et al., 1997 and 1998). The miniature cone penetration generates a smaller pressure bulb than the CPT does. Therefore, the miniature cone penetration identifies thin soil layers. In the silty clay embankment, a fine-grained soil layer, both CPT and CIMCPT results exhibit similar patterns indicating the verification of the implementation of the CIMCPT system.

Several studies (Tumay et al., 1997 and 1998; Kurup and Tumay, 1999; Mohammad te al., 2000; Titi et al., 2000) have shown the reliability and repeatability of the CIMCPT test results. A statistical analysis was performed on the cone test results to determine the coefficient of variation. In a data set, average the CIMCPT test results along the depth and estimate the standard deviation as well as coefficient of variation. The average value of all the CIMCPT test results in a data set at a selected depth is considered for the resilient modulus evaluation from the cone penetration test results. The coefficient of variation of CIMCPT results of silty clay is shown in Figure 4.3. A high variation of tip resistance, as shown in Figure 4.3, was observed in the top layer of this site which consists of a gravel base of 0.3 m. But below the top 0.3 m, only a small variation among the CIMCPT results can be observed.

Figure 4.4 presents the field testing layout for the PRF-heavy clay. Out of eight CIMCPTs five were satisfactory while the other three were erroneous due to the

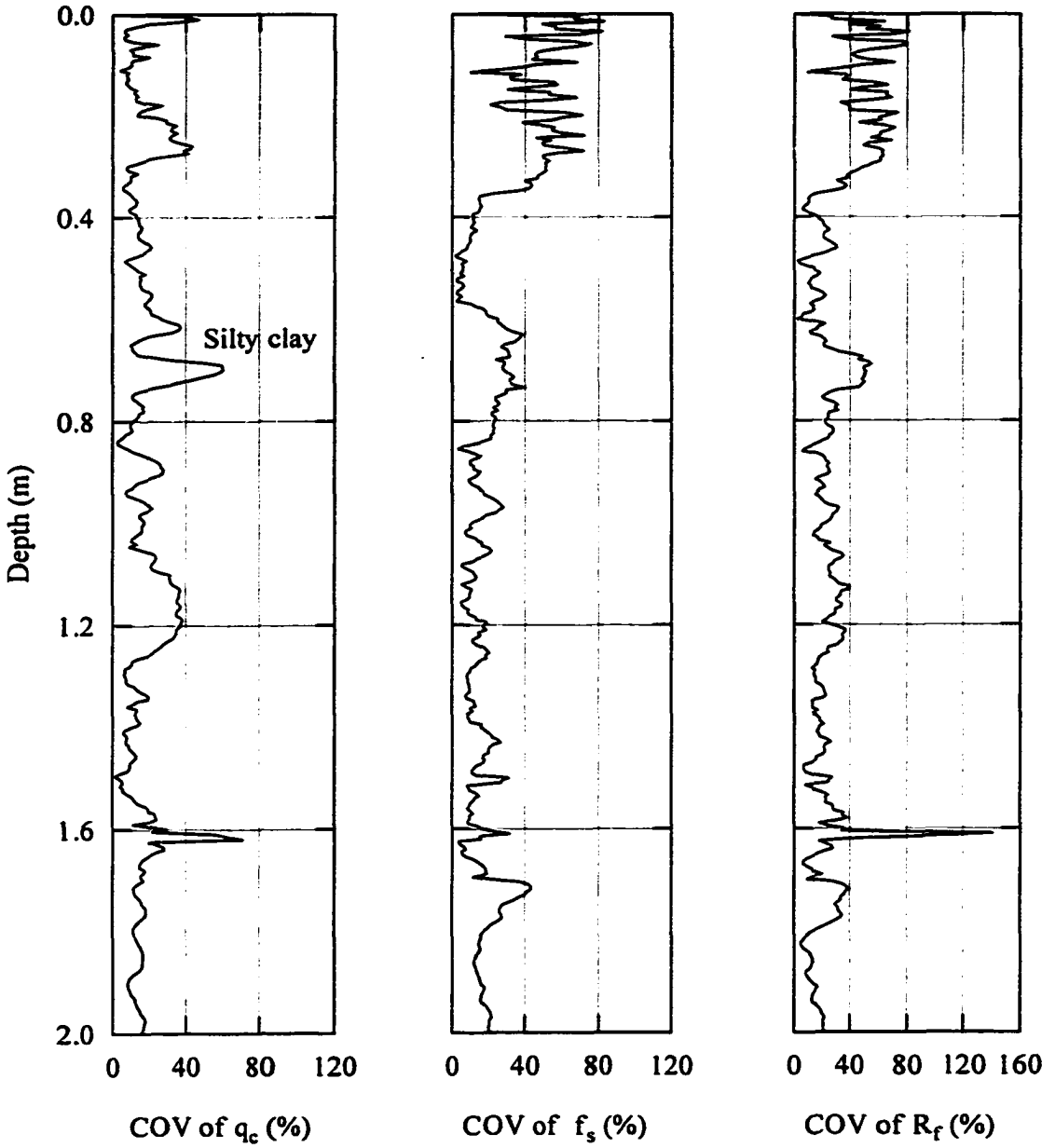

Legend: q_c - Tip resistance, f_s - Sleeve friction, R_f - Friction ratio

Figure 4.3 Coefficient of variation of CIMCPT for the cone test of the PRF-silty clay

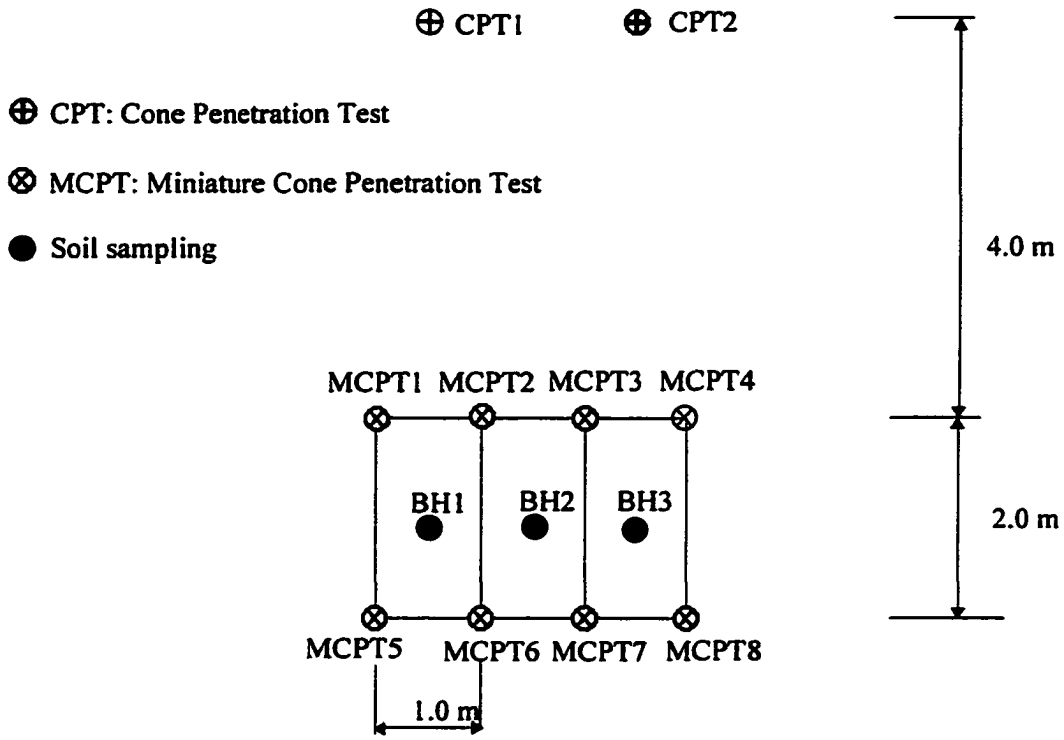

Figure 4.4 Field test layout for the PRF-heavy clay

malfunction in the data acquisition system. Therefore, only five of the eight CIMCPTs (test Nos. 1, 3, 5, 6, and 8) were used in the data analysis. Figure 4.5 depicts the cone penetration test results for the PRF-heavy clay for field test set1. The miniature cone recorded low tip resistance and high sleeve friction due to soft clayey nature of this soil. The coefficient of variation of the test results is depicted in Figure 4.6. According to the testing layout, shown in Figure 4.4, a high coefficient of variation in heavy clay may be attributed to the soil variability resulting from the difference in the distance among the test locations of CIMCPTs. The soil deposit may not be homogeneous in all the test points.

Figure 4.7 presents the field testing layout for the LA-42/ I-10 site. Figures 4.8 depicts the cone penetration test results. The top layer (0 to about 0.5 m) forms with a stiff, desiccated deposit. Therefore, the tip resistance showed high variability in the top layer. The following soil deposit is a heavily overconsolidated, desiccated silty clay/ clayey silt with occasional sand pockets (Chen and Mayne, 1994). When the miniature cone penetrometer encounters a sand pocket, a high tip resistance was expected. Below the top layer, the CPT and CIMCPT soundings reflect the similar patterns with different magnitudes. Figure 4.9 shows the coefficient of variation of the tip resistance and the sleeve friction. A large deviation of the cone test results can be observed in the top layer. Below the top layer, a small deviation of the cone test results can be observed. The average *COV* of the tip resistance is 18.5 percent for the miniature cone whereas, that is 12.5 percent for the 15 cm^2 cone. The average COV of the sleeve friction is 18.2 percent for the miniature cone whereas, that is 16 percent for the 15 cm^2 cone. Because of the high sensitivity of the miniature cone and its capability to identify thin soil layers, the

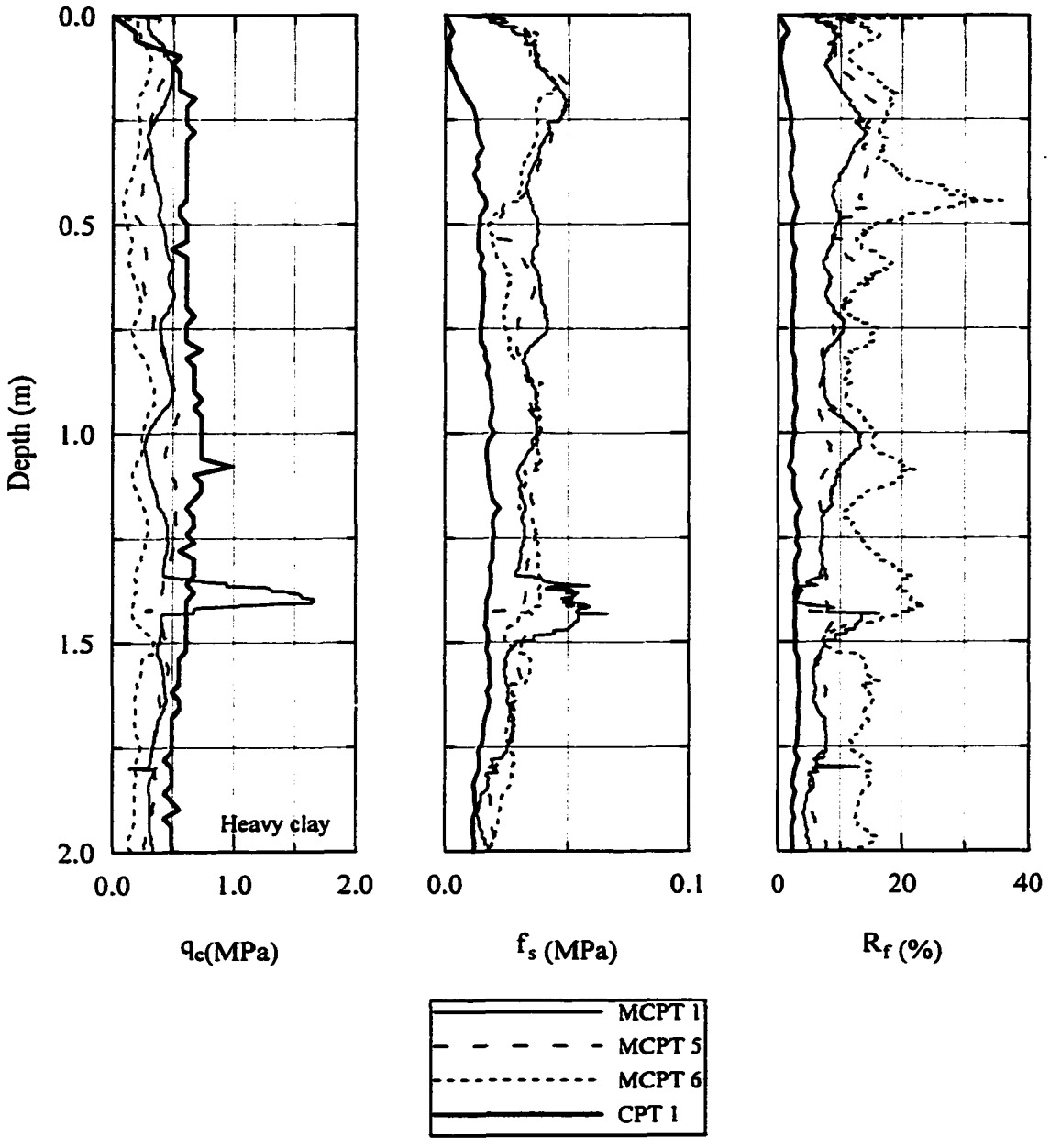

Legend: q_c - Tip resistance, f_s - Sleeve friction, R_f - Friction ratio

Figure 4.5 Cone penetration test results of the PRF-heavy clay (set #1)

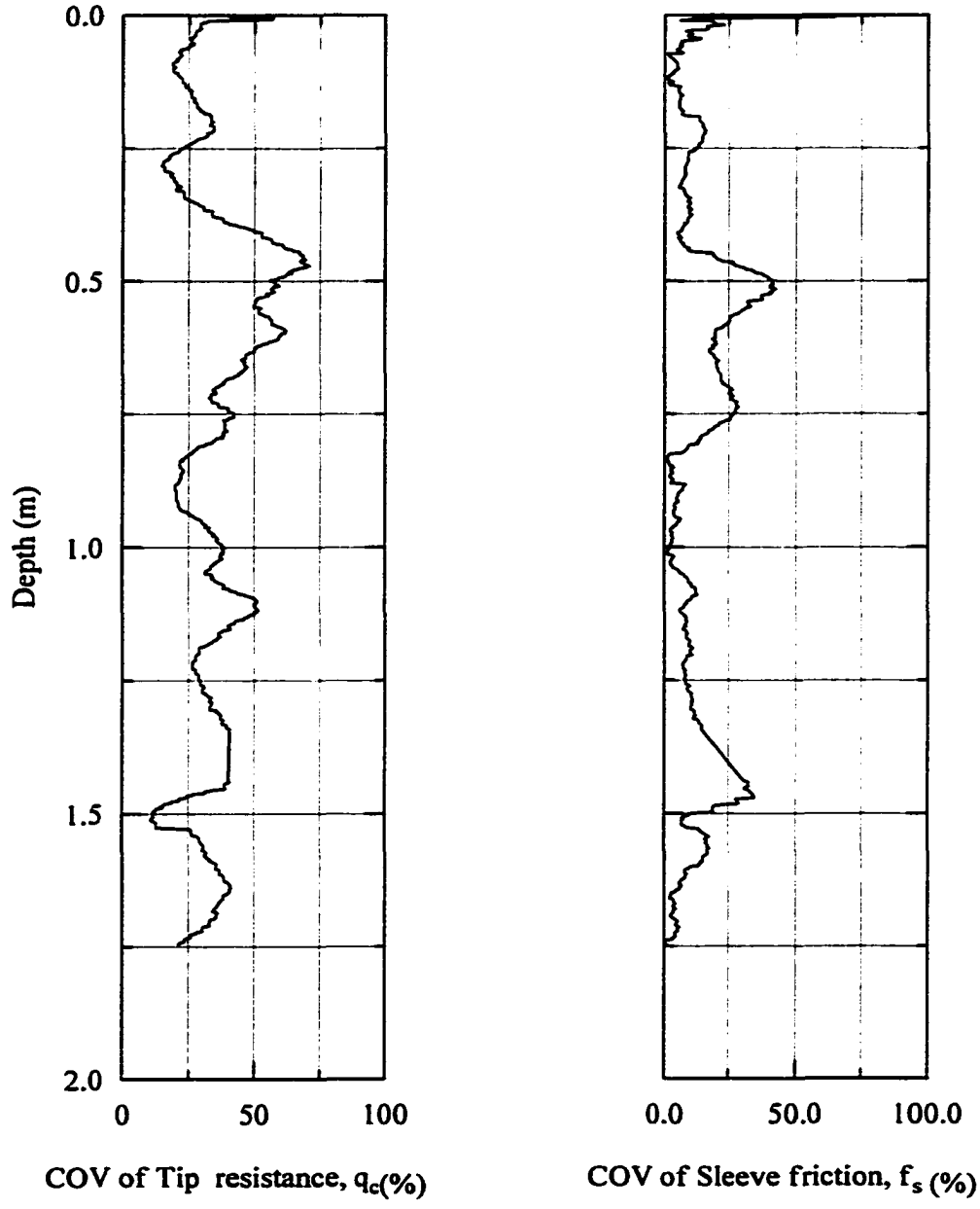

Figure 4.6 Coefficient of variation of CIMCPT for the cone test of the PRF-heavy clay

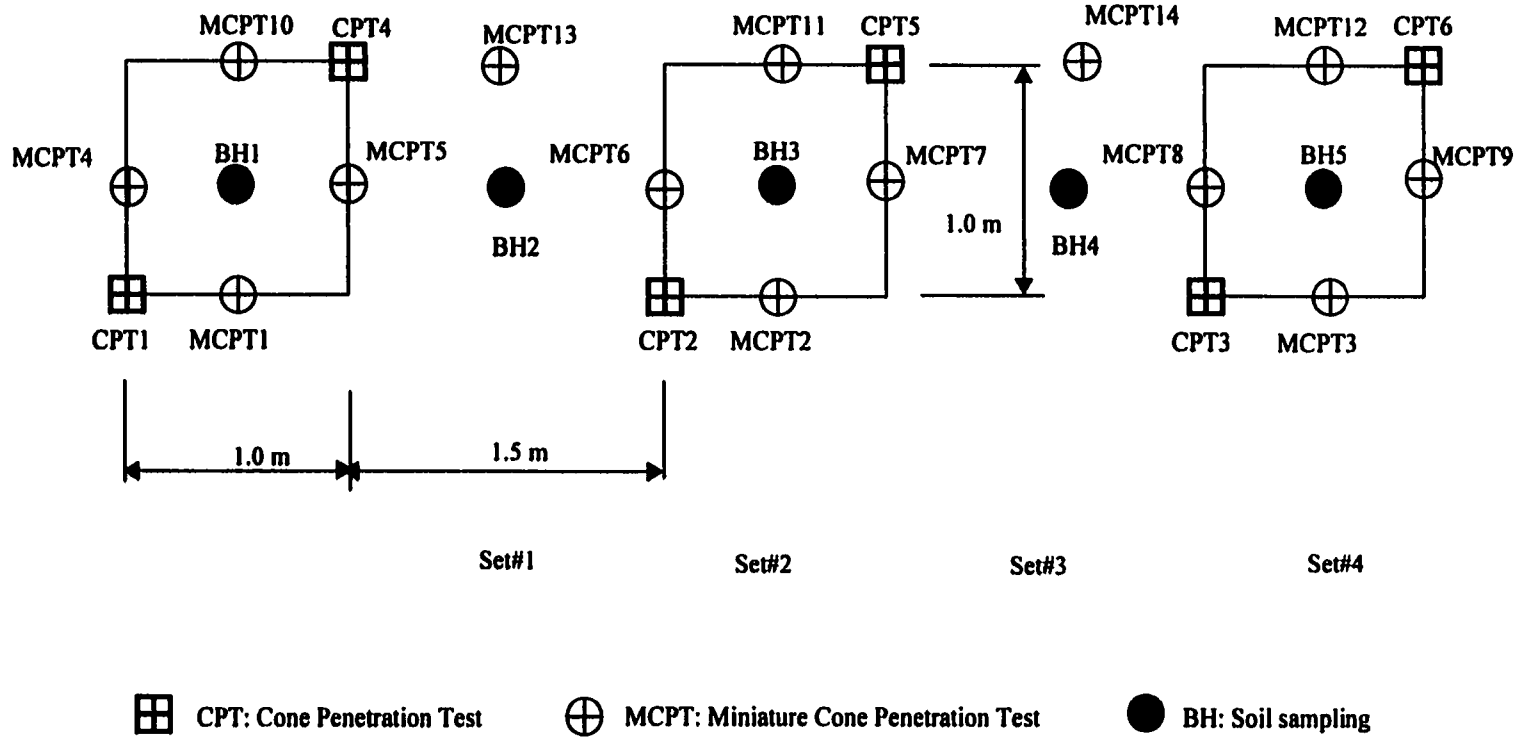

Figure 4.7 Field test layout for the LA-42/I-10 site

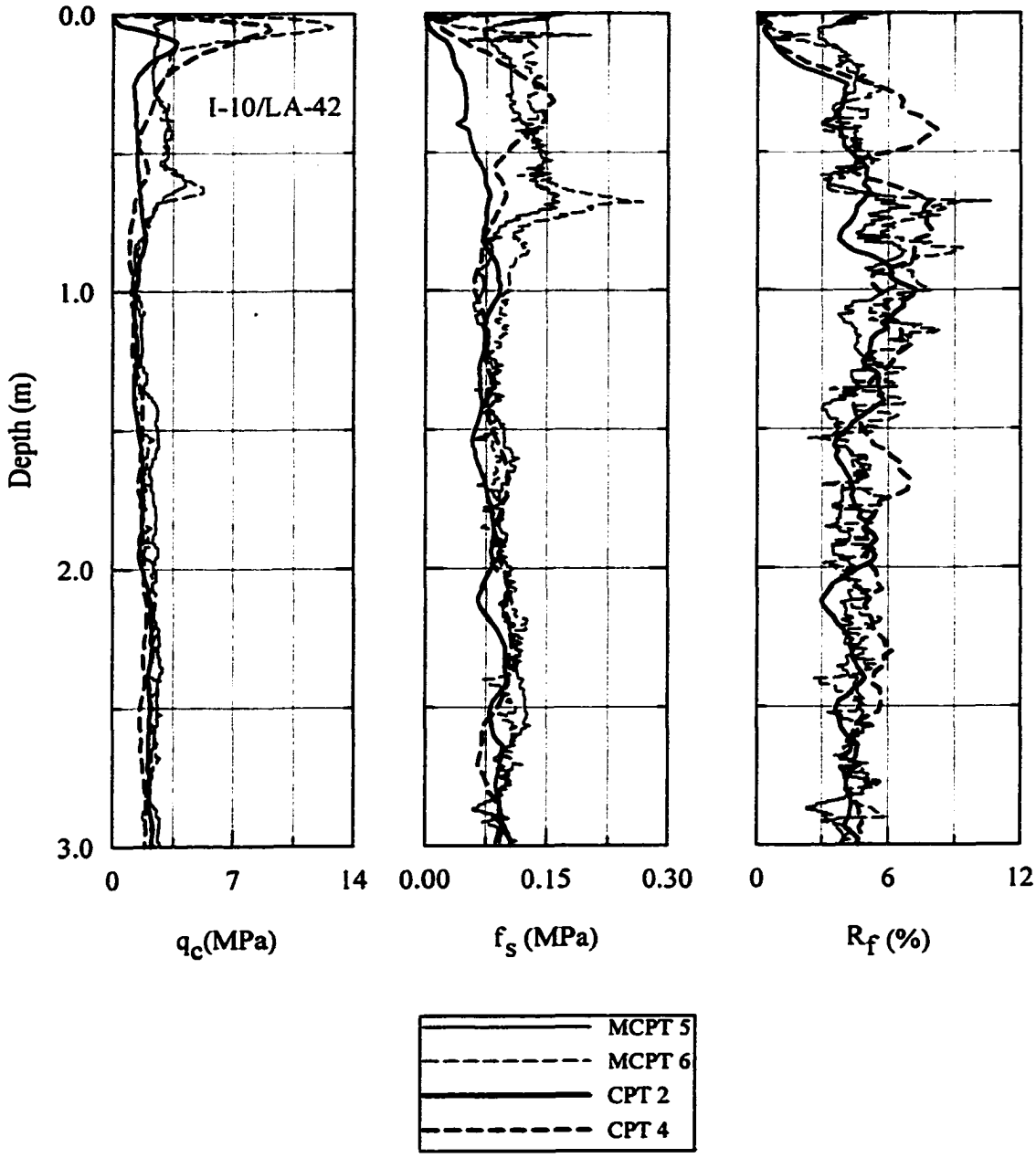

Figure 4.8 Cone penetration test results of the LA-42/I-10 site (set #1)

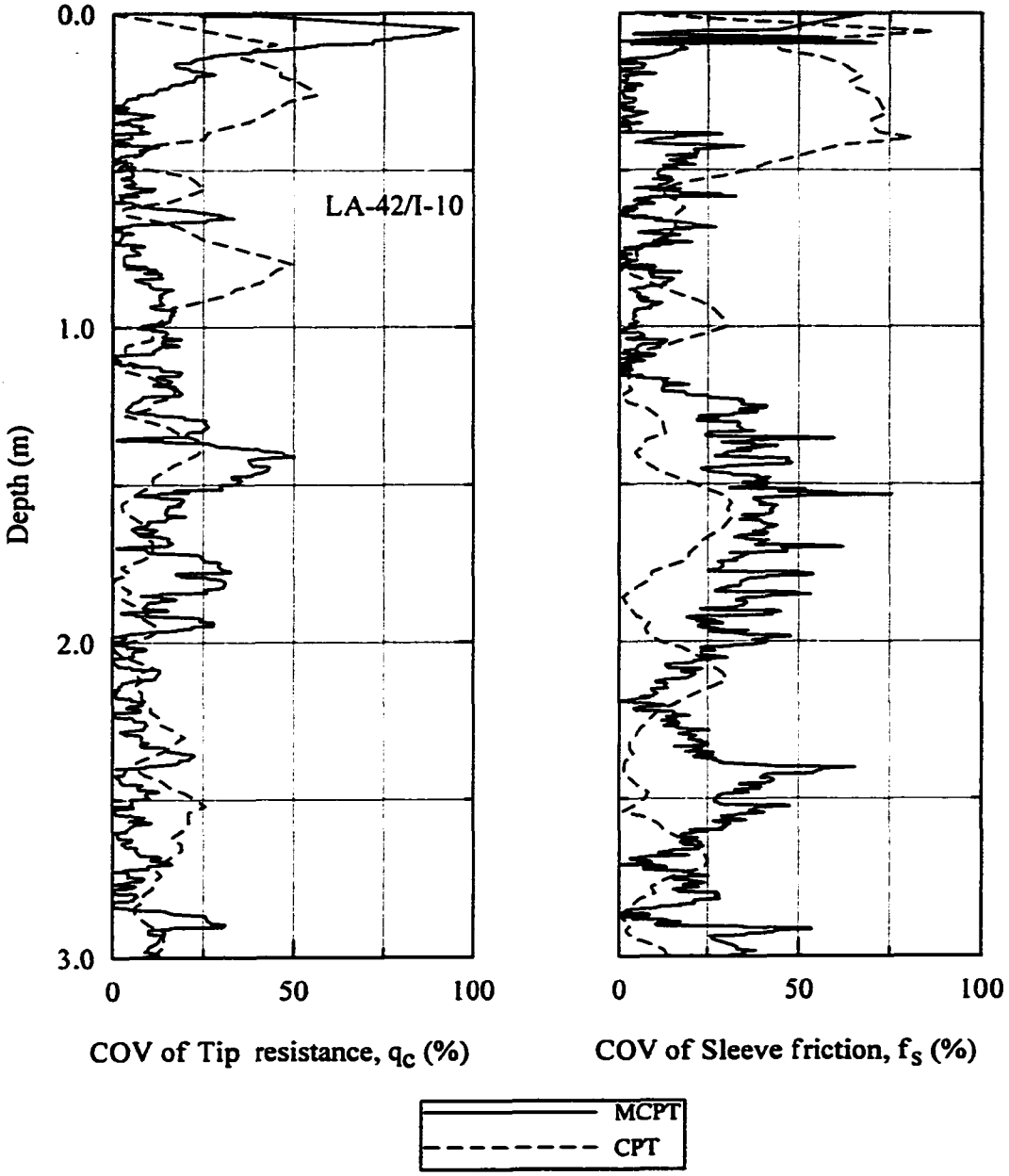

Legend: q_c - Tip resistance, f_s - Sleeve friction, R_f - Friction ratio

Figure 4.9 Coefficient of variation for the cone test of the LA-42/I-10 site

coefficient of variation for the CIMCPT sounding is slightly higher than that of the CPT results, particularly at the top layer (Tumay et al., 1997).

Figure 4.10 presents the field testing layout for the LA-15 site. Figure 4.11 depicts the cone penetration test results. The CPT and CIMCPT soundings reflect the similar patterns. Due to the scale effects, the tip resistance of the miniature cone penetration is slightly higher than that of the CPT (Tumay et al., 1997). The coefficient of variation of the test results is depicted in Figure 4.12. The coefficient of variation profiles of both CPT and CIMCPT follow the same pattern. But the coefficient of variation of the CIMCPT is slightly greater than that of the CPT. This is attributed to the high sensitivity of the miniature cone penetrometer (Tumay et al., 1997).

Figure 4.13 presents the field testing layout for the LA-89 site. Figure 4.14 depicts the cone penetration test results. The cone penetration results indicate the natural soil under the subgrade is a soft material as its tip resistance is very low. The CPT and CIMCPT soundings reflect the similar pattern with different magnitudes. The coefficient of variation of the test results is depicted in Figure 4.15. In the top layer (0 to about 0.4 m) the coefficient of variation is high due to the high sensitivity of the miniature cone penetrometer. But the coefficient of variation of CIMCPT results is small in the bottom layers. The coefficient of variation profiles of both CPT and CIMCPT follow similar patterns up to top 2 m.

Figure 4.16 presents the field testing layout for the Siegen Lane site. Figure 4.17 depicts the cone penetration test results. The CPT and CIMCPT soundings reflect the similar patterns with different magnitudes. The coefficient of variation profiles of both CPT and CIMCPT follow similar patterns (Figure 4.18).

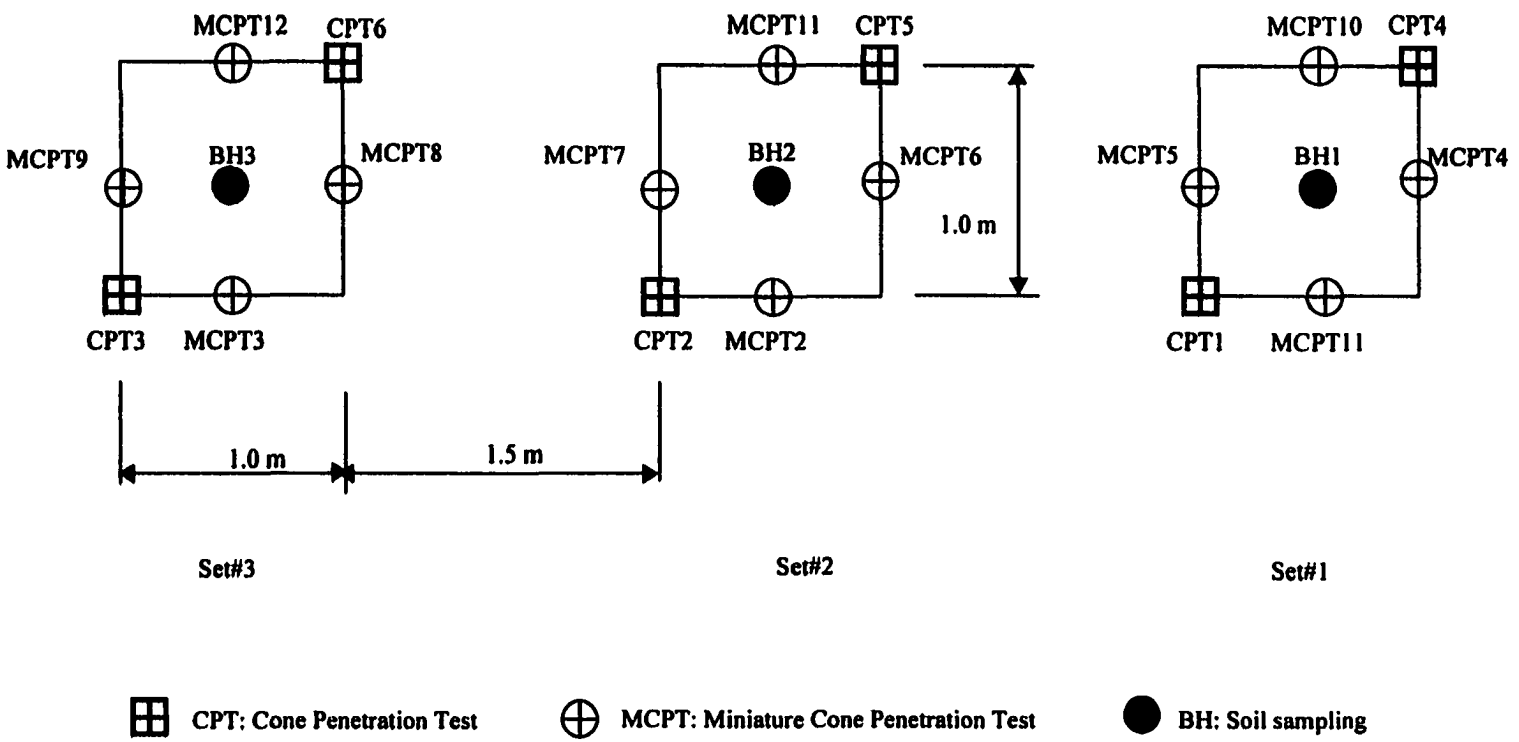

Figure 4.10 Field test layout for the LA-15 site

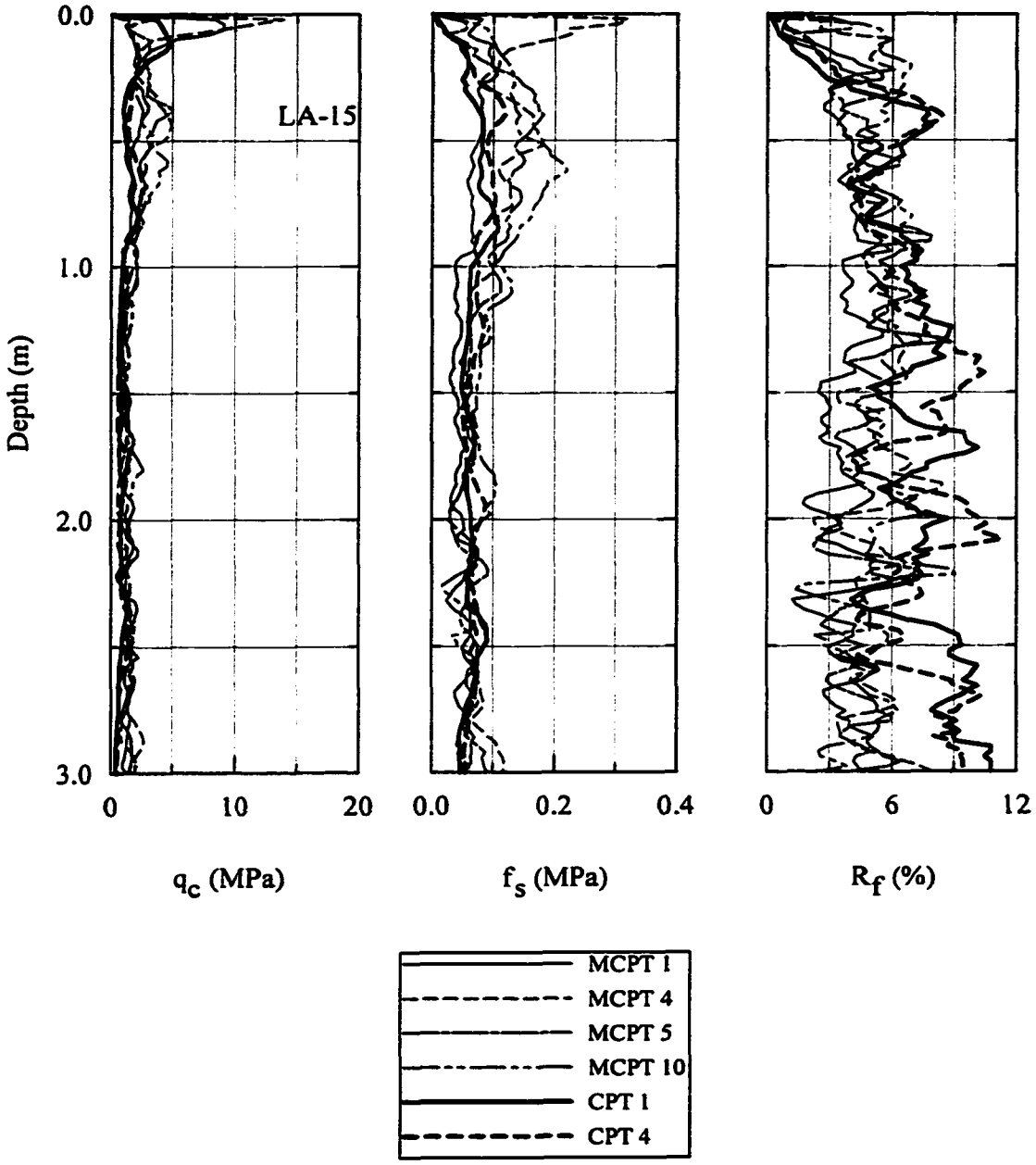

Figure 4.11 Cone penetration test results of the LA-15 site (set #1)

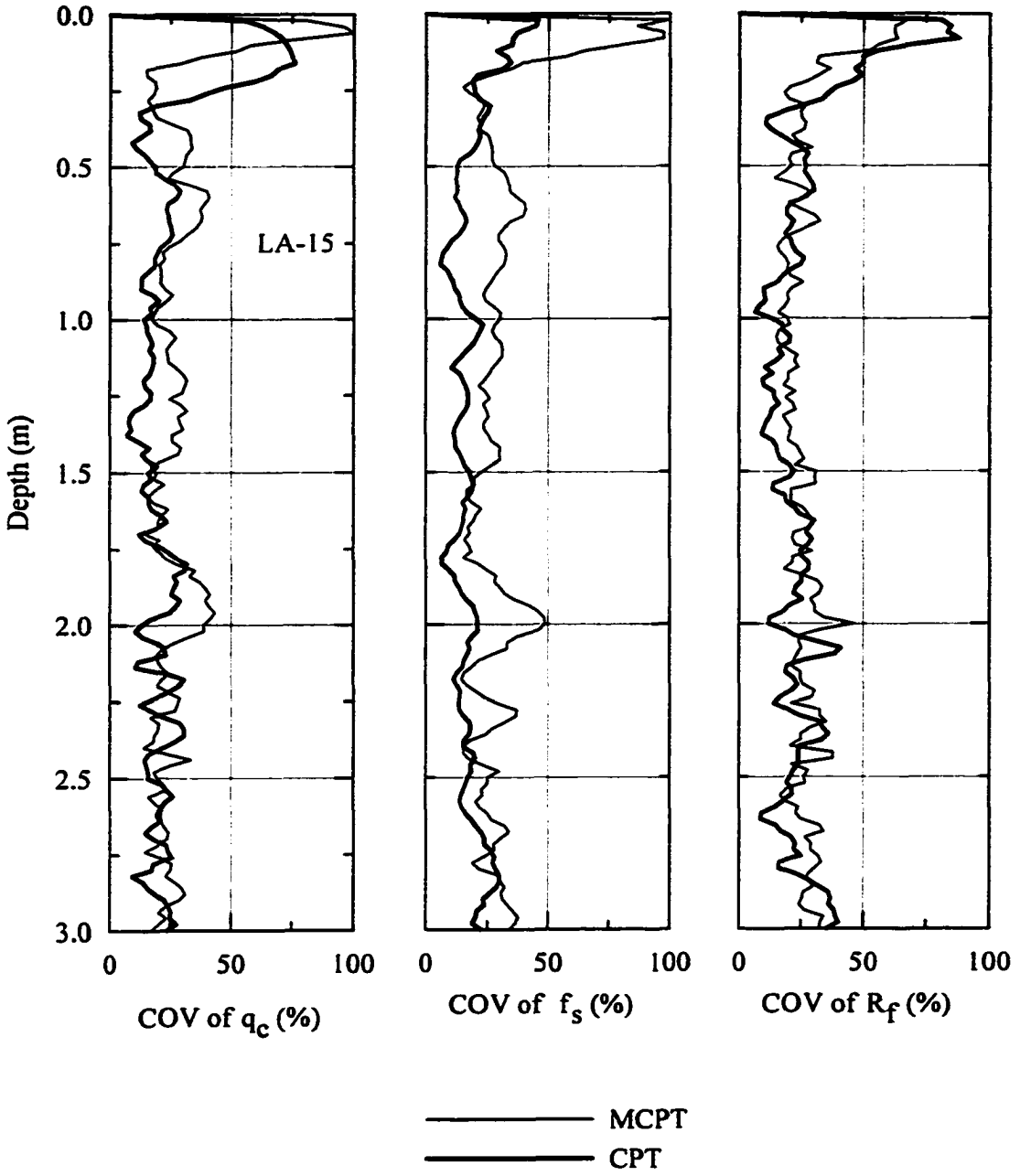

Figure 4.12 Coefficient of variation for the cone test of the LA-15 site

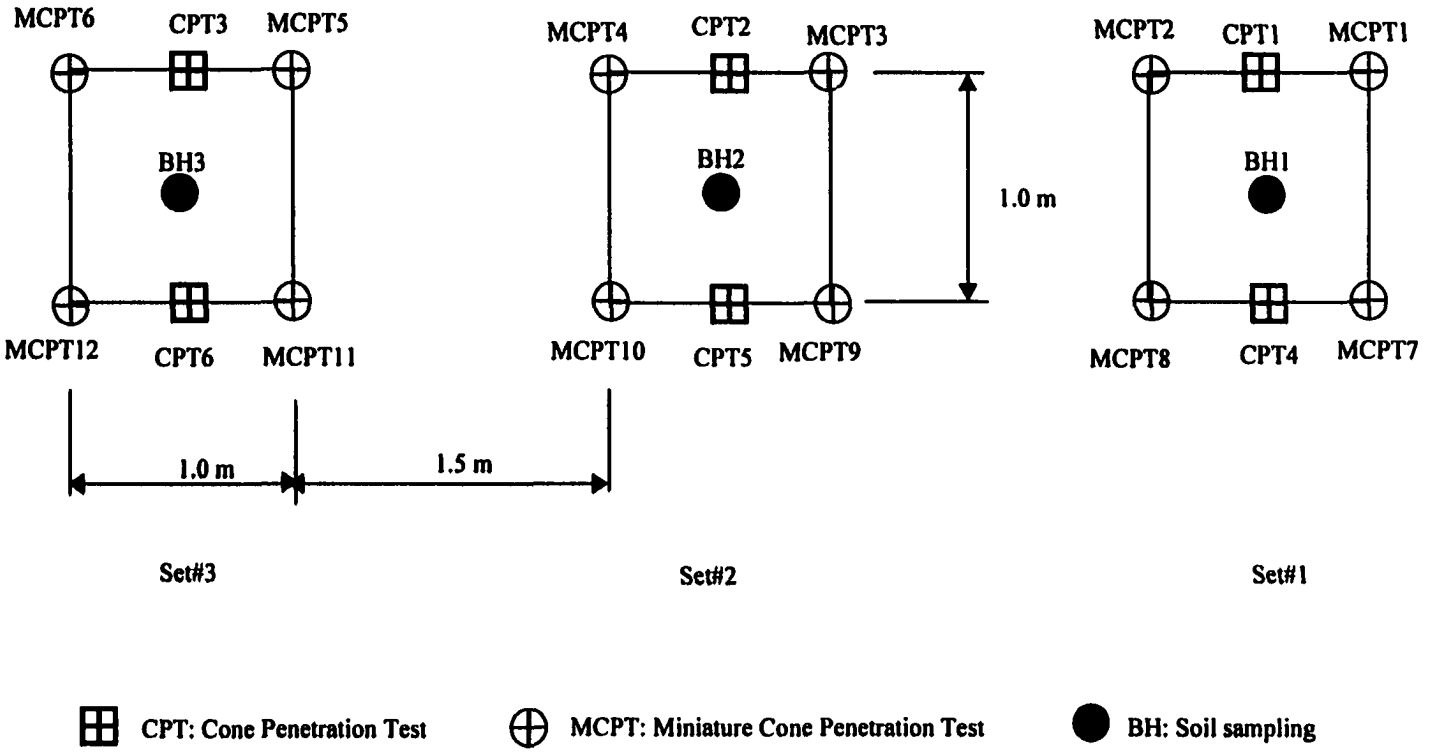

Figure 4.13 Field test layout for the LA-89 site

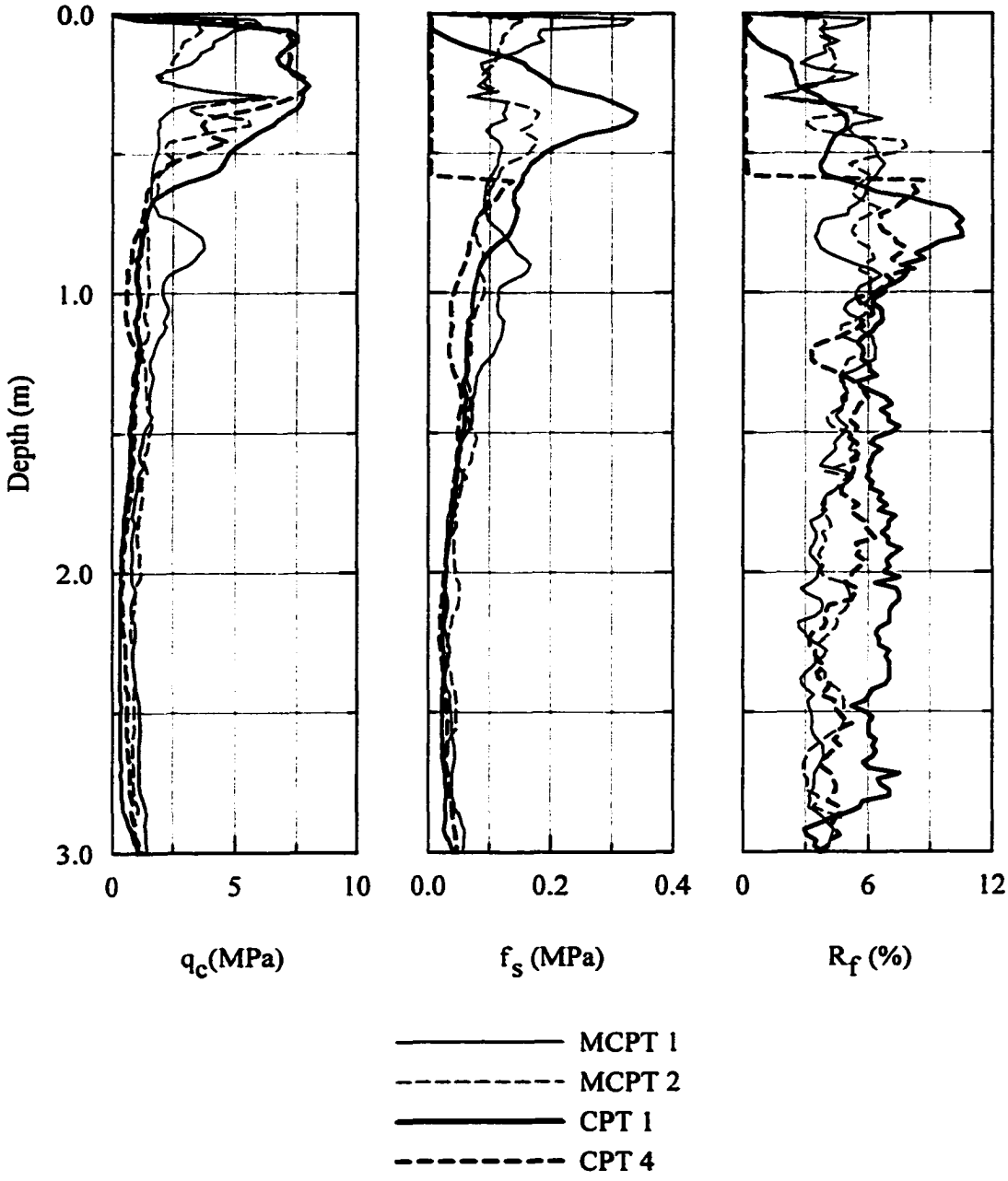

Legend: q_c - Tip resistance, f_s - Sleeve friction, R_f - Friction ratio

Figure 4.14 Cone penetration test results of the LA-89 site (set #1)

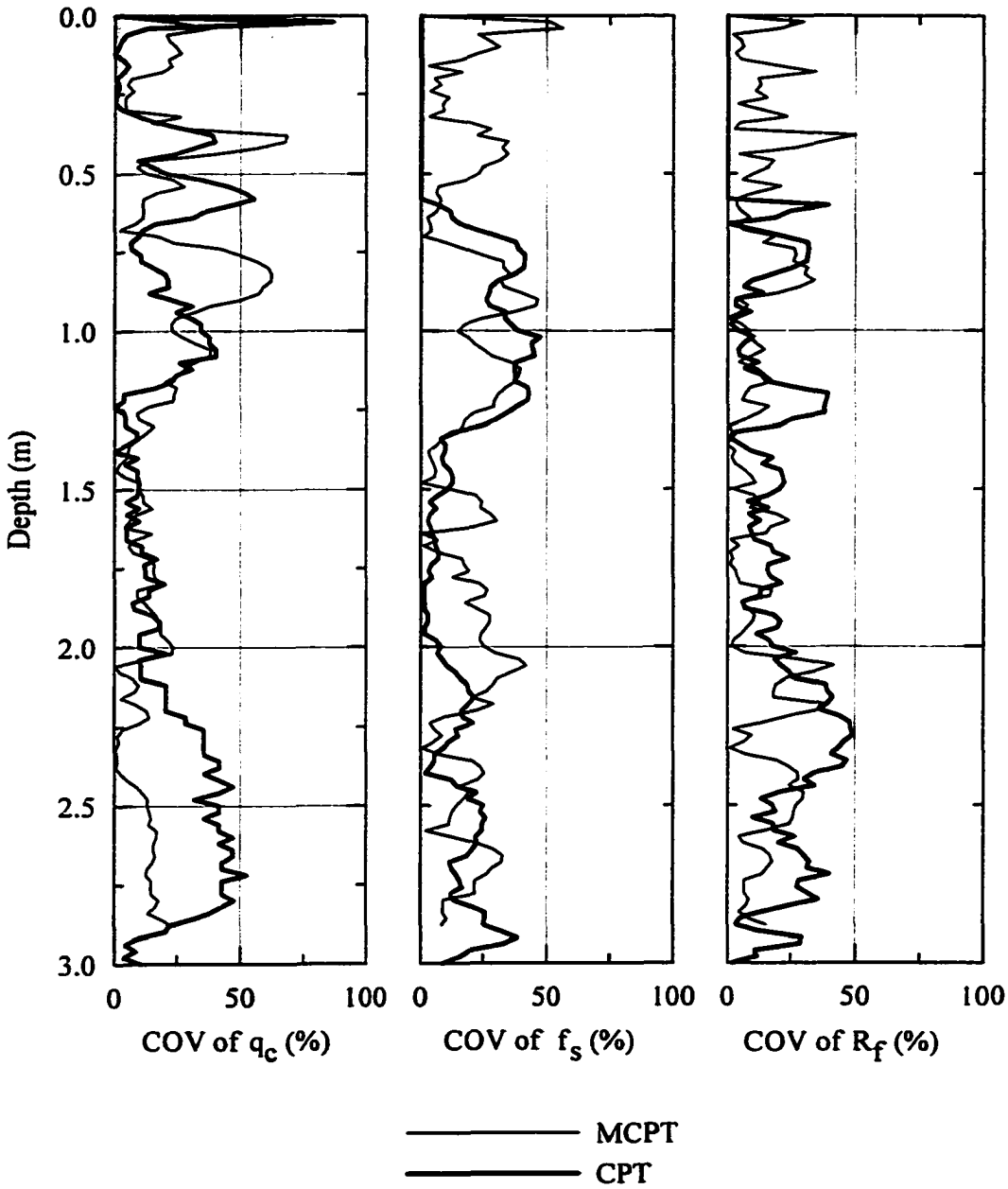

Legend: q_c - Tip resistance, f_s - Sleeve friction, R_f - Friction ratio

Figure 4.15 Coefficient of variation of CIMCPT for LA-89

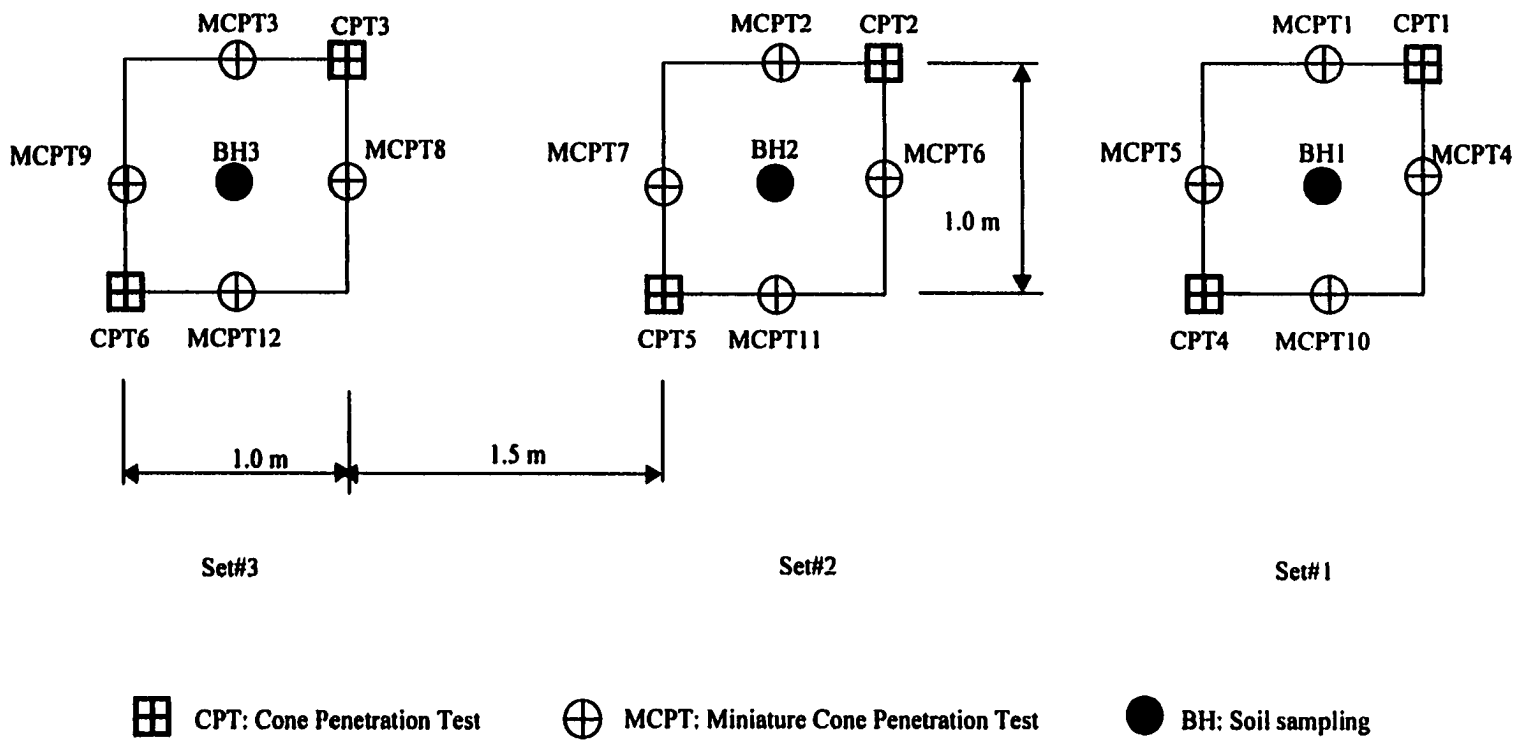

Figure 4.16 Field test layout for the Siegen Lane site

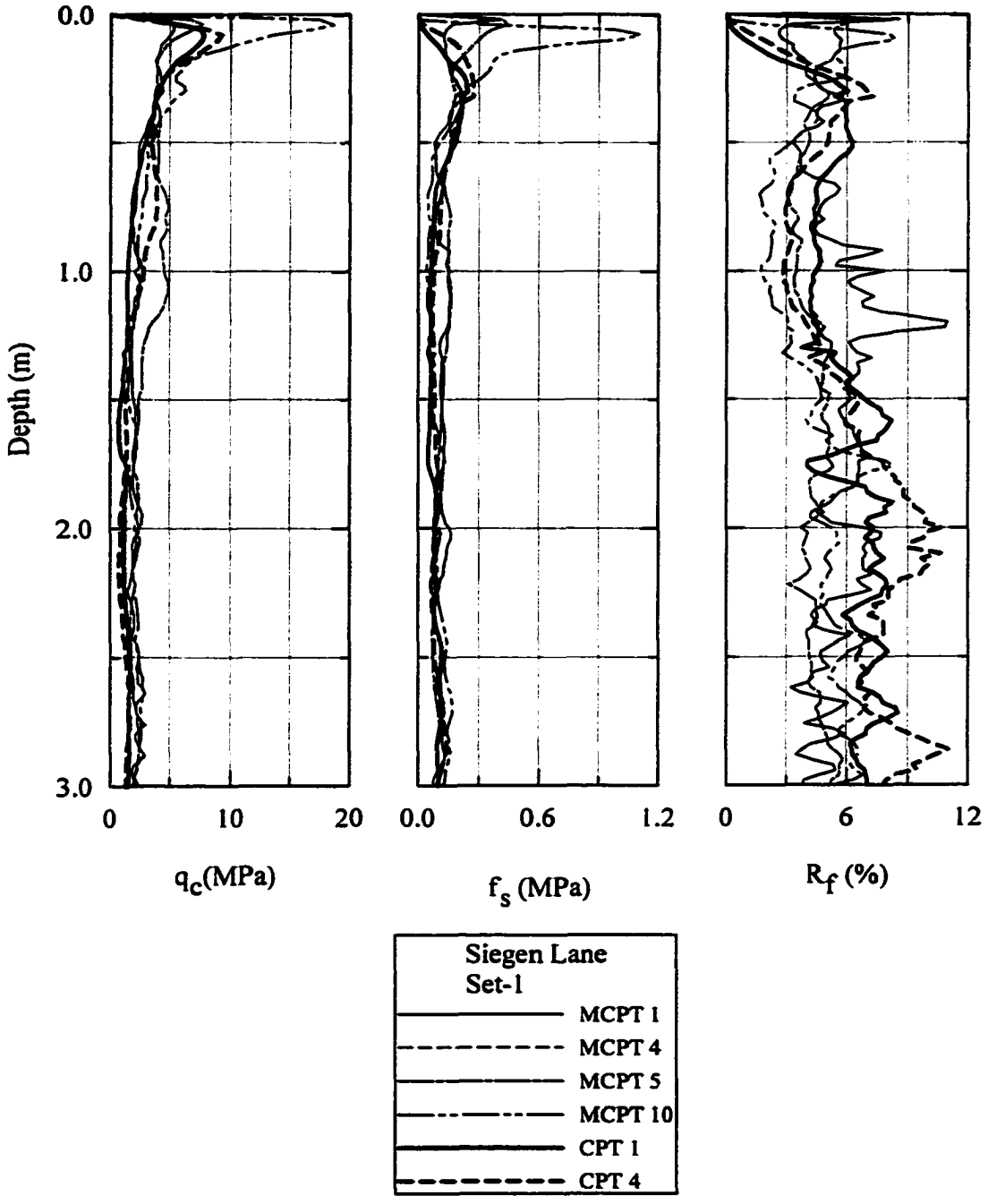

Figure 4.17 Cone penetration test results of the Siegen Lane site (set #1)

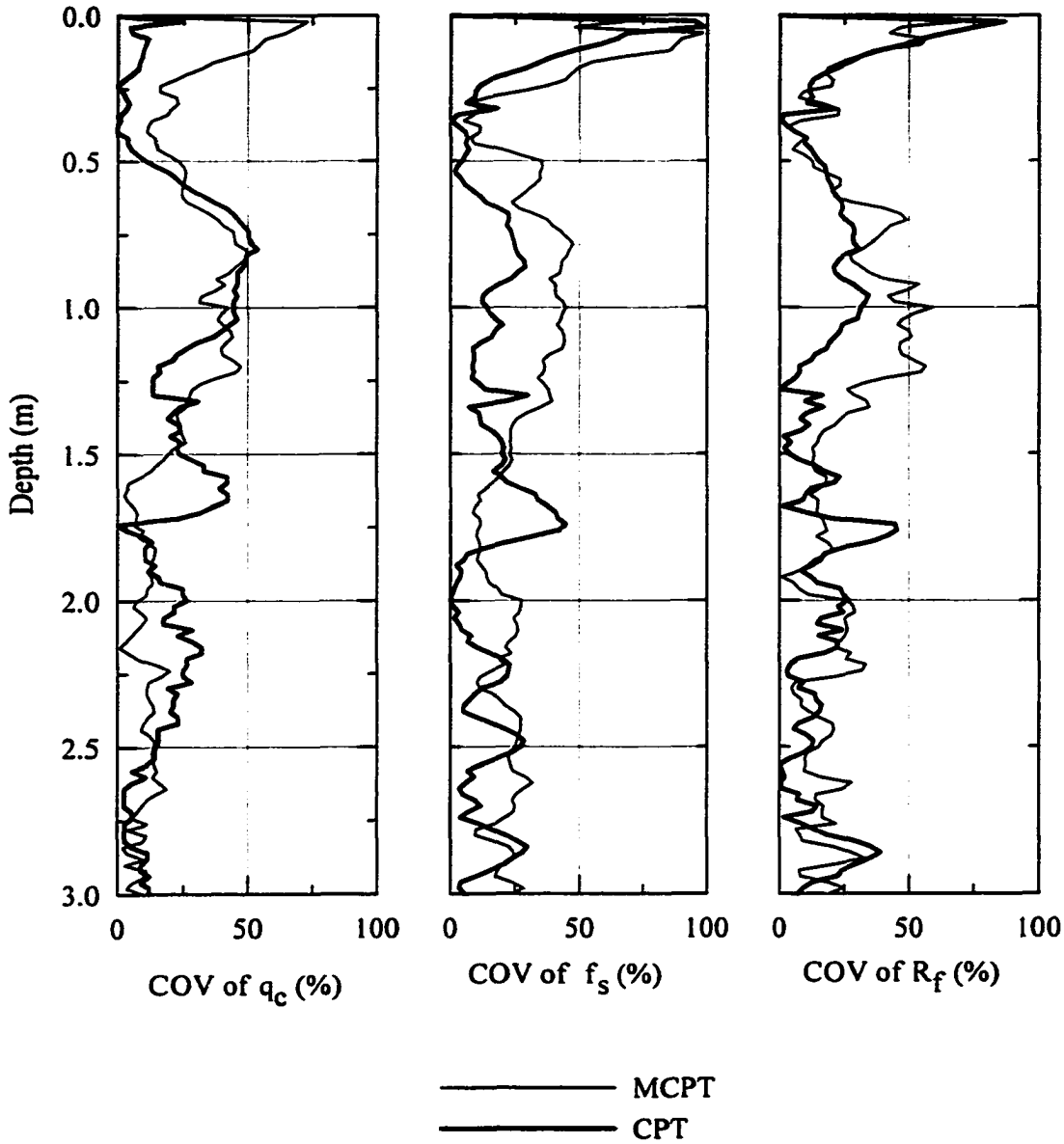

Legend: q_c - Tip resistance, f_s - Sleeve friction, R_f - Friction ratio

Figure 4.18 Coefficient of variation of the CIMCPT for Siegen Lane

Figure 4.19 presents the cone test results of the LA-28 site. The CPT and CIMCPT soundings reflect the similar patterns. As shown in Figure 4.19, coarse-grained soil, such as sand, exhibits higher cone tip resistance and low friction ratio than those of fine-grained soil, such as silty clay, as shown Figure 4.2. Fine-grained soil, such as clay, exhibits low cone tip resistance and high friction ratio. The coefficient of variation of the test results is depicted in Figure 4.20. The coefficient of variation of the CIMCPT follows the same pattern as that of CPT. But the values of coefficient of variation of the CIMCPT results are slightly higher than that of CPT. This is due to the fact that high sensitivity of the miniature cone penetration. The miniature cone penetrometer is capable of identifying small variation in a soil layer (Tumay et. al, 1997).

The soil at Larose site consists of dense fine sand. In such soil, sand particles will rearrange their orientation during penetration to let the state of compactness increase around the cone. The increase of the density of the sand, due to the penetration of the cone, results in an increase in the soil resistance to the cone penetration. Therefore, a larger thrust is needed to push the cone into the ground. At Larose site, the maximum allowable thrust to push the miniature cone was reached with very little advancement of the cone. Therefore, no CIMCPT were conducted at this site.

Comparison of the CPT data and CIMCPT data for most of the investigated sites has shown that the cone penetration test parameters and coefficient of variation of the CIMCPT results follow almost the same pattern as those of CPT. Even though, the values of the tip resistance and coefficient of variation of the CIMCPT results are slightly higher than those of CPT, these results imply the verification of the implementation of the CIMCPT results. This observation was also made by Tumay et al.,

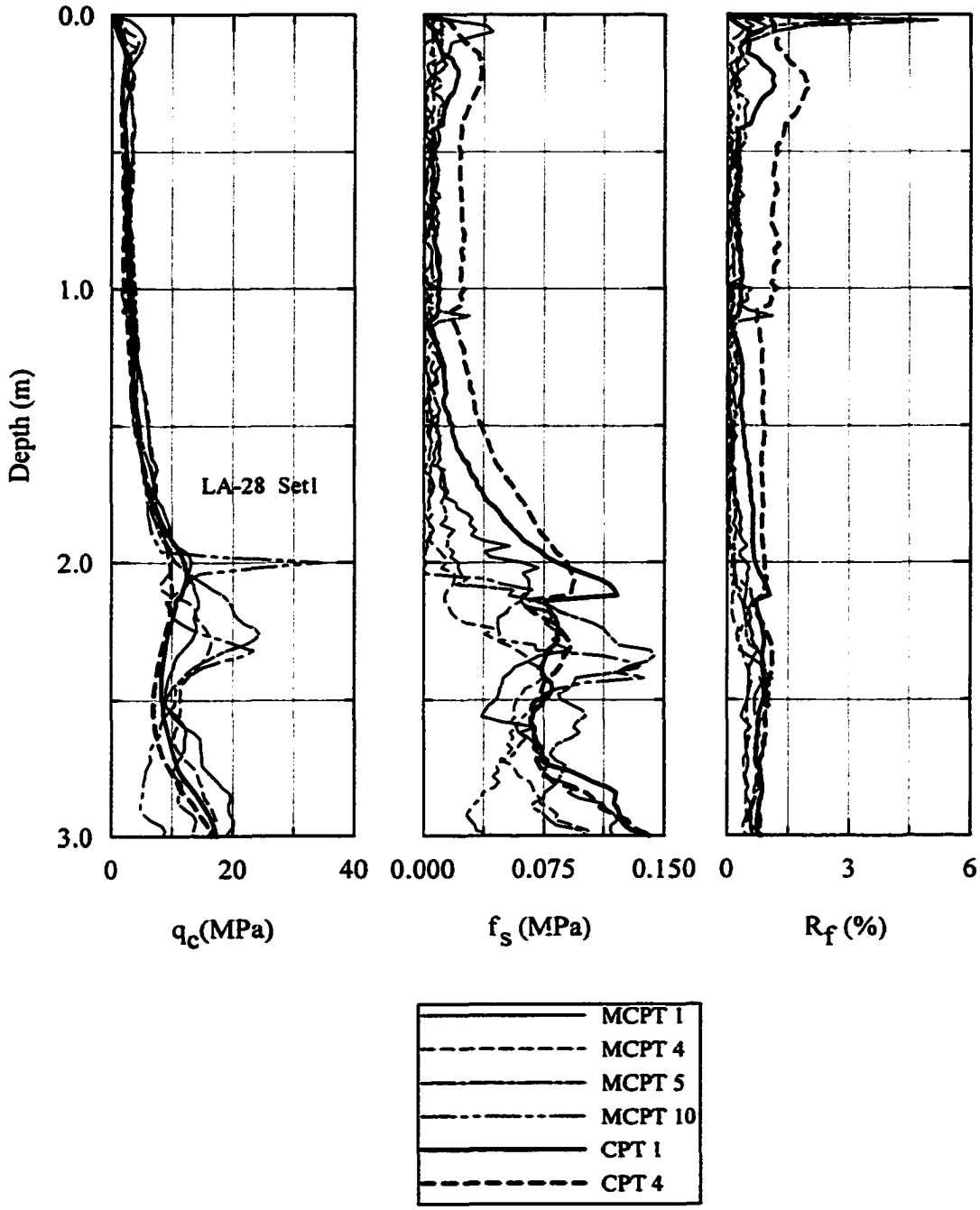

Figure 4.19 Cone penetration test results of the LA-28 site (set #1)

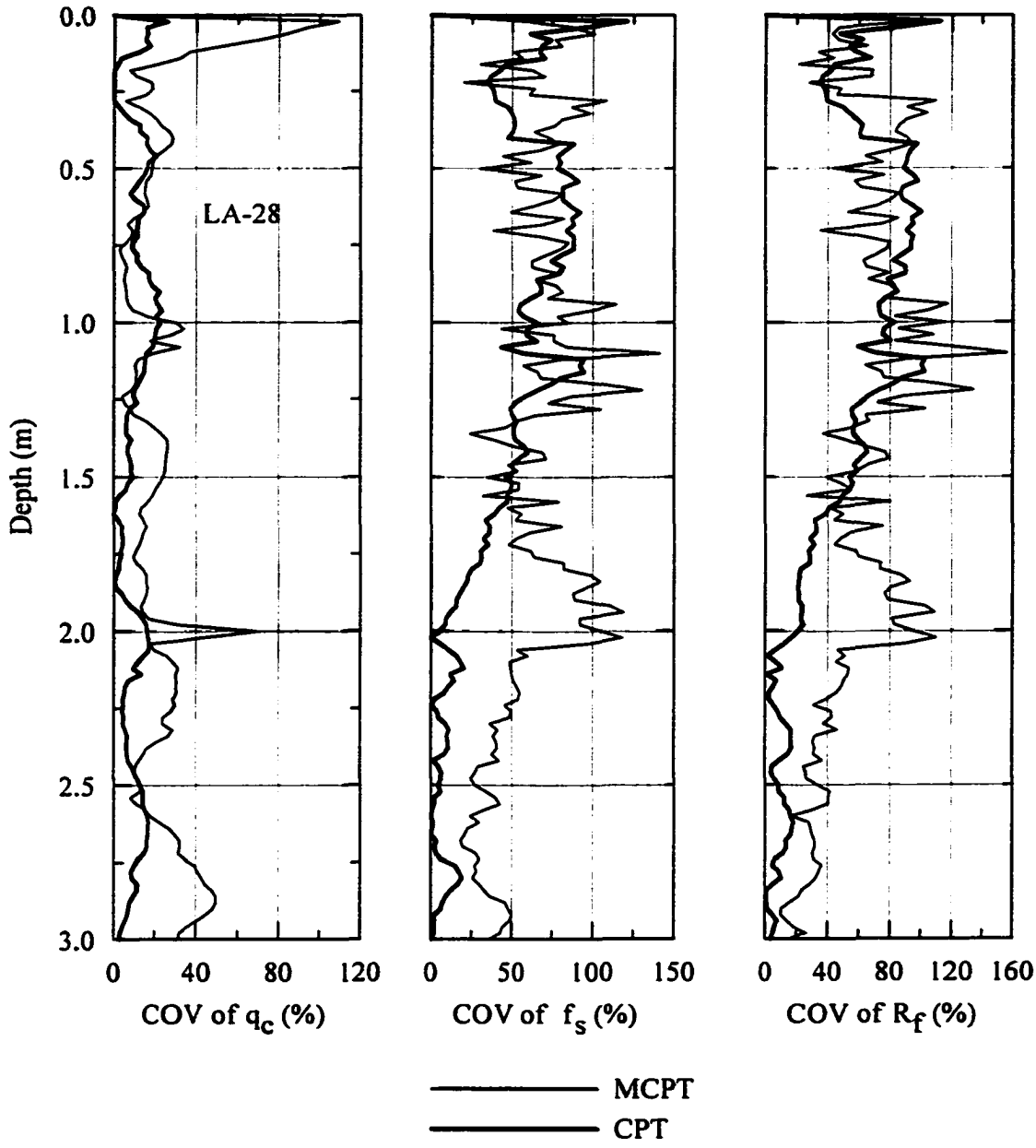

Figure 4.20 Coefficient of variation for LA-28 (Set#1)

(1997), Kurup and Tumay (1999), and Titi et al. (2000). Several conversion factors are available (Tumay et al., 1992; Tumay et al., 1997; Kurup et al., 1999; Mohammad et al., 2000; Titi et al., 2000) to convert the CIMCPT into the CPT test results. In general, for fine-grained soil, the tip resistance of the CIMCPT is about 11 percent greater than that of the 15 cm^2 cone and the sleeve friction of the CIMCPT is about 9 percent less than that of the 15 cm^2 cone (Titi et al., 2000).

4.3 Resilient Modulus Test Results

The resilient modulus test was performed with three confining stresses and five deviator stress levels for each confining stress. The test results of each confining stress were connected with a linear regression line. This line represents the measured resilient modulus at different deviator stress levels, expected in the pavements.

Figure 4.21 depicts the laboratory measured resilient modulus, obtained from the AASHTO T-294 test, for PRF-silty clay. As shown in Figure 4.21, the laboratory measured resilient modulus increases as the confining pressure increases, whereas it decreases as the deviator stress increases. This result indicates the stress dependency of the resilient modulus. This result is consistent with the previous studies (Fredlund et al., 1977; Ullidtz, 1987; Nataatmadja et al., 1989; Kamal et al., 1993; Mohammad et al., 1994; Mohammad et al., 1995; Puppala et al., 1996; Mohammad et al., 1998; Mohammad et al., 1999). The resilient modulus of the silty clay at depth of 0.8 m is lower than that at depth of 1.0 m. At 0.8 m, water content and dry unit weight of the silty clay are 25.4 percent and 15.9 kN/m^3, whereas at 1.0 m, those of the silty clay soil sample are 23.0 percent and 16.5 kN/m^3 respectively. At 1.0 m, water content of the silty clay soil sample is lower than that at 0.8 m. At 1.0 m, dry unit weight of the silty clay soil

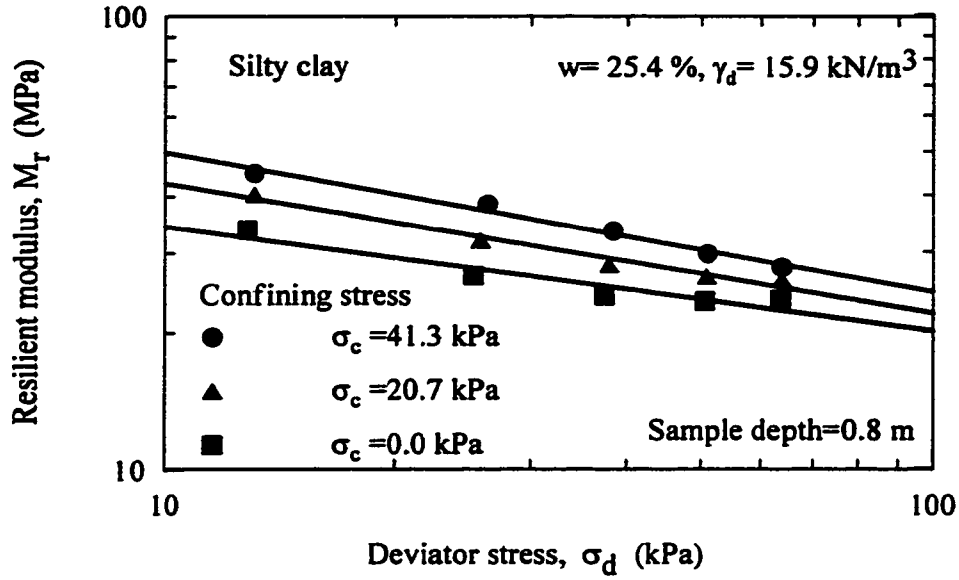

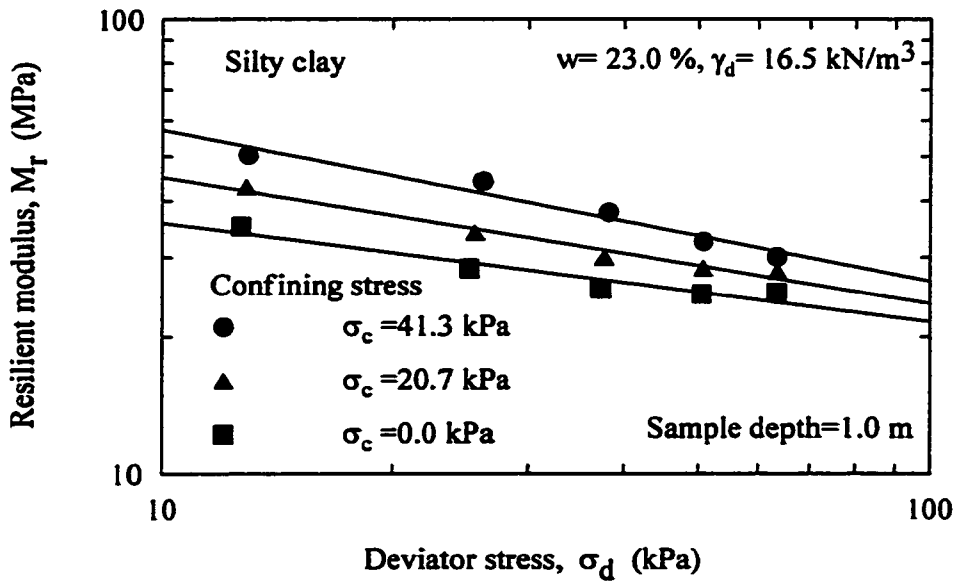

Figure 4.21 Resilient modulus of *PRF*-silty clay at borehole 1

sample is greater than that at 0.8 m. The lower the dry unit weight the lower the resilient modulus. The lower the moisture content the higher the resilient modulus. The effective deviator stress in clay decreases and hence the resilient modulus decreases as the dilational properties increases with the moisture content. These observations were also made by previous studies (Allen, 1989; McGee, 1989; Monismith, 1989; Mohammad et al., 1995; Drumm et al., 1997; Mohammad et al., 2000). This is the reason to exhibit higher resilient modulus values of the soil sample at 1.0 m depth of silty clay as compared to those at 0.8m.

Figure 4.22 shows the the resilient modulus values of the PRF-heavy clay. The resilient modulus of the PRF-heavy clay is lower than that of the PRF-silty clay. This is because the heavy clay is a softer material with a higher moisture content and a lower dry unit weight. The in-situ water contents of the silty clay soil samples vary from 21 to 25 percent, whereas those of the heavy clay soil samples vary from 59 to 65 percent. The dry unit weights of the silty clay soil samples are also greater than those of the heavy clay soil samples. The lower resilient modulus of the heavy clay is attributed to both of these reasons. Hence, it reflects a lower stiffness resulting a lower resilient modulus. As shown in Figure 4.22, the resilient modulus values of heavy clay at depth of 0.8 m are not significantly different from those at depth of 1.0 m. At 0.8 m, water content and dry unit weight of heavy clay are 61.6 percent and 9.9 kN/m^3 whereas, at 1.0 m, those are 65.1 percent and 9.9 kN/m^3 respectively. Since both the samples showed the same dry unit weight, a significant difference in the resilient modulus at these high moisture contents may not be exhibited. Confining pressure also showed a little effect on the resilient modulus of the heavy clay at these high moisture contents.

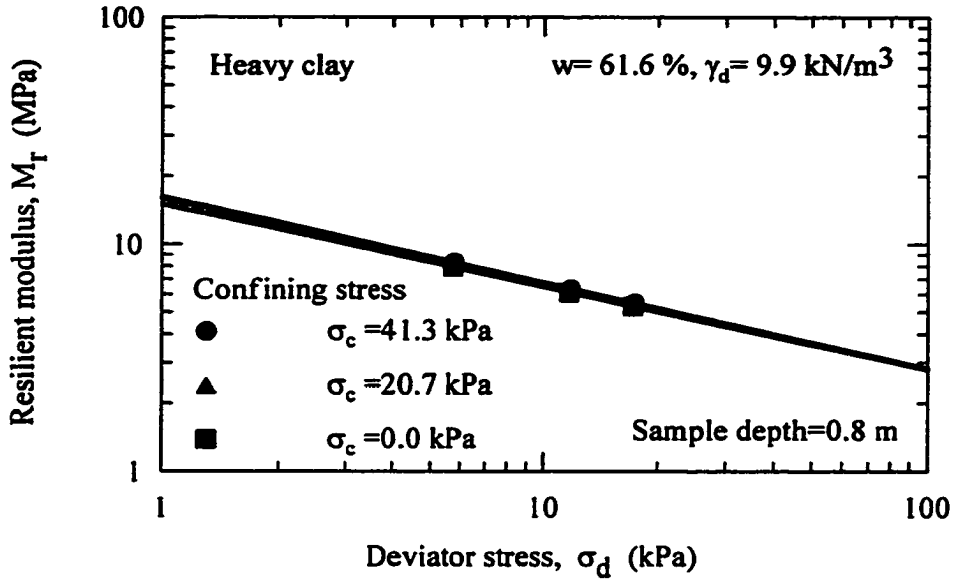

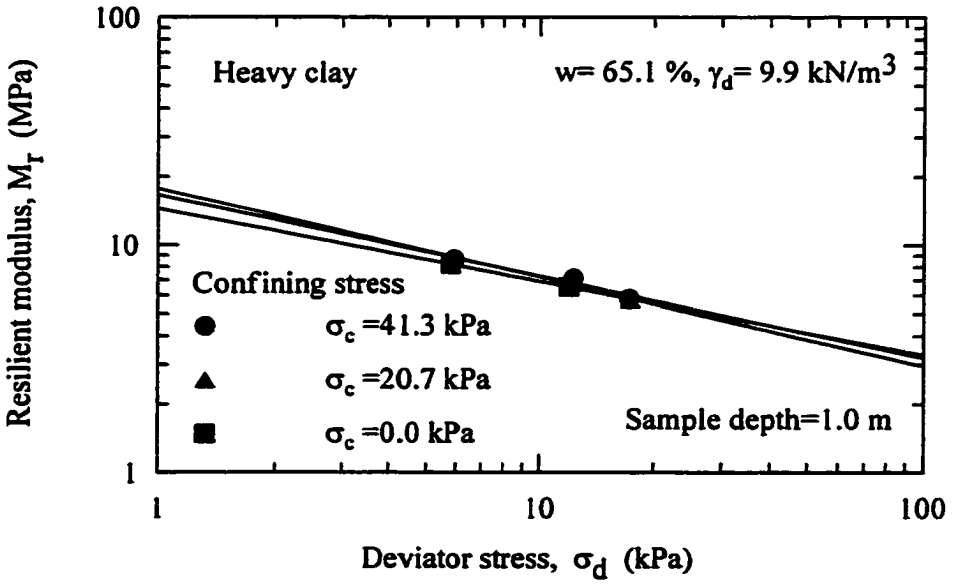

Figure 4.22 Resilient modulus of *PRF*-heavy clay at borehole 1

The resilient modulus of the LA-42/I-10 clay at depth of 0.8 m is higher than that at depth of 1.0 m (Figure 4.23). At 0.8 m, water content and dry unit weight of this clay are 19.6 percent and 17.2 kN/m^3, whereas at 1.0 m, those of this clay are 23.0 percent and 16.5 kN/m^3 respectively. At 1.0 m, water content of the LA-42/I-10 soil sample is higher than that at 0.8 m. At 1.0 m, dry unit weight of the LA-42/I-10 soil sample is lower than that at 0.8 m. As explained previously, the resilient modulus of the LA-42/I-10 clay at depth of 0.8 m is higher than that at depth of 1.0 m due to these higher unit weight and lower water content of the 0.8 m depth soil sample.

The resilient modulus of the LA-15 clay at depth of 0.8 m is higher than that at depth of 1.0 m (Figure 4.24). At 0.8 m, water content and dry unit weight of this clay are 24.1 percent and 17.3 kN/m^3 whereas, at 1.0 m, those are 23.0 percent and 16.2 kN/m^3 respectively. At 1.0 m, water content of the LA-15 soil sample is lower than that at 0.8 m by 1.1 percent. At 1.0 m, dry unit weight of the LA-15 soil sample is lower than that at 0.8 m. In this case, the higher resilient modulus at depth of 0.8 m is attributed to the higher unit weight at this depth. This result indicates that the effect of the dry unit weight is more significant than that of the water content on the resilient properties of soil.

Figure 4.25 shows the resilient modulus of the LA-89 clay. The resilient modulus of the top soil sample is higher than that of the bottom soil sample. The water content and dry unit weight of the top soil sample are 26.8 percent and 16.1 kN/m^3 respectively. In the bottom soil sample, the water content and dry unit weight are 28.6 percent and 15.9 kN/m^3 respectively. In the bottom soil sample, the water content is higher than that in the top soil sample. In the bottom soil sampie, the dry unit weight is lower than that in the top soil sample. Similar to previous explanation, the resilient modulus of the top soil

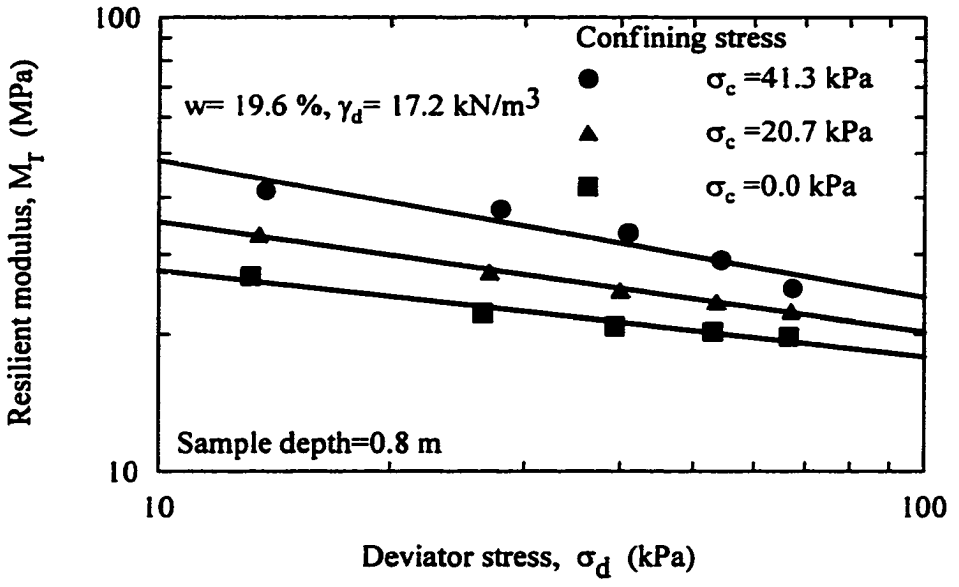

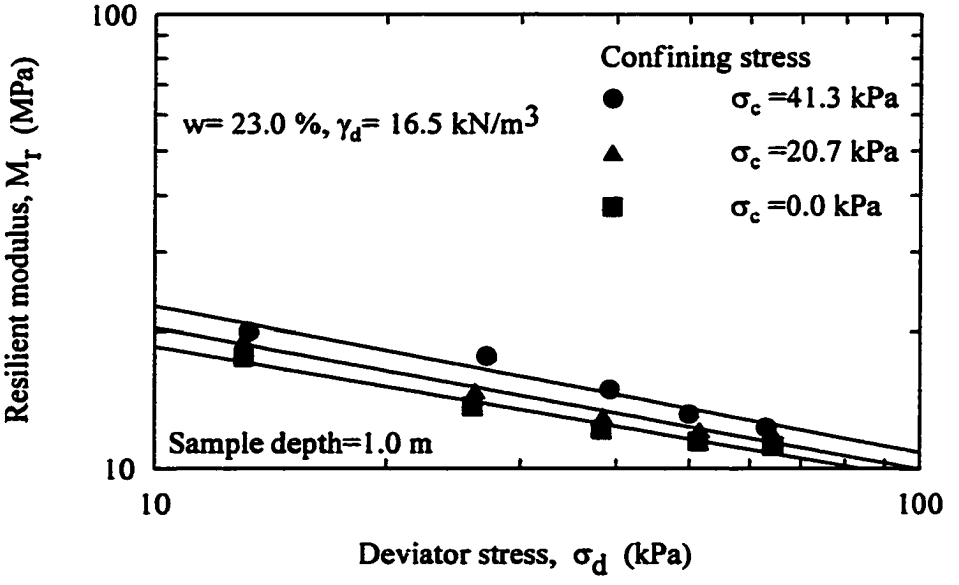

Figure 4.23 Resilient modulus of LA42/I-10 clay at borehole 2

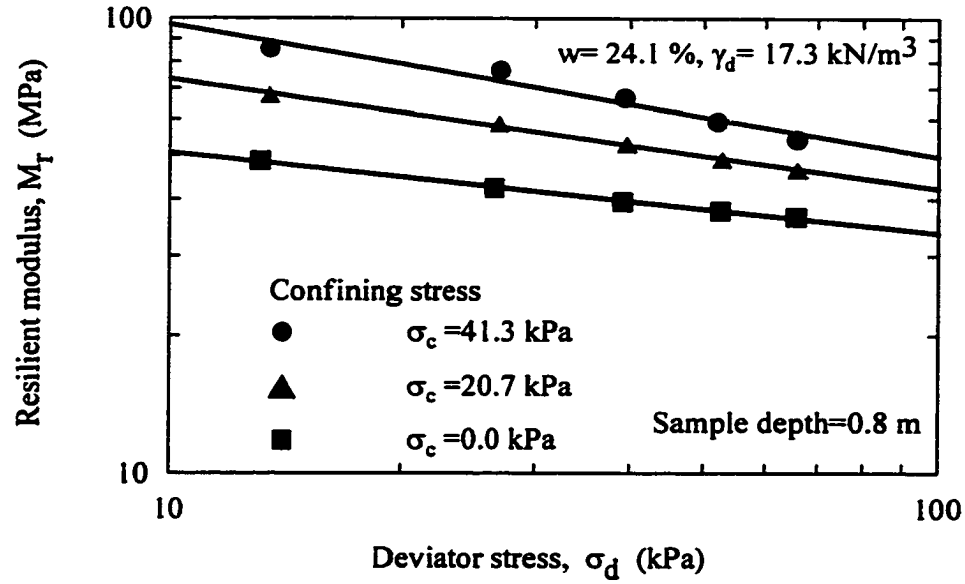

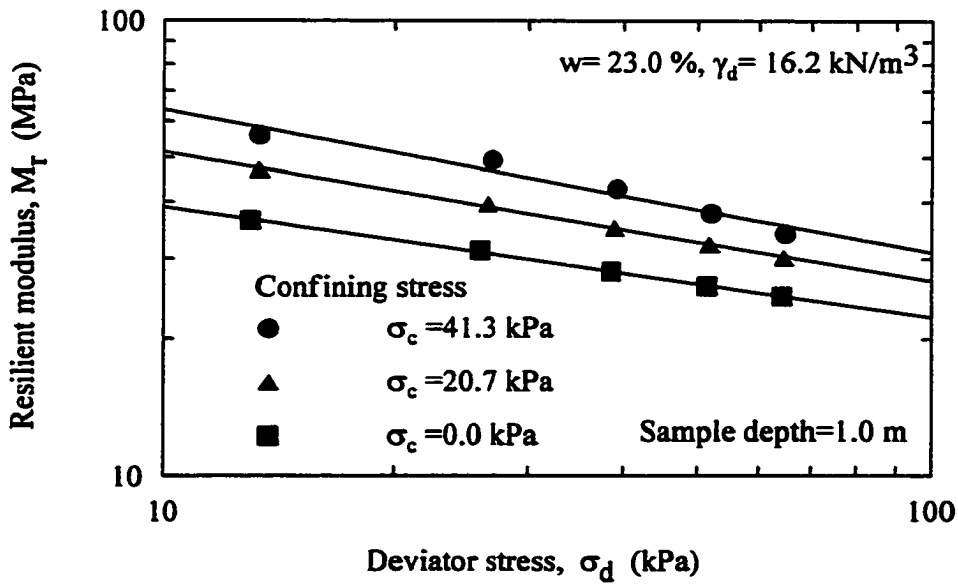

Figure 4.24 Resilient modulus of LA-15 clay at borehole 1

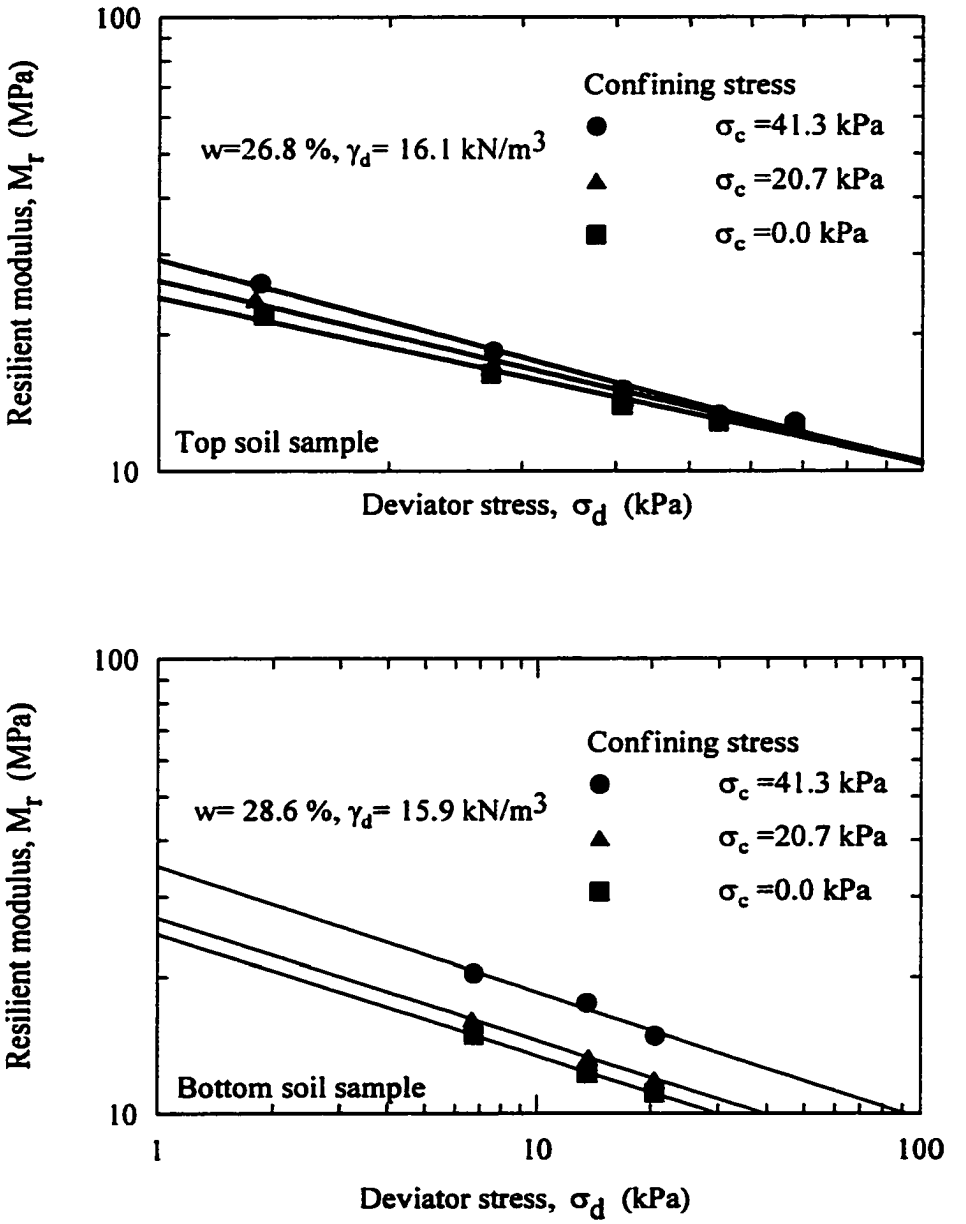

Figure 4.25 Resilient modulus of LA-89 clay at borehole 2

sample is higher than that in the bottom soil sample due to these higher unit weight and lower water content of top soil sample.

Figure 4.26 depicts the resilient modulus of the Siegen Lane clay. The resilient modulus of the top soil sample is higher than that of the bottom soil sample. In the top sample, water content and dry unit weight of this clay are 9.5 percent and 18.3 kN/m^3, whereas in the bottom sample, those are 22.5 percent and 17.1 kN/m^3 respectively. The water content of the bottom soil sample is higher than that of the top soil sample. In the bottom soil sample, dry unit weight of the soil sample is lower than that in the top soil sample. Similar to previous explanation, the resilient modulus of the top soil sample is higher than that of the bottom soil sample due to these higher unit weight and lower water content of it. The top layer (0 to about 0.5 m) of the Siegen Lane site consists a stiff, desiccated deposit. The water content of this top layer is 9.5 percent with respect to the optimum water content of 17.5 percent. As shown in Figure 43, the resilient properties of this soil at low confining stresses exhibited a little deviation from the behavior of fine-grained soils due to the dry and desiccated nature of the top soil layer.

As shown in Figure 4.27, for coarse-grained soil at LA-28 site, the resilient modulus increases with the bulk stress and confining stress. This is also a typical behavior of sands. This result is also consistent with the previous studies (Rada et al., 1981; Mohammad et al., 1994; Mohammad et al., 1998; Mohammad et al., 1999). As the bulk stress increases stiffness of coarse-grained soil increases. As the confining stress increases dilational properties decreases. Appendix A presents the resilient modulus test results. A laboratory resilient modulus test on the field soil samples covers a range of possible confining and deviator stress levels which are expected under various

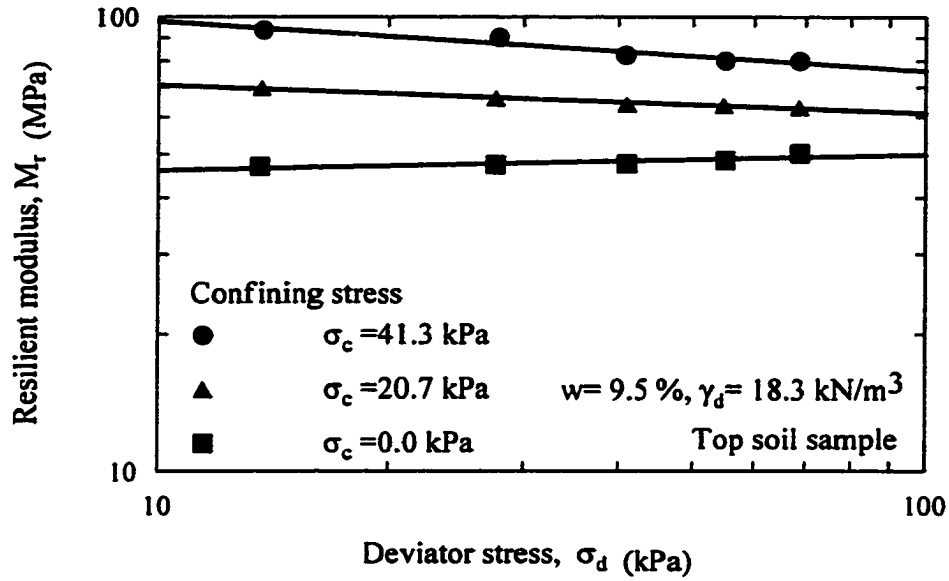

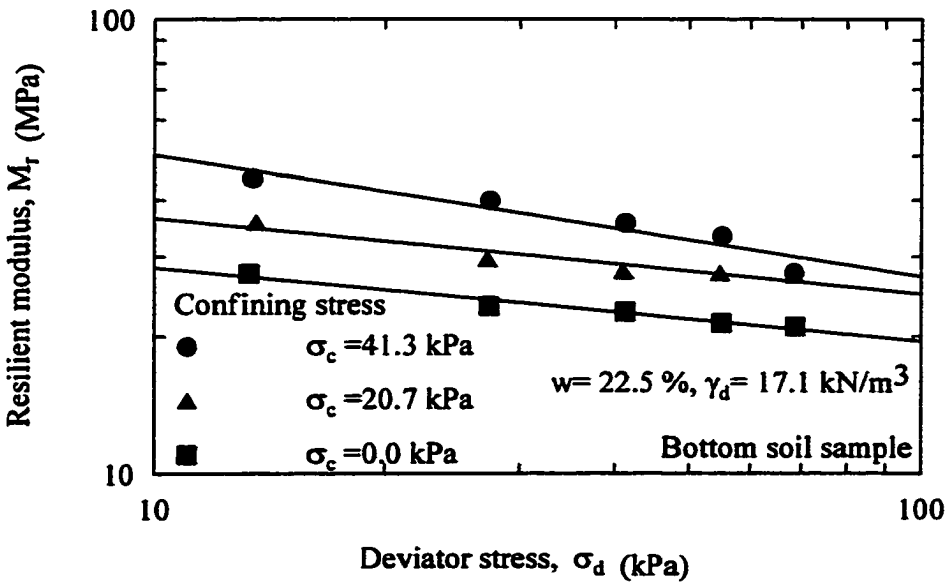

Figure 4.26 Resilient modulus of Siegen Lane clay

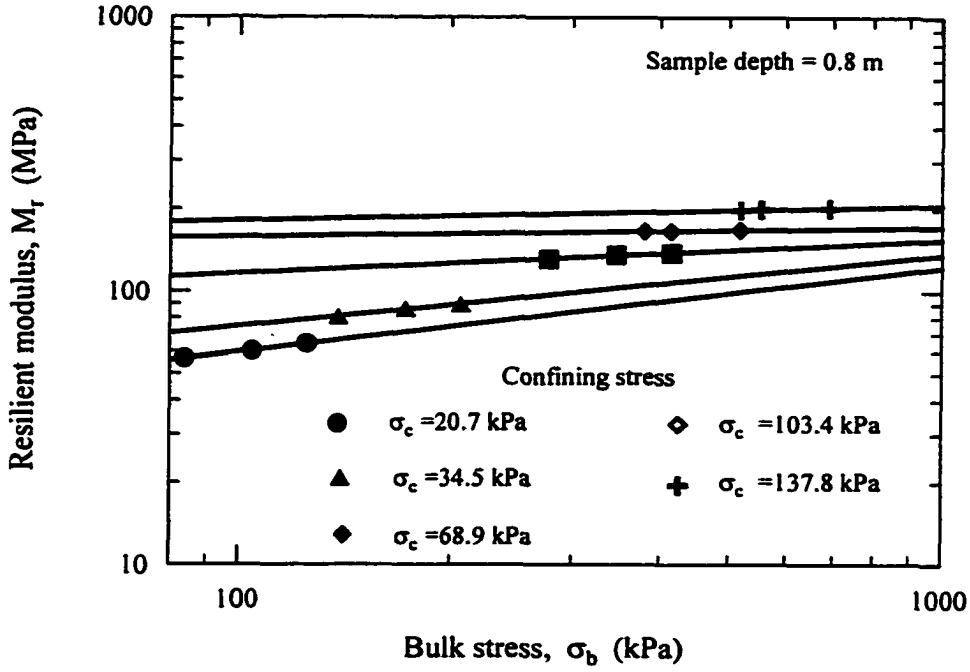

Figure 4.27 Resilient modulus of LA-28 sand

in-situ and traffic stress conditions. As explained in Figure 4.28, the depth of the soil sample retrieved from the field is used to estimate the in-situ stresses. Based on the in-situ stress levels, a corresponding resilient modulus, denoted as the field resilient modulus, can be interpolated from the laboratory resilient modulus test results. Figure 4.28 illustrates the interpolation procedure used in this study. Tables 4.3 and 4.4 contain the summary of the field and laboratory test parameters. The moduli of elasticity (E) were estimated from the laboratory repeated load triaxial testing. By averaging two or more in-situ resilient modulus values of a soil type in Table 4.4, the modulus of elasticity was estimated. The poisson's ratio (ν) was assumed. Table 4.5 contains the elastic properties of soils.

4.4 Model Development

In this portion of the study, an attempt was made to establish models to predict the resilient modulus from the cone penetration measurements. The cone penetration, resilient modulus, and soil property test results were used in the model development. The main variables, affecting the resilient modulus from the cone penetration parameters were identified. The main parameters considered in these models are the soil type, tip resistance, sleeve friction, resilient modulus, moisture content, dry unit weight, deviator stress, and confining stress. Since this study aimed to use the CIMCPT in subgrade soil characterization, its data was used in the model development. The CPT data is to be converted to the CIMCPT data before using the following models.

From Tables 4.3 and 4.4, test results of silty clay and heavy clay were selected for fine-grained soil models. Before the regression analysis, the variables were arranged to satisfy several physical conditions.

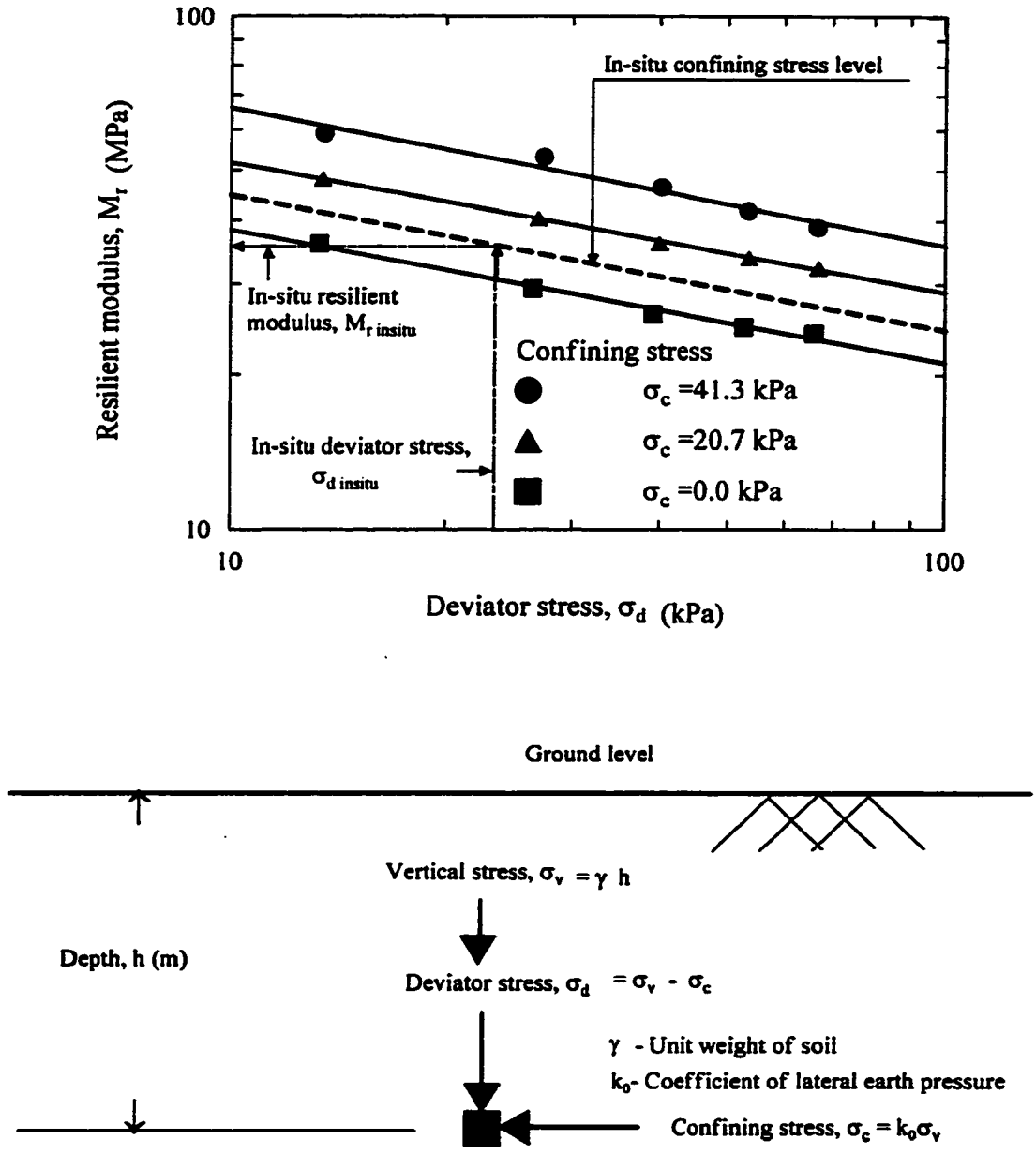

Figure 4.28 Interpolation procedure for resilient modulus

Table 4.3 Summary of field cone penetration and laboratory tests on soils

	Depth (m)	q_c (MPa)	f_s (MPa)	Water content(%)	Dry unit weight (kN/m³)
PRF-Silty clay					
BH1	0.8	2.50	0.0662	25.4	15.9
BH1	1	3.20	0.0714	23.0	16.5
BH2	0.8	2.69	0.0905	20.8	16.8
BH3	0.8	2.82	0.0733	23.2	16.9
BH3	1	3.15	0.0921	21.5	17.0
PRF-Heavy clay					
BH1	0.8	0.28	0.0185	61.6	9.9
BH1	1	0.31	0.0201	65.1	9.9
BH2	0.8	0.32	0.0229	60.4	10.2
BH2	1	0.40	0.0229	62.5	10.0
BH3	0.8	0.39	0.0185	59.0	10.2
BH3	1	0.38	0.0178	59.5	10.3
I-10/LA-42 clay					
BH1	0.8	2.08	0.1040	21.5	16.9
BH2	0.8	1.88	0.1122	19.6	17.2
BH2	1	1.13	0.0556	23.0	16.5
BH3	0.8	2.01	0.1194	21.4	16.3
BH4	0.8	1.82	0.0943	20.8	16.8
BH4	1	1.24	0.0623	22.5	16.4
LA-15 clay					
BH1	0.8	2.85	0.1509	24.1	17.3
BH1	1	2.08	0.1141	23.0	16.2
BH2	0.8	2.07	0.1233	28.4	16.8
BH2	1	2.14	0.0968	27.3	15.3
BH3	0.8	3.07	0.1345	18.8	17.8
BH3	1	2.05	0.1095	31.4	15.2
LA-89 clay					
BH1	0.6	1.74	0.0990	24.9	18.1
BH2	0.8	1.36	0.1076	26.8	16.1
BH2	1.6	0.50	0.0619	28.6	15.9
BH3	0.6	1.79	0.1043	24.6	17.1
Siegen Lane clay					
BH1	0.6	3.10	0.1241	9.5	18.3
BH1	1.2	1.32	0.1560	22.5	17.1
BH2	0.8	3.36	0.1134	16.7	17.1
BH2	1.2	3.66	0.1166	21.9	17.3
BH3	1.3	1.61	0.1050	23.1	15.4

Legend: q_c -Cone tip resistance, f_s -Cone sleeve friction, BH -Borehole

Table 4.4 Summary of the stress analysis on the investigated soils

	Depth (m)	In-situ			In-situ and traffic			Percent difference of M_r (%)
		σ_c (kPa)	σ_d (kPa)	M_{ri} (MPa)	σ_c (kPa)	σ_d (kPa)	M_{rt} (MPa)	
PRF-silty clay								
BH1	0.8	12.4	4.5	48.4	15.8	10.6	40.0	17.4
BH1	1	15.7	5.3	50.4	18.9	11.1	42.9	14.9
BH2	0.8	12.4	4.5	54.1	15.8	10.6	45.2	16.5
BH3	0.8	12.4	4.5	63.4	15.8	10.6	49.9	21.2
BH3	1	15.7	5.3	60.7	18.9	11.1	54.7	9.9
PRF-heavy clay								
BH1	0.8	11.9	1.3	14.3	17.1	5.7	8.2	42.7
BH1	1	14.9	1.6	14.6	20.0	5.7	8.9	39.0
BH2	0.8	11.9	1.3	24.7	17.1	5.7	12.6	48.9
BH2	1	14.9	1.6	26.2	20.0	5.7	18.2	30.5
BH3	0.8	11.9	1.3	24.8	17.1	5.7	13.4	45.9
BH3	1	14.9	1.6	24.5	20.0	5.7	17.3	29.4
I-10/LA-42 clay								
BH1	0.8	8.6	7.8	43.3	12.2	14.0	38.0	12.2
BH2	0.8	8.5	7.8	32.2	12.2	14.0	29.7	7.8
BH2	1	10.7	9.7	19.6	14.2	15.6	17.3	11.9
BH3	0.8	8.3	7.6	33.4	11.9	13.8	28.2	15.5
BH4	0.8	8.4	7.7	34.9	12.1	13.9	30.9	11.6
BH4	1	10.5	9.6	18.0	14.1	15.4	16.0	11.3
LA-15 clay								
BH1	0.8	13.0	4.1	77.4	18.1	9.4	70.9	8.4
BH1	1	15.1	4.8	58.3	20.2	9.5	51.8	11.1
BH2	0.8	13.1	4.1	52.8	18.2	9.4	54.5	-3.2
BH2	1	14.8	4.7	53.0	19.8	9.4	50.8	4.2
BH3	0.8	12.9	4.1	83.3	18.0	9.4	77.7	6.7
BH3	1	15.2	4.8	56.9	20.2	9.5	46.4	18.5
LA-89 clay								
BH1	0.6	9.1	3.7	45.6	13.9	9.5	43.3	5.0
BH2	0.8	11.6	4.8	36.1	16.5	9.9	26.7	25.9
BH2	1.6	23.2	9.5	14.9	27.8	13.5	13.7	8.1
BH3	0.6	9.1	3.7	53.8	13.9	9.5	36.8	31.6
Siegen Lane clay								
BH1	0.6	8.1	4.0	54.6	12.7	10.2	59.8	-9.5
BH1	1.2	16.8	8.3	35.9	21.2	13.0	35.1	2.2
BH2	0.8	10.7	5.3	61.1	15.3	10.8	71.9	-17.7
BH3	1.3	16.3	8.0	33.2	20.7	12.6	32.3	2.7

Legend: σ_c - Confining stress , σ_d - Deviator stress, M_{ri} - Resilient modulus under in-situ condition, M_{rt} - Resilient modulus under traffic condition, BH- Borehole, Percent difference of $M_r = (M_{ri}-M_{rt})100 / M_{ri}$

Table 4.5 Elastic properties of the investigated soil sites

Elastic Property	Field site						Assumed pavement	
	PRF- Silty clay	*PRF*- Heavy clay	*I-10/ LA-42* Clay	*LA-15* Clay	*LA-89* Silty clay loam	Siegen Lane Clay	Asphalt surface 89 mm (3.5")	Base 216 mm (8.5")
E (MPa)	49.4	21.5	30.2	63.6	37.6	41.2	4134.0	1034.0
ν	0.35	0.35	0.35	0.35	0.35	0.35	0.35	0.35

Legend: E- elastic modulus, ν - Possion's ratio

These physical conditions were based on the field and laboratory test results. The physical conditions for the models are given below.

1. The resilient modulus increases as the tip resistance, confining stress, and dry unit weight of soil increase.
2. The resilient modulus decreases as the moisture content increases.
3. The resilient modulus decreases as the deviator stress for fine-grained soil increases.
4. The resilient modulus increases as the bulk stress for coarse-grained soil increases.
5. The variables in the models are input as nondimensional form.

Appendix B presents the procedure for the model development. The ratio of the resilient modulus to confining stress, was computed for each data set and it was input in the linear regression model as the dependent variable. The all variables were arranged according to the required conditions as in the nondimensional forms. After several trials of regression analysis, a constant power term for the confining stress was estabiished as 0.55. The ratio of the resilient modulus to confining stress to the 0.55 power was input as the dependent variable in the model. In this way, the shape of the model was predefined before the regression analysis. Then a linear multiple regression analysis was performed by the Statistical Analysis System (SAS) program to develop models between the resilient modulus and the cone penetration data. Four models, two of them for the fine-grained soil in-situ and traffic conditions and the other two for the coarse-grained soil in-situ and traffic conditions, were developed.

4.4.1 Proposed Model for Fine-grained Soils (In-situ)

As described in the previous section, a linear multiple regression analysis was performed using the *SAS* program to develop the following model between the cone data

and the resilient modulus. This model was based on the test results of the silty clay and heavy clay.

$$\frac{M_r}{\sigma_c^{0.55}} = \frac{1}{\sigma_v}\left(31.79q_c + 74.81\frac{f_s}{w}\right) + 4.08\frac{\gamma_d}{\gamma_w} \qquad (4.1)$$

where, M_r- resilient modulus (MPa), σ_c- confining (minor principal) stress (kPa), σ_v- vertical (major principal) stress (kPa), q_c- tip resistance(MPa), f_s- sleeve friction (MPa), w- water content (as a decimal), γ_d- dry unit weight (kN/m^3), γ_w- unit weight of water (kN/m^3).

In this regression model, the coefficient of multiple determination, R^2, is as high as 0.99 and root mean squared error, RMSE, is as low as 1.37. There are no extremely large residuals. The residuals showed no outliers or erroneous observations. There is no evidence in the residuals to imply that the model is inappropriate. The model, given in equation (4.1), was developed using data from PRF silty clay and heavy clay, and it was used to predict the resilient modulus of soil from other sites such as LA-42/ I-10, LA-15, LA-89, and Siegen Lane. Figure 4.29 depicts the comparison of the predicted resilient and the measured resilient moduli. Most of the data fall close to the line of equality. The measured and predicted modulus values are not significantly different.

4.4.2 Proposed Model for Coarse-grained Soils (In-situ)

For sand, CIMCPT test has shown difficult to penetrate. Lime stabilized recycled cement soil in LA-89 behaves like sand in the resilient modulus testing, showing an increase in resilient modulus with bulk stress. The test results of LA-28 and LA-89,

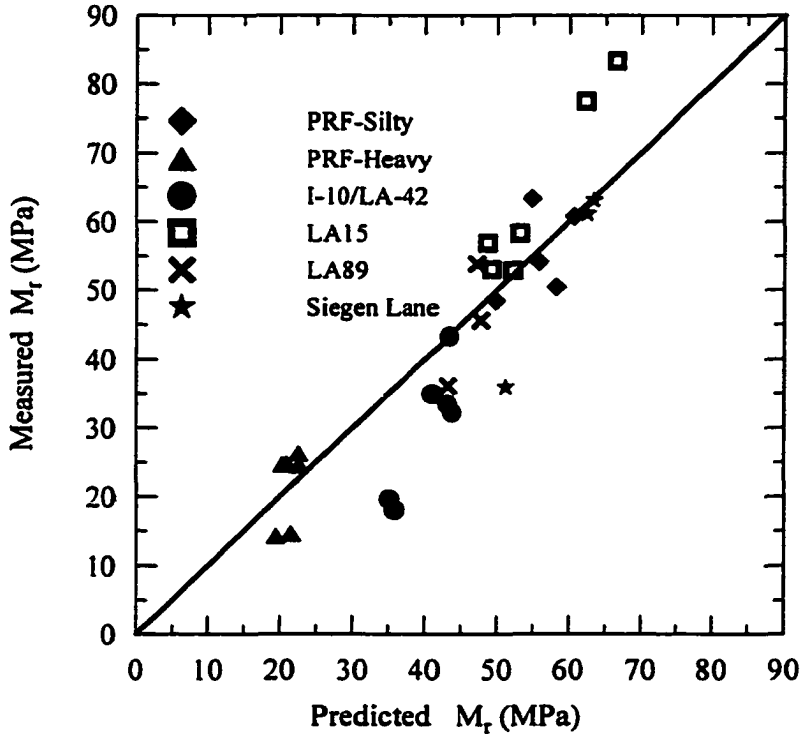

Figure 4.29 Prediction of in-situ resilient modulus for fine-grained soil

Tables 4.6 and 4.7, are used in the regression analysis for sand. As the resilient modulus increases with the confining stress and bulk stress in sand, following correlation between the cone data and the resilient modulus was developed using data from the *LA-28* sand and LA-89 lime stabilized recycled soil cement.

$$\frac{M_r}{\sigma_c^{0.55}} = 6.66\frac{(q_c\sigma_b)}{\sigma_v^2} - 32.99\frac{f_s}{q_c} + 0.52\frac{\gamma_d}{(w\gamma_w)} \qquad (4.2)$$

where, M_r- resilient modulus (MPa), σ_c- confining (minor principal) stress (kPa), σ_v- vertical (major principal) stress (kPa), q_c- tip resistance(MPa), f_s- sleeve friction (MPa), w- water content (as a decimal), γ_d- dry unit weight (kN/m^3), γ_w- unit weight of water (kN/m^3), and σ_b - bulk stress.

In this regression model, the coefficient of multiple determination, R^2, is as high as 0.99 and root mean squared error, RMSE, is as low as 0.96. There are no extremely large residuals. The residuals showed no outliers or erroneous observations. There is no evidence in the residuals to imply that the model is inappropriate. In the AASHTO T-294 resilient modulus test procedure, crushability and angularity were not addressed and therefore, these properties were not covered in this study.

The model, given in equation (4.2), was developed using data from the LA-28 sand and the LA-89 lime stabilized recycled soil cement. Figure 4.30 depicts the comparison of the predicted resilient and the measured resilient moduli. Most of the data fall close to the line of equality. The measured and predicted modulus values are not significantly different.

Table 4.6 Summary of the field and laboratory tests on the LA-28 sand and LA-89 lime treated recycled cement soil

	Depth (m)	q_c (MPa)	f_s (MPa)	w (%)	γ_d (kN/m^3)
LA-28					
BH1	0.8	2.3	0.0148	11.0	19.4
BH1	1	2.1	0.0250	16.3	17.2
BH2	0.8	2.3	0.0217	11.1	17.7
BH3	0.8	2.4	0.0238	10.3	17.5
LA-89					
BH1	0.4	6.5	0.3240	18.8	15.8
BH3	0.4	8.1	0.3690	17.9	17.2

Table 4.7 Summary of the stress analysis on the LA-28 sand and LA-89 lime treated recycled soil cement

	Depth (m)	In-situ			In-situ and Traffic		
		M_r (Mpa)	σ_c (kPa)	σ_d (kPa)	M_r (Mpa)	σ_c (kPa)	σ_d (kPa)
LA-28							
BH1	0.8	34.6	9.13	8.09	43.3	13.40	13.70
BH1	1	24.0	10.61	9.41	34.8	14.90	15.00
BH2	0.8	40.1	10.44	9.26	44.4	13.50	13.80
BH3	0.8	32.4	8.18	7.26	38.9	12.50	12.80
LA-89							
BH1	0.4	43.2	5.55	1.95	52.2	10.20	9.69
BH3	0.4	53.9	5.99	2.16	75.0	10.60	9.85

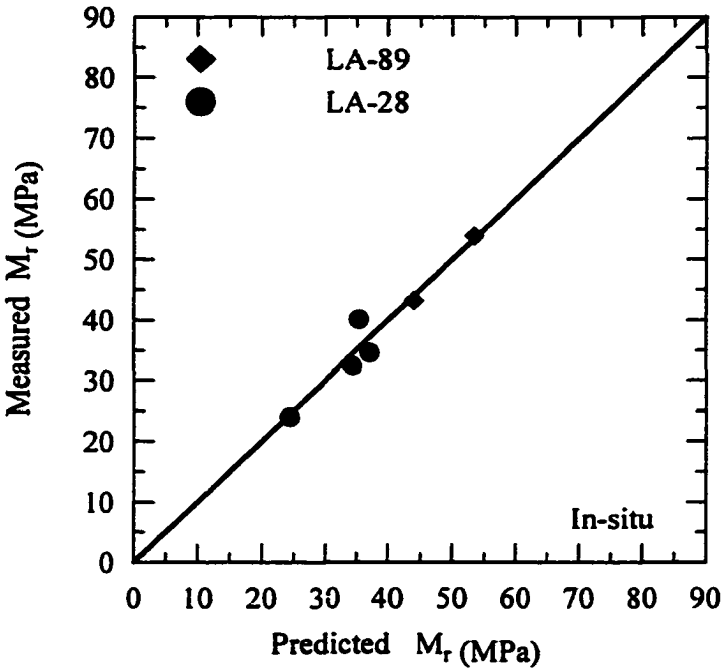

Figure 4.30 Prediction of in-situ resilient modulus for coarse-grained soil

4.4.3 Analysis for Traffic Loadings

4.4.3.1 Traffic Stress Model for Fine-grained Soil

Table 4.5 shows the difference between the resilient modulus values of the in-situ and in-situ with traffic loading conditions. Section 4.6 explains the sensitivity of the resilient modulus on the overlay thickness. Therefore, it is required to develop different models for traffic stress conditions to predict the resilient modulus from the cone test results. In this analysis, a fictitious pavement configuration with a standard dual wheel 80 kN (18 kips) truck loading (1 ESAL) was placed on each type of soil site as shown in Figure 4.31. For this traffic loading, stresses in the soil at a particular depth were computed by using the computer code for the analysis of linear-elastic pavement systems, ELSYM5. The in-situ stresses and traffic stresses were superimposed to compute combined major and minor (confining stress) principal stresses, at this soil element. From the major and minor principal stresses, deviator stress was calculated. From the laboratory resilient modulus tests at these confining stress and deviator stress, resilient modulus under this traffic loading was estimated. These results are presented in Tables 4.4 and 4.5.

The following model between the cone data and the resilient modulus was developed by using data of silty clay and heavy clay, as given Tables 4.4 and 4.5, for traffic stress condition. The resilient modulus, major principal stress, and minor principal stress in this model were based on the traffic loading condition. The model for fine-grained soil under traffic stress:

$$\frac{M_r}{\sigma_3^{0.55}} = 47.03\frac{q_c}{\sigma_1} + 170.40\frac{f_s}{\sigma_1 w} + 1.67\frac{\gamma_d}{\gamma_w} \qquad (4.3)$$

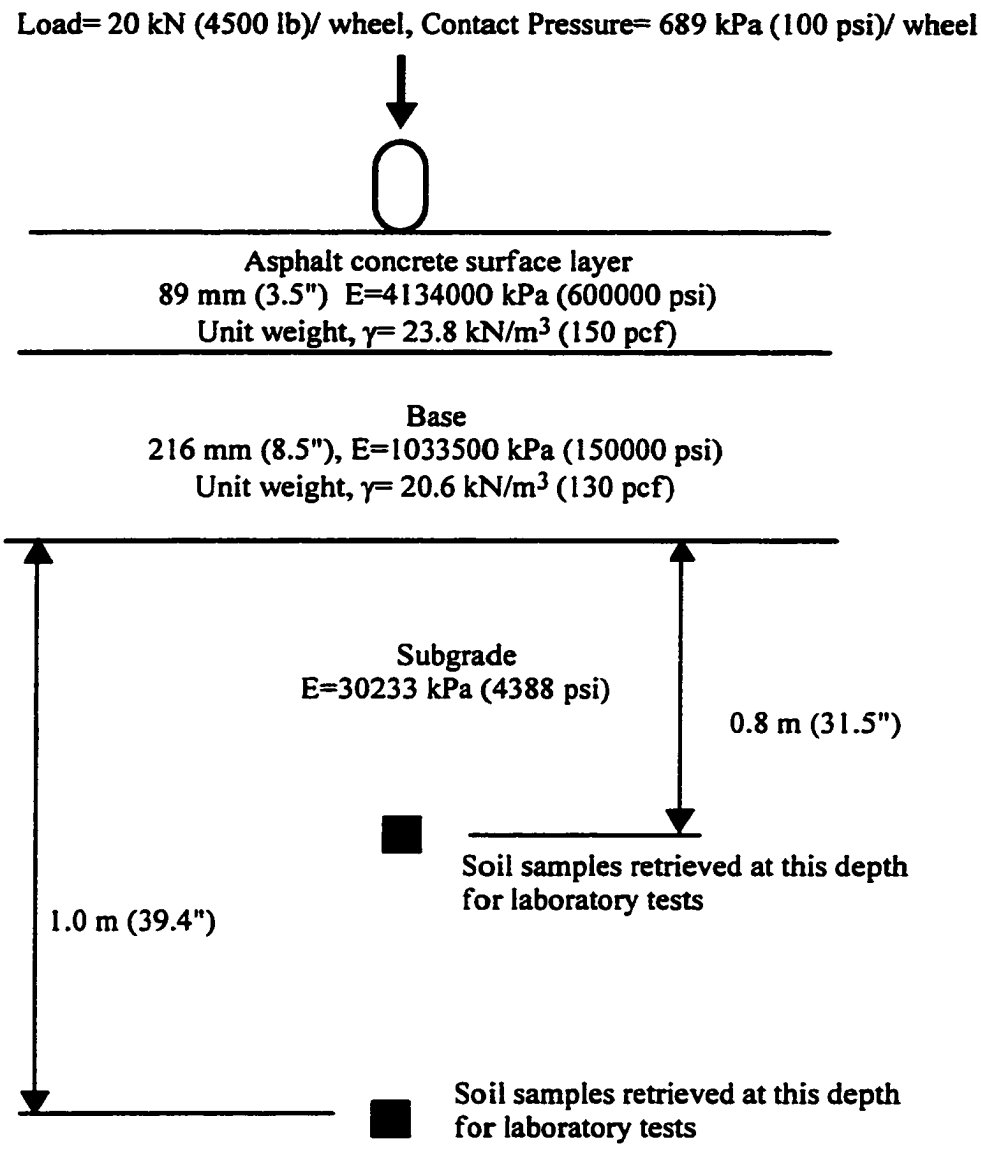

Figure 4.31 A typical pavement structure for the traffic stress analysis

where, *Mr*- resilient modulus (MPa), σ_3- minor principal stress (σ_c- confining) (kPa), σ_1- major principal stress (σ_v- vertical stress) (kPa), q_c- tip resistance(MPa), f_s- sleeve friction (MPa), *w*- water content (as a decimal), γ_d- dry unit weight (kN/m^3), γ_w- unit weight of water (kN/m^3).

In this regression model, the coefficient of multiple determination, R^2, is as high as 0.99 and root mean squared error, RMSE, is as low as 0.80. There are no extremely large residuals. The residuals showed no outliers or erroneous observations. There is no evidence in the residuals to imply that the model is inappropriate. The model, given in equation (4.3), was developed using the data from PRF- silty clay and heavy clay, and it was used to predict the resilient modulus of soil from other sites such as LA-42/ I-10, LA-15, LA-89, and Siegen Lane. Figure 4.32 depicts the comparison of the predicted and the measured resilient moduli. Most of the data fall close to the line of equality. The measured and predicted modulus values are not significantly different.

4.4.3.2 Traffic Stress Model for Coarse-grained Soil

As described in Section 4.5.3.1, a traffic stress analysis was performed on Field test-LA89, Field test-LA28, and controlled test granular soils. As shown in Figure 4.31, a fictitious pavement configuration, with a standard dual wheel 80 kN (18 kips) truck loading (1 ESAL) was placed on each type of soil in controlled test. For LA-89 and LA-28, results of the stress analysis are presented in Table 4.6 and 4.7. A traffic stress model, given in equation (4.4), was developed by using data, from Field test at LA-89 and LA-28. A linear multiple regression analysis using the SAS program was performed for developing this model. Traffic stress model for coarse-grained materials:

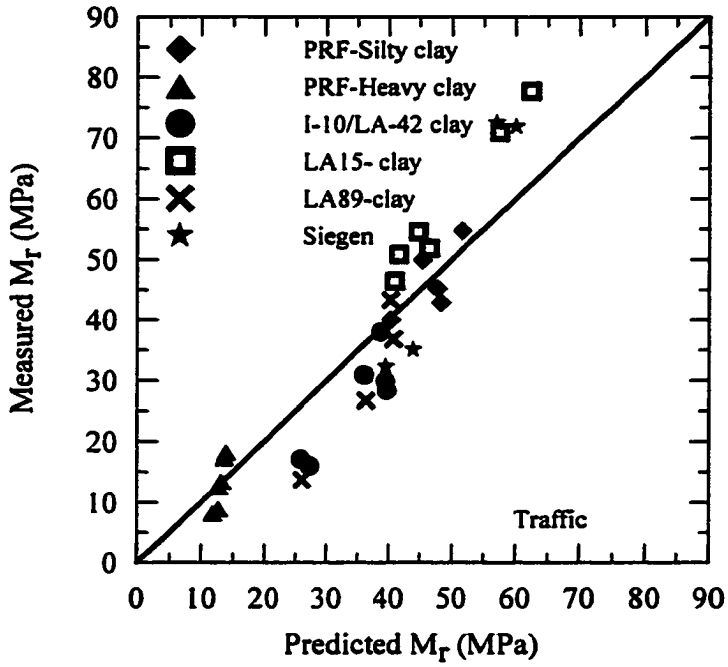

Figure 4.32 Prediction of resilient modulus of fine-grained soil from traffic stress model

$$\frac{M_r}{\sigma_3^{0.55}} = 18.95\frac{q_c\sigma_b}{\sigma_1^2} + 0.41\frac{\gamma_d}{\gamma_w w} \qquad (4.4)$$

where, M_r- resilient modulus (MPa), σ_c- confining (minor principal) stress (kPa), σ_v- vertical (major principal) stress (kPa), q_c- tip resistance(MPa), w- water content (as a decimal), γ_d- dry unit weight (kN/m^3), γ_w- unit weight of water (kN/m^3), and σ_b - bulk stress.

In this regression model, the coefficient of multiple determination, R^2, is as high as 0.99 and root mean squared error, RMSE, is as low as 1.25. There are no extremely large residuals. The residuals showed no outliers or erroneous observations. There is no evidence in the residuals to imply that the model is inappropriate. The model, given in equation (4.4), was developed using data from the LA-28 sand and the LA-89 lime stabilized recycled cement soil. Figure 4.33 depicts the comparison of the predicted resilient and the measured resilient moduli. Most of the data fall close to the line of equality. The measured and predicted modulus values are not significantly different.

4.5 Analysis of the Laboratory Cone Penetration Test

Effects of compaction, boundary, and moisture-unit weight on the laboratory cone test results are discussed. Simplified design charts are presented. The proposed models are also Verified. Four soil types were selected for the test. These are heavy clay, silty clay, and silt from the PRF site and sand from a local supplier. They are dried in the ovens and then pulverized to the proper size for compaction. Silt and sand represent the cohesionless soil while heavy clay and silty clay represent the cohesive soil.

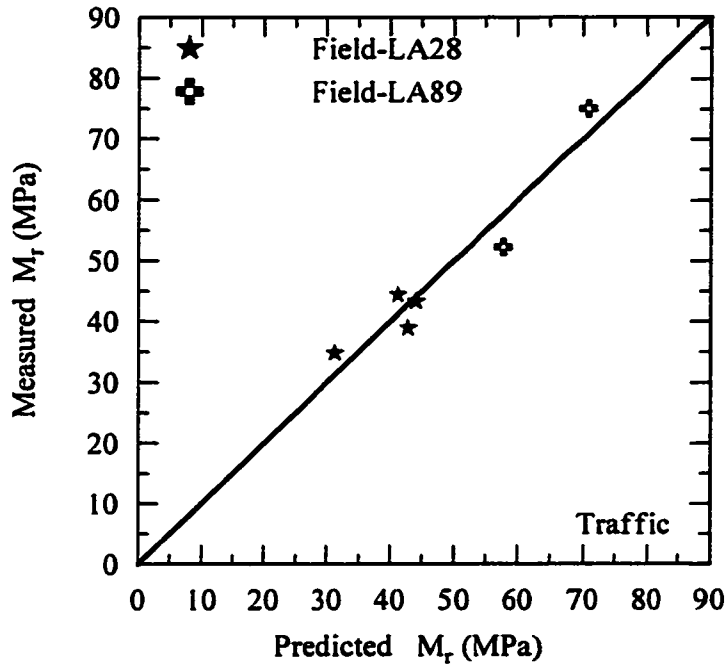

Figure 4.33 Predicted and measured resilient modulus for coarse-grained soil (traffic)

Tables 4.1 and 4.8 present, the properties of these soils. Moisture- unit weight curves for silty clay, heavy clay, silt, and sand are shown in Figures 4.34, 4.35, 4.36, and 4.37, respectively. Three points from a moisture unit weight curve were selected for soil compaction. These three points were one at dry side, another at optimum and the other at wet side.

4.5.1 Effects of Compaction

The layered compaction effect is illustrated in Figure 4.38. When a compaction effort is applied on the top of a soil layer, the highest unit weight is expected at the top of the layer while it decreases along the depth. Contrary to this, at the top of the layer, enough confinement is not found to develop a high unit weight due to the compaction. This results in lower unit weight in the top and bottom of the soil layer. In addition to this effect, compaction efforts applied on top layers may also be distributed in the already compacted bottom layers (Figure 4.38). Therefore, change in the unit weight of the layers can be expected due to the effect of the compaction. Figure 4.38, a schematic diagram, illustrates this behavior in a soil sample. Variation in the unit weight in a sample along the depth may be reflected in the cone test results.

4.5.2 Boundary Effects

The effects of the boundary of the container, used for soil sample preparation, may influence on the test results. Penetrating a cone in a soil mass, replaces a volume of soil equal to its own volume causing disturbances in surrounding soil. This results in ground heave at shallow penetration while primarily radial soil movement at deep penetrations. But boundary effects can be minimized by selecting the cone testing locations away from the container's inner surface. Effect of the boundary condition on

Table 4.8 Properties of the soils used in the laboratory cone penetration test

Property \ Soil type	PRF-Silt	Sand
Passing sieve #200 (%)	39	2
Clay (%)	9	0
Silt (%)	30	2
Organic content (%)	NA	NA
Liquid limit (LL) (%)	NP	NP
Plastic limit (PL) (%)	NP	NP
Plasticity index (PI)	NP	NP
Specific gravity (G_s)	2.69	2.67
Angle of internal friction (ϕ) (°)	28.0	28.0
Optimum water content (w_{opt}) (%)	15.2	8.1
Maximum dry unit weight (γ_{dmax}) (kN/m^3)	17.2	16.4
Soil classification (USCS)	SM (Silty sand)	SP (Poorly graded sand)
Soil classification (AASHTO)	A-4 (Sandy loam)	A-3 (Fine sand)

Legend: NA- not available and NP- non plastic

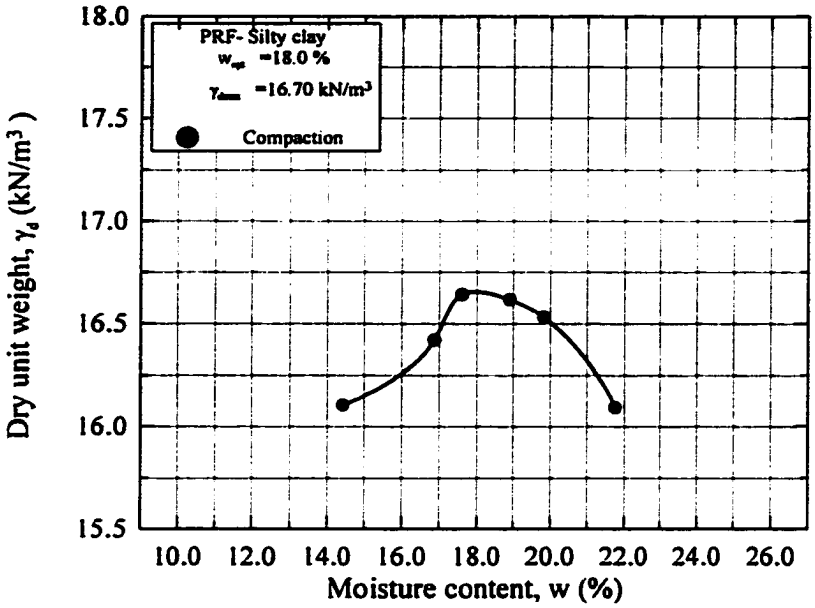

Figure 4.34 Moisture-unit weight relationship of PRF-silty clay

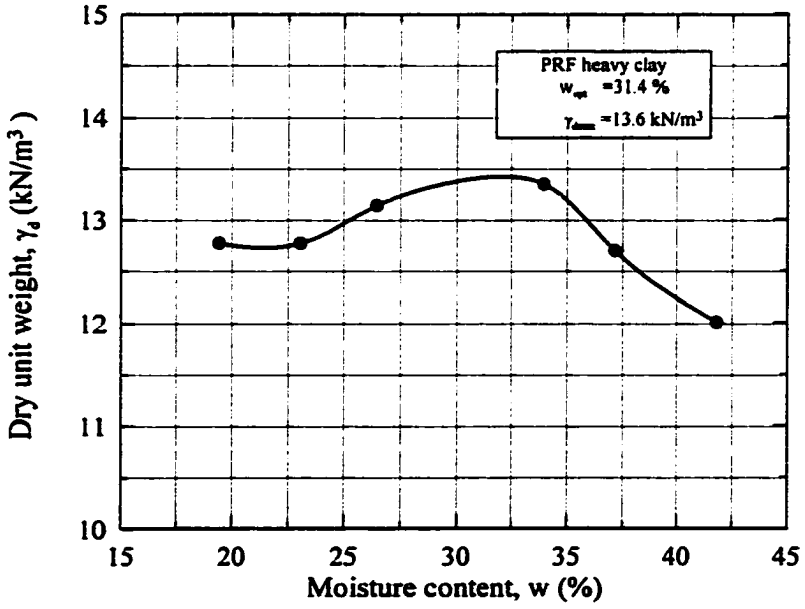

Figure 4.35 Moisture-unit weight relationship of PRF-heavy clay

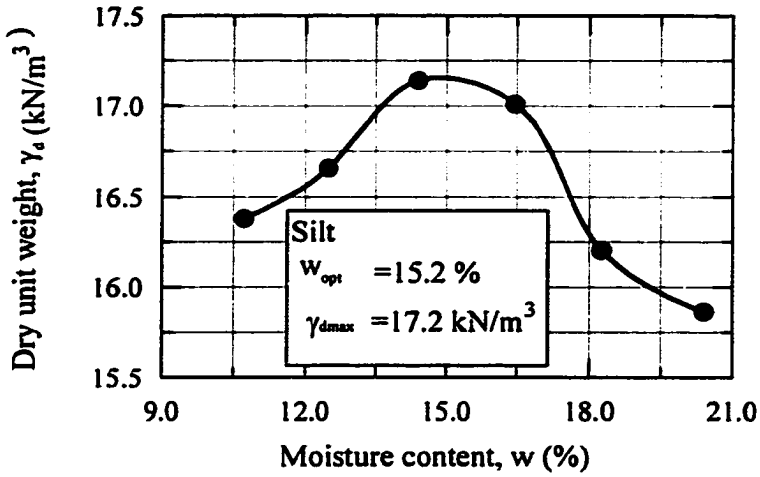

Figure 4.36 Moisture-unit weight relationship of silt

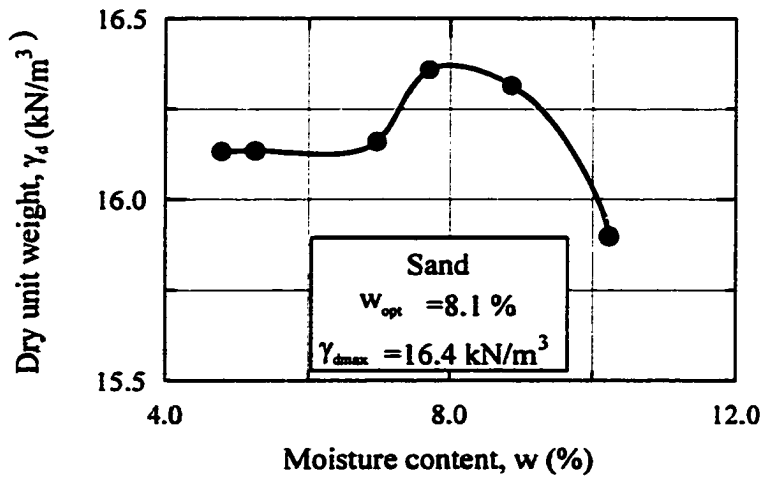

Figure 4.37 Moisture-unit weight relationship of sand

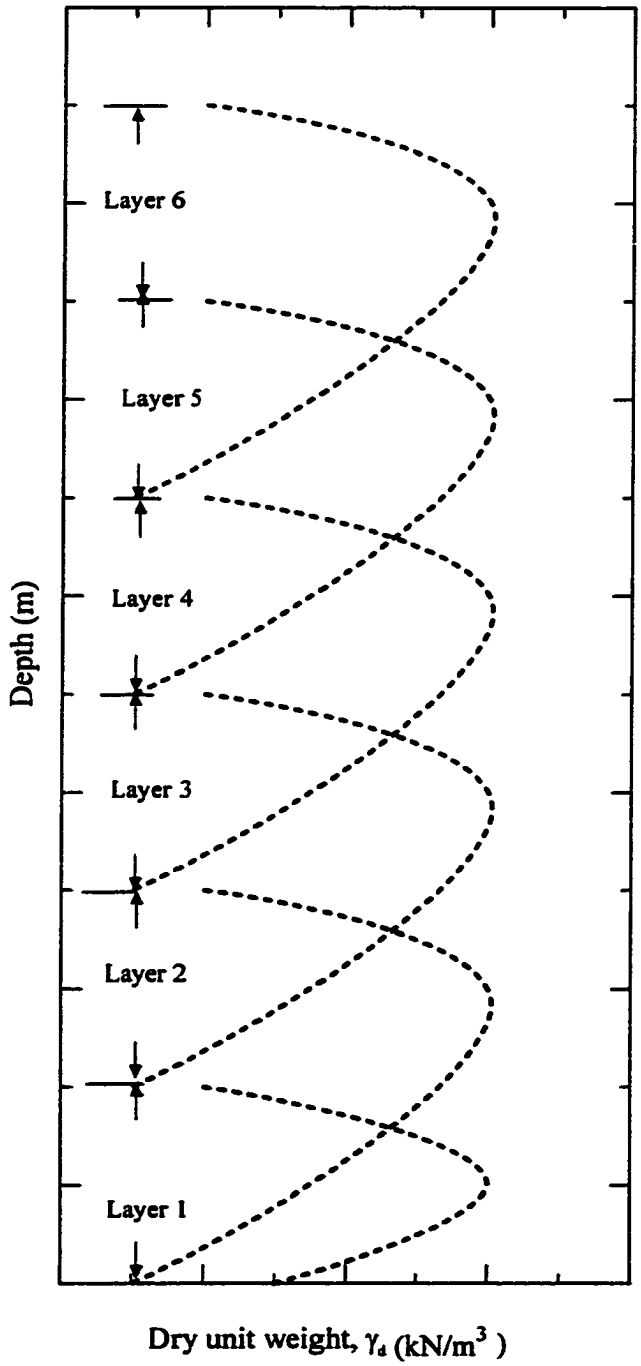

Figure 4.38 Effect on the layered compaction of soils

cone testing results depends on the diameter ratio, the soil sample diameter to cone diameter. Several studies (Holden, 1971; Schmertmann, 1978; Parkin and Lunne, 1982; Kurup, 1990) discussed the boundary effects on the cone penetration test results. Kurup (1990) reported that the sample size and boundary condition had no effect on the cone test results for diameter ratio larger than about 15. This suggests that little boundary effect be observed when a diameter ratio is larger than 15. According to Figure 3.10 in Chapter 3, the effective diameter ratio, maintained in this study, was 36 at the center. The effective diameter ratio was 17 at other four locations. This indicates a satisfactory clear distance was maintained in this study to avoid the boundary effects. Testing layout, shown in Figure3.10 in Chapter 3, allows to perform cone penetration at different locations. This allows to check the uniformity of the sample.

4.5.3 Laboratory Cone Penetration Test Results

In order to verify the homogeneity of the compacted soil sample and repeatability of the miniature cone penetration test results, five locations were selected for cone tests. Averaging the cone tip resistance along the depth of soil sample was performed by excluding a thickness, used for compacting a soil layer, of about 0.125 m from the top and 0.25 m from the bottom of the sample. This procedure allows to avoid the end effects of the soil sample. This is illustrated in Figure 4.39. It is observed that the tip resistance varies with the depth of the soil sample. This is due to the fact that several layers were used for the soil compaction and the influence from the compaction of top layers may be expected on the already compacted lower layers.

Figure 4.39 shows the laboratory cone penetration test results of silty clay at dry side. The variation in the cone penetration test results along the depth of the sample, as

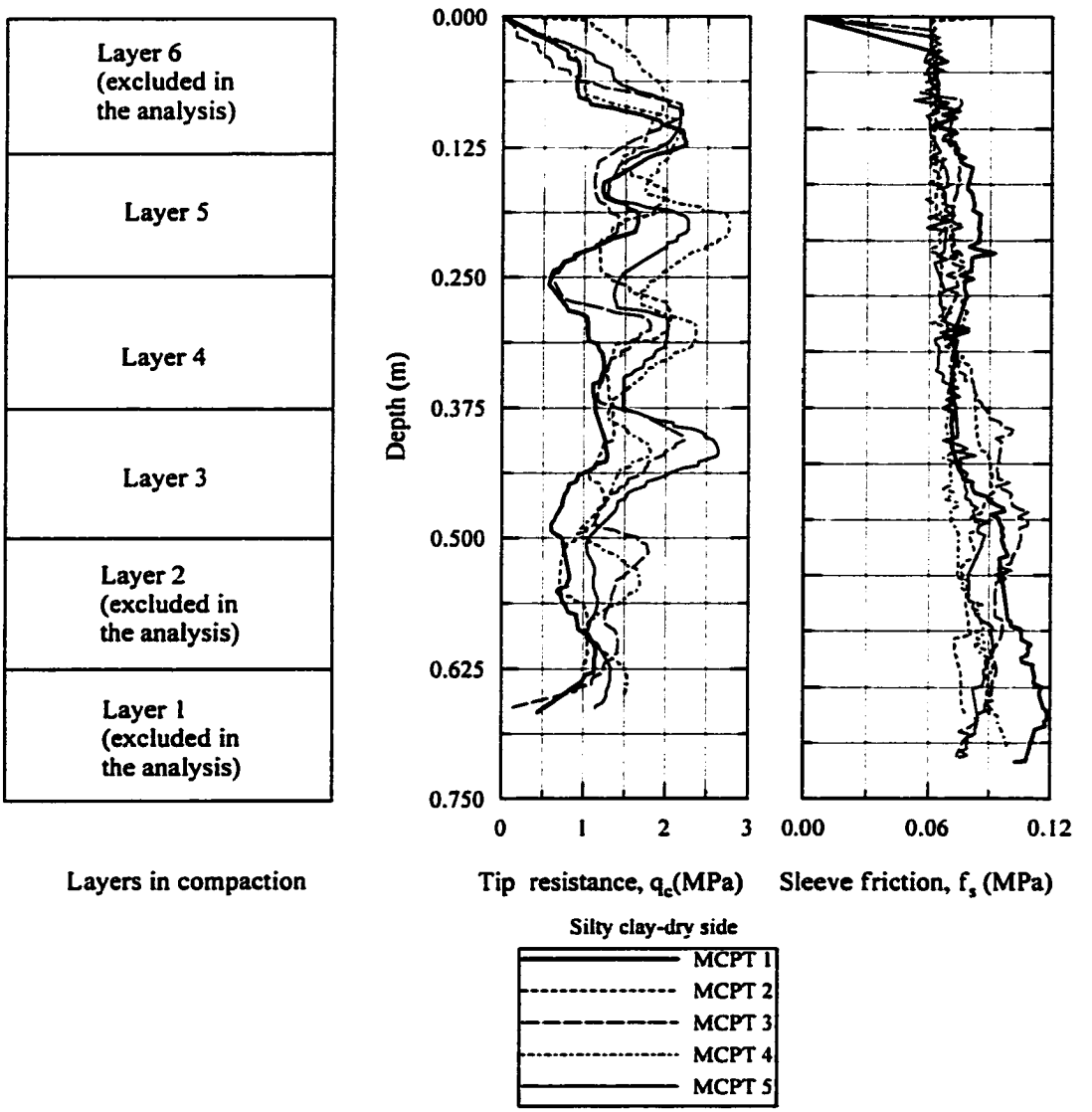

Figure 4.39 Laboratory cone penetration of silty clay at dry side

shown in Figure 4.39, is a result from the variation in the compaction along the depth as explained in Section 4.5.1. The cone penetration test results of all five tests in a sample were considered from 0.125 m to 0.5 m to estimate the average tip resistance, sleeve friction, and coefficient of variation. The cone tip resistance of dry side showed an average value of 1.5 MPa, standard deviation of 0.3 MPa,. The coefficient of variation is depicted in Figure 4.40. This result shows a variation in tip resistance in different compacted layers. For the depth of data analysis, 0.125 m to 0.5 m, the average coefficient of variation of tip resistance for silty clay-dry side is 21 %. This variation in the cone test results is due to the effect of layered compaction.

Figure 4.41 presents the cone penetration test results at the optimum. The cone tip resistance along the depth of the sample is a result from the variation in the compaction along the depth as explained in Section 4.4.1. Comparison of Figures 4.39 and 4.41 shows that tip resistance at the optimum sample is higher than that of the dry side. This due to the fact that the unit weight of optimum is greater than that of dry side. The higher the unit weight the higher the tip resistance. Figure 4.42 shows the coefficient of variation at the optimum. The average coefficient of variation of tip resistance for silty clay-optimum is 25 %. This is also due to the compaction effects on the cone penetration test results. Due to the compaction effects and the high sensitivity of the miniature cone penetrometer and its capability to identify thin soil layers, the above variation in the laboratory miniature cone penetration test results is expected. As shown in Figure 4.43, the lowest tip resistance was observed in the wet side soil sample. The highest stiffness in the optimum sample is the reason for the highest tip resistance. A combined effect of moisture content and dry unit weight exists on the tip resistance. Figure 4.44 shows

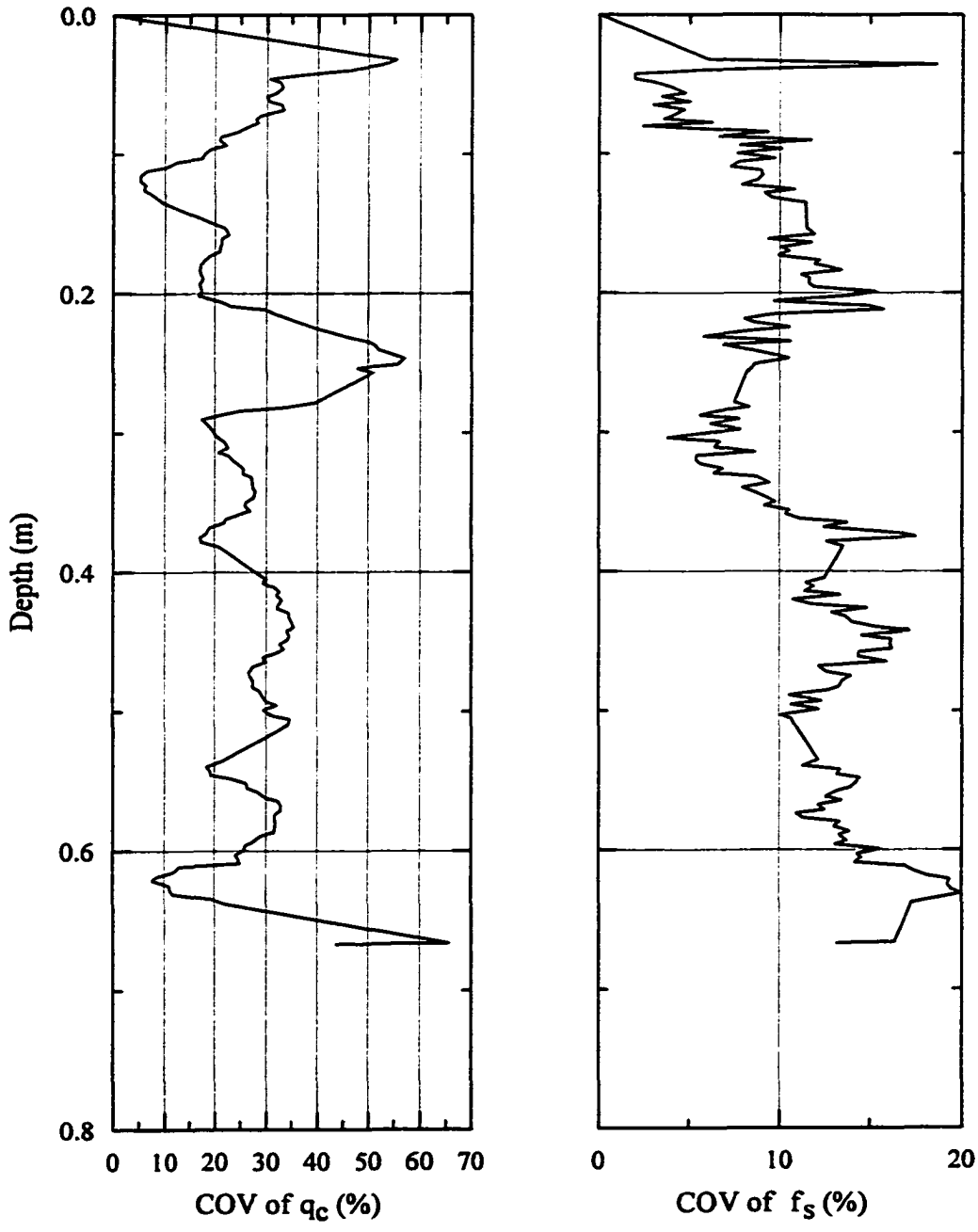

Figure 4.40 Coefficient of variation of laboratory cone penetration of silty clay at dry side

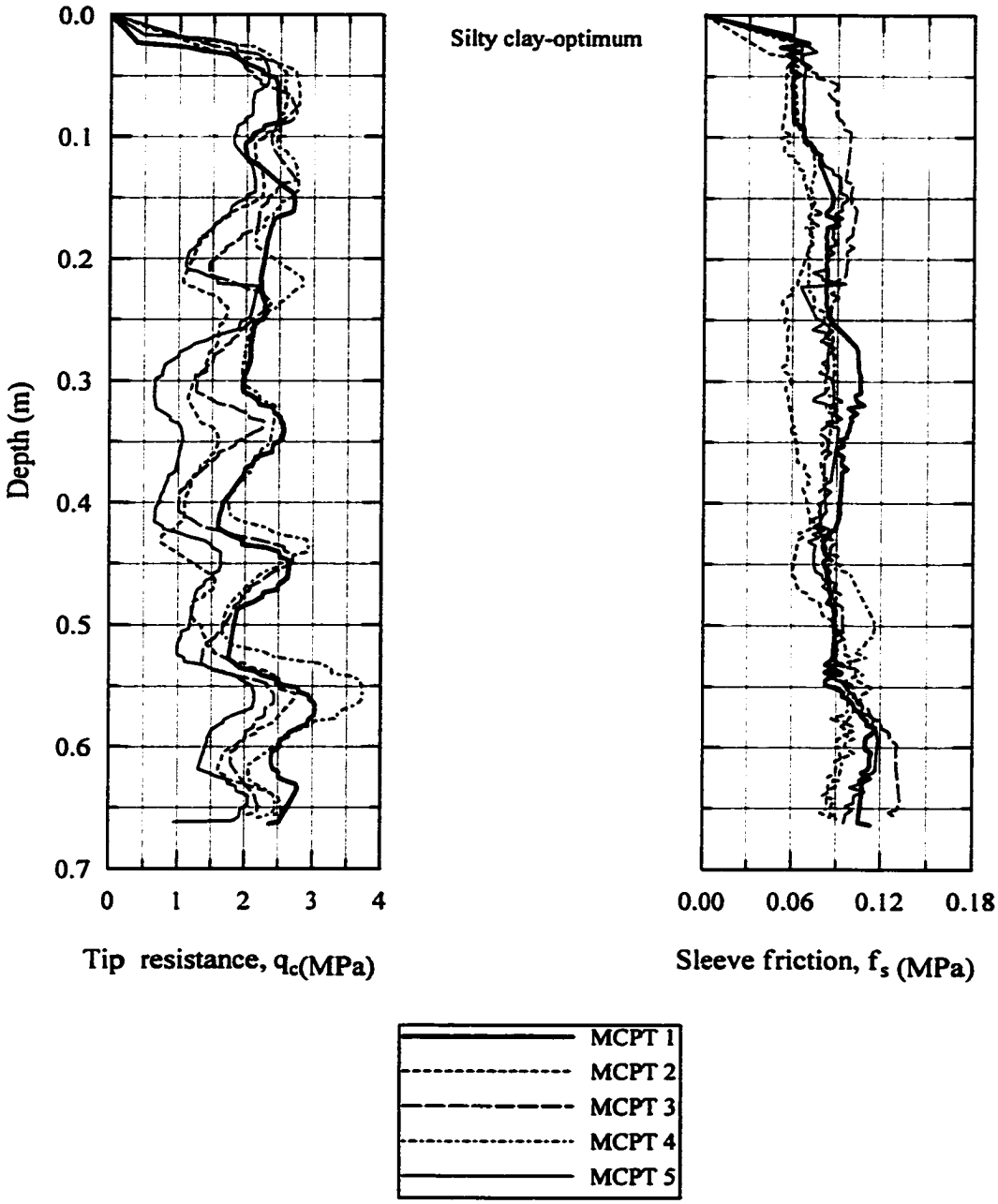

Figure 4.41 Laboratory cone penetration of silty clay at optimum

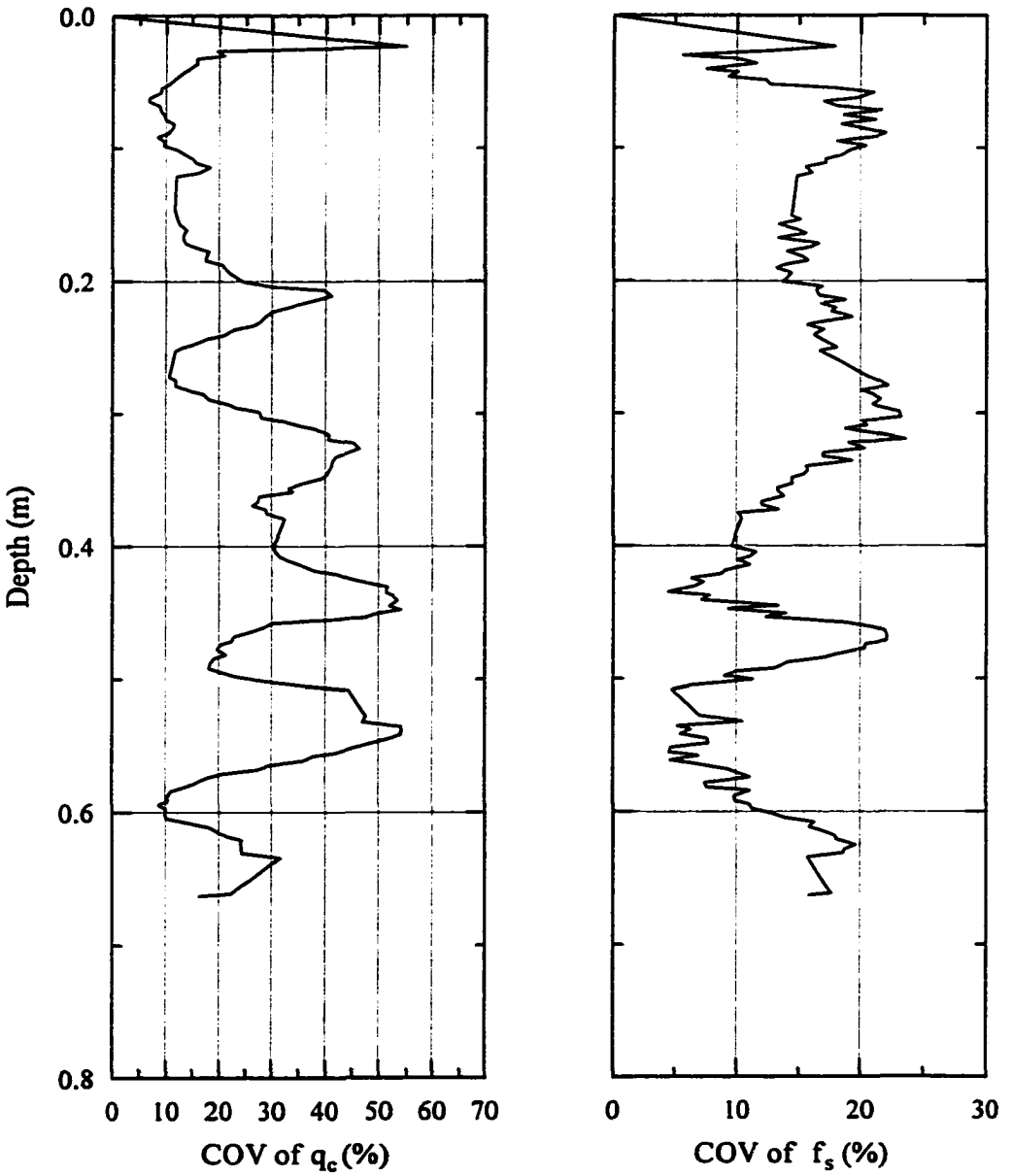

Figure 4.42 Coefficient of variation of laboratory cone penetration of silty clay at optimum

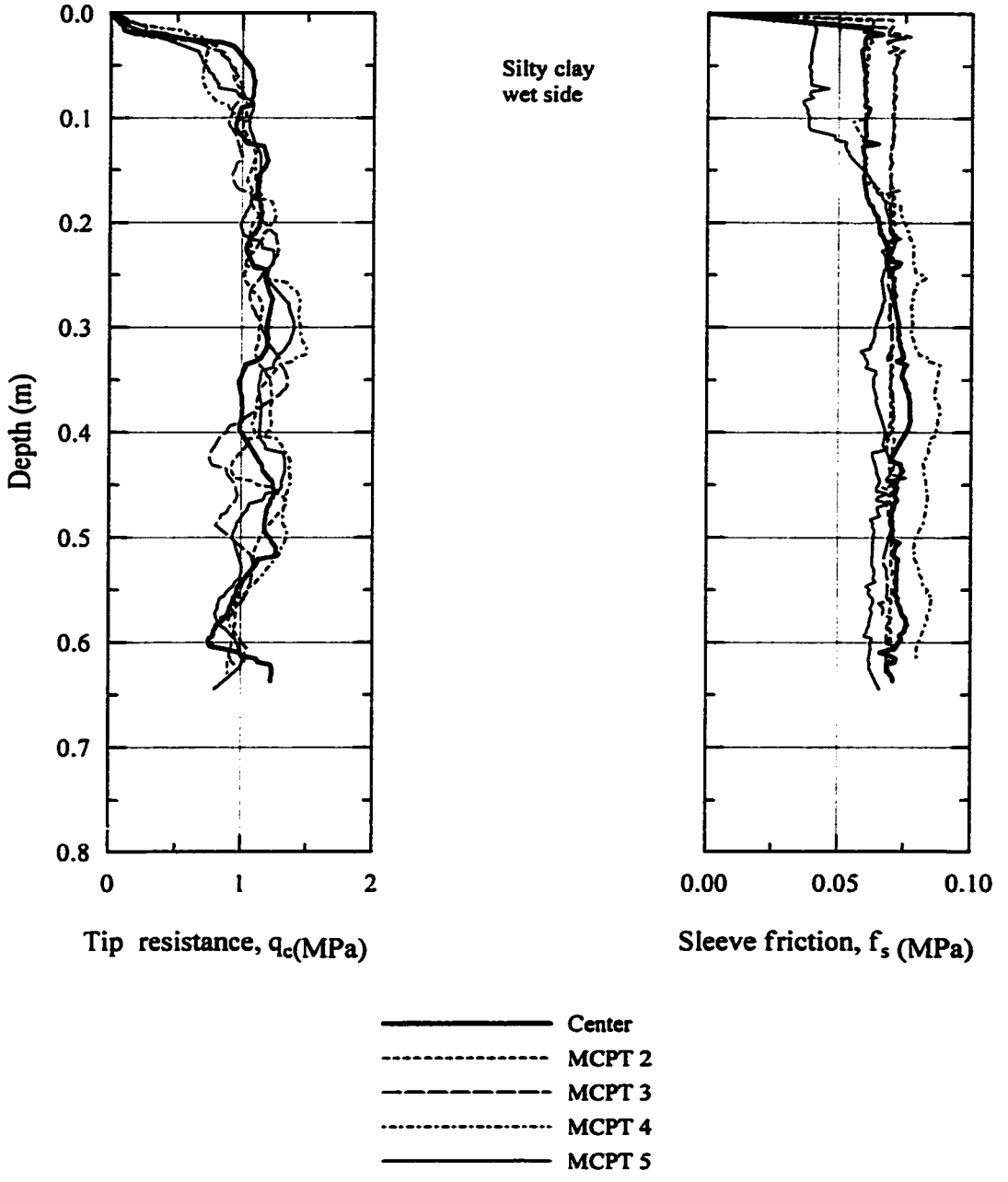

Figure 4.43 Laboratory cone penetration of silty clay at wet side

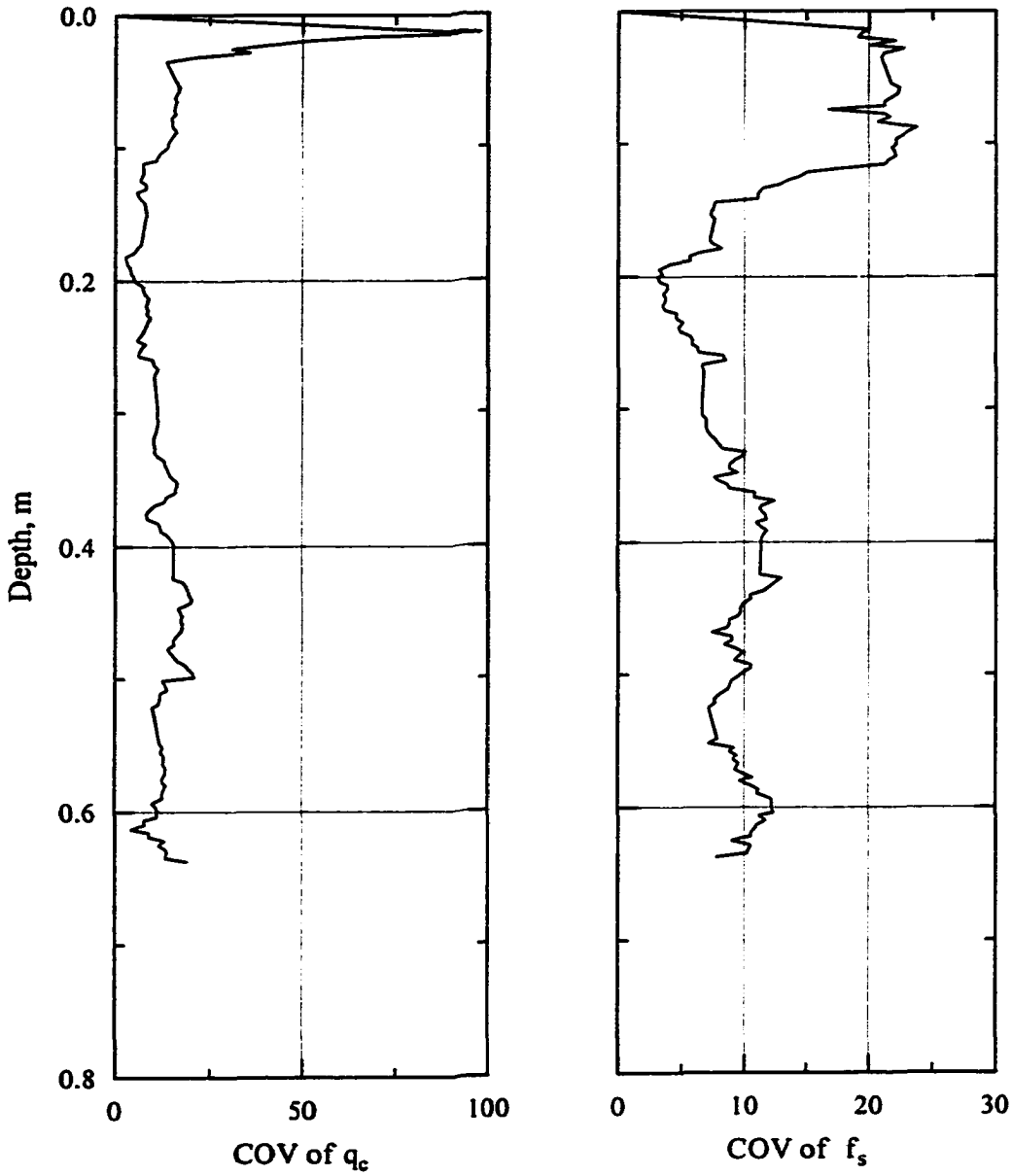

Figure 4.44 Coefficient of variation of laboratory cone penetration of silty clay at wet side

the coefficient of variation at the wet side. For the depth of data analysis, 0.125 m to 0.5 m, average coefficient of variation of tip resistance for silty clay-wet side is 11.6 %.

Figure 4.45 shows the cone penetration test results at the dry side of the heavy clay. The average tip resistance of heavy clay- dry side is 1.3 MPa. The average tip resistance of heavy clay- dry side is less than that of silty clay-dry side. This is due to the soft nature of heavy clay. As shown in Figure 4.46, for the range of data analysis, coefficient of variation of tip resistance for heavy clay dry side, optimum, and wet side are 13 %, 15 %, and 23 % respectively.

Figure 4.47 shows the cone penetration test results at the optimum of the heavy clay. The average tip resistance of heavy clay- optimum is 1.6 MPa. The average tip resistance of heavy clay-optimum is also less than that of silty clay-optimum. Coefficient of variation of tip resistance for heavy clay-optimum is 15 %.

Figure 4.48 present the cone penetration test results at the wet side of the heavy clay. The tip resistance at optimum sample is higher than that of the dry side and wet side samples because the highest stiffness is occurred at the optimum. The lowest tip resistance was observed in the wet side soil sample due to the highest moisture content.

Cone test result for silt is depicted in Figure 4.49 shows that tip resistance varies with the depth. The highest tip resistance was observed in the optimum sample. The lowest tip resistance was recorded in the wet side sample. For the range of data analysis, coefficient of variation of tip resistance for silt dry side, optimum, and wet side are 15 %, 9 %, and 7 % respectively. Coefficient of variation of water content for silt dry side, optimum, and wet side are 4.0 %, 3.0 %, and 2.2 %.

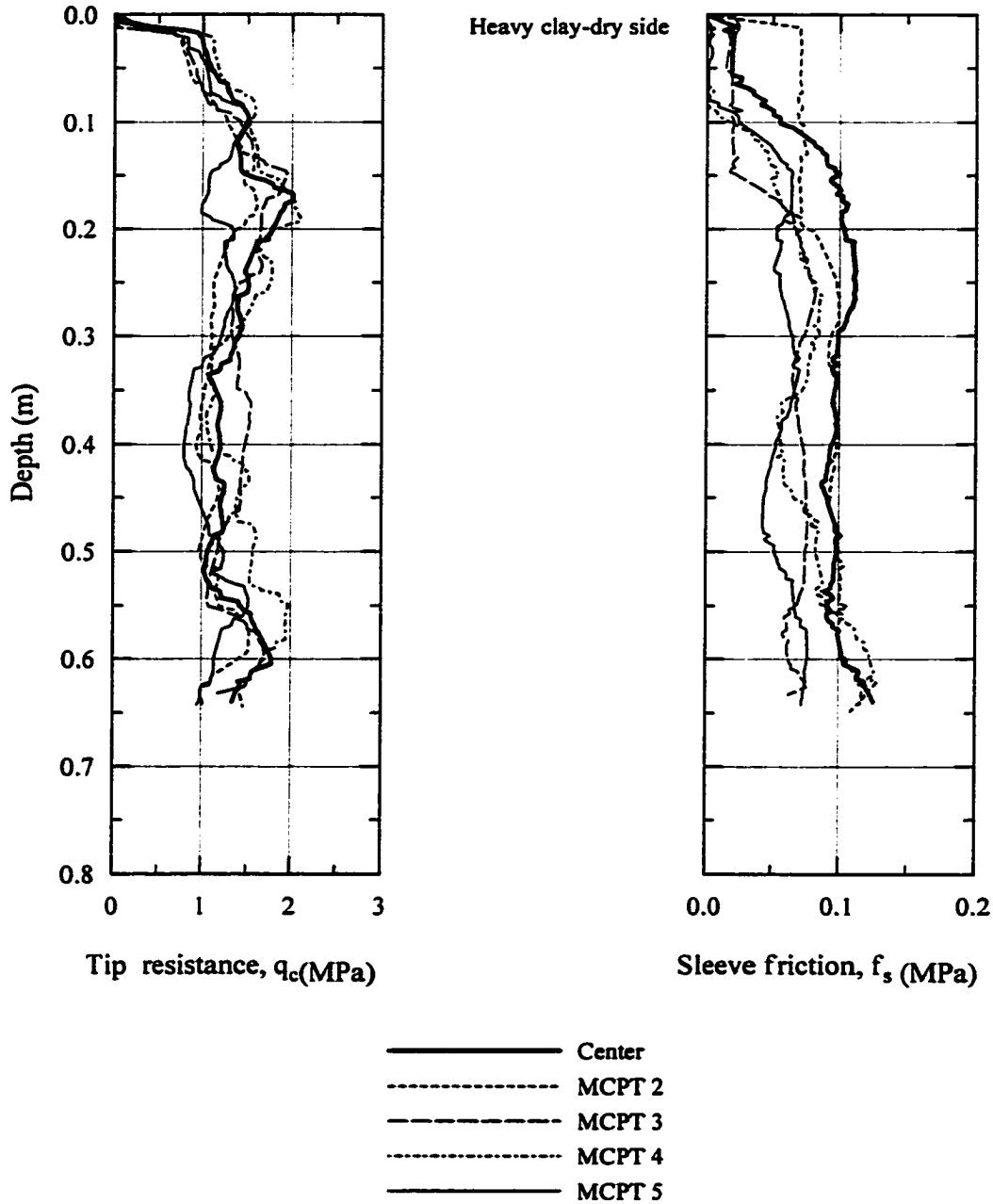

Figure 4.45 Laboratory cone penetration of heavy clay at dry side

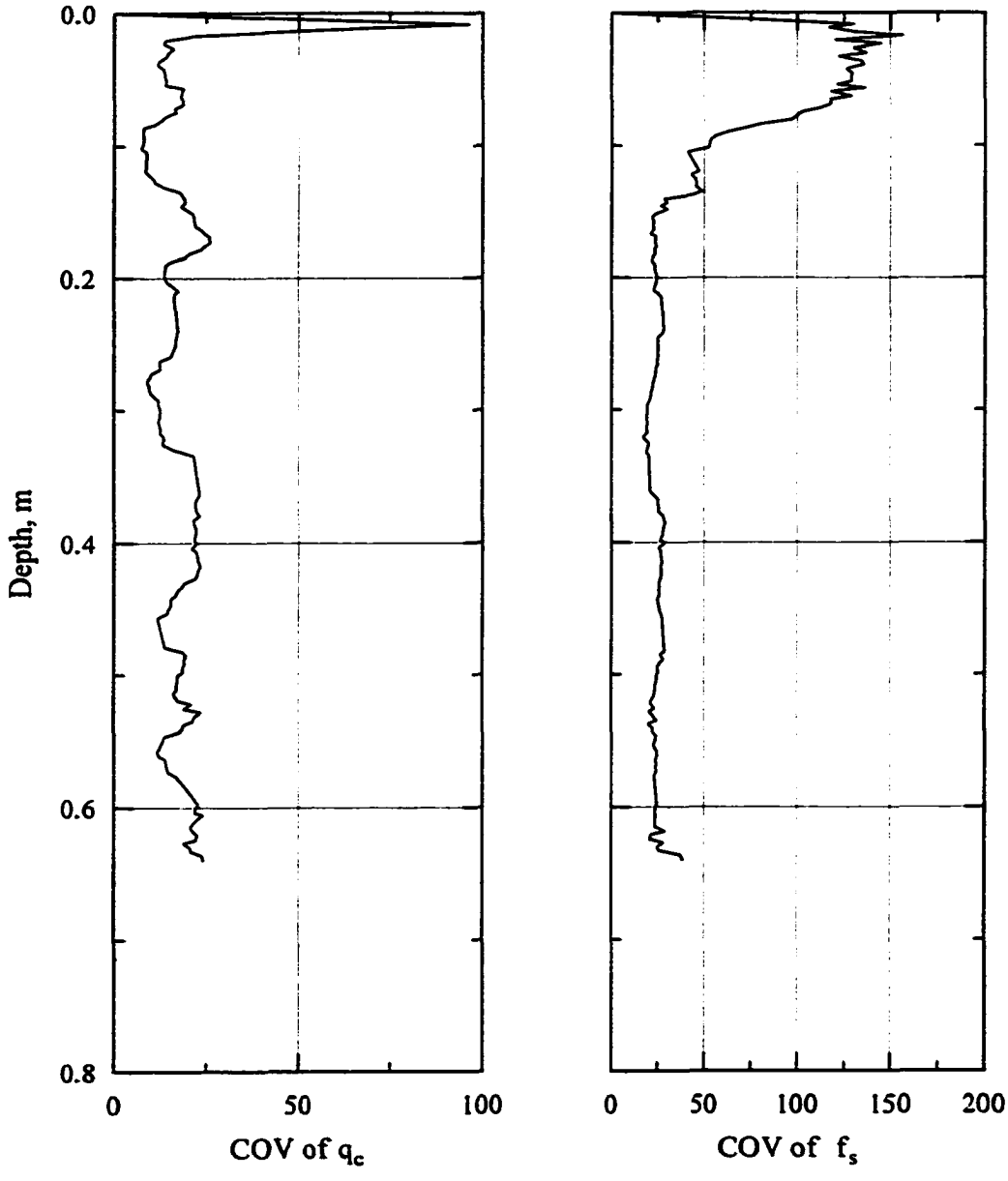

Figure 4.46 Coefficient of variation of laboratory cone penetration of heavy clay at dry side

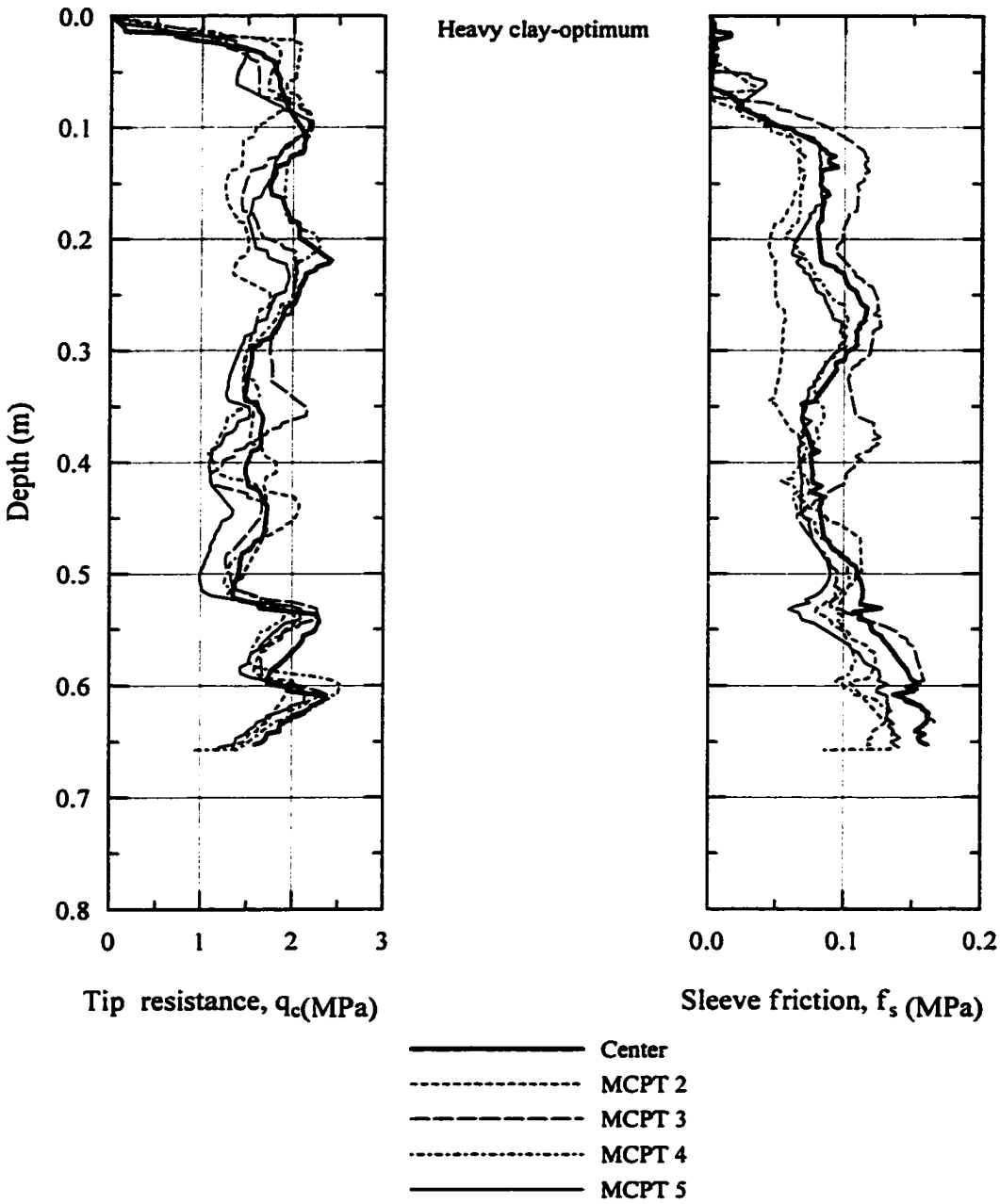

Figure 4.47 Laboratory cone penetration of heavy clay at optimum

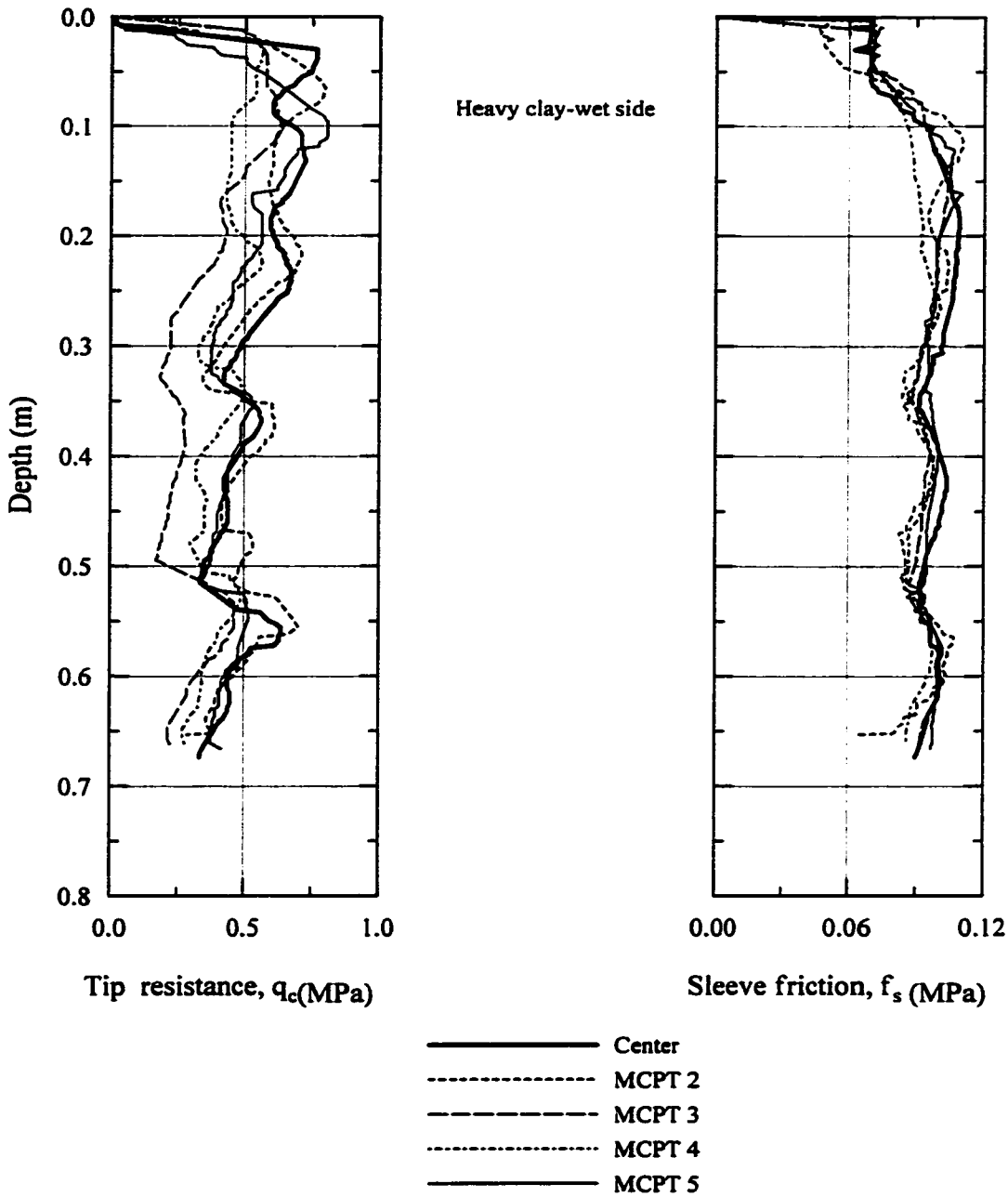

Figure 4.48 Laboratory cone penetration of heavy clay at wet side

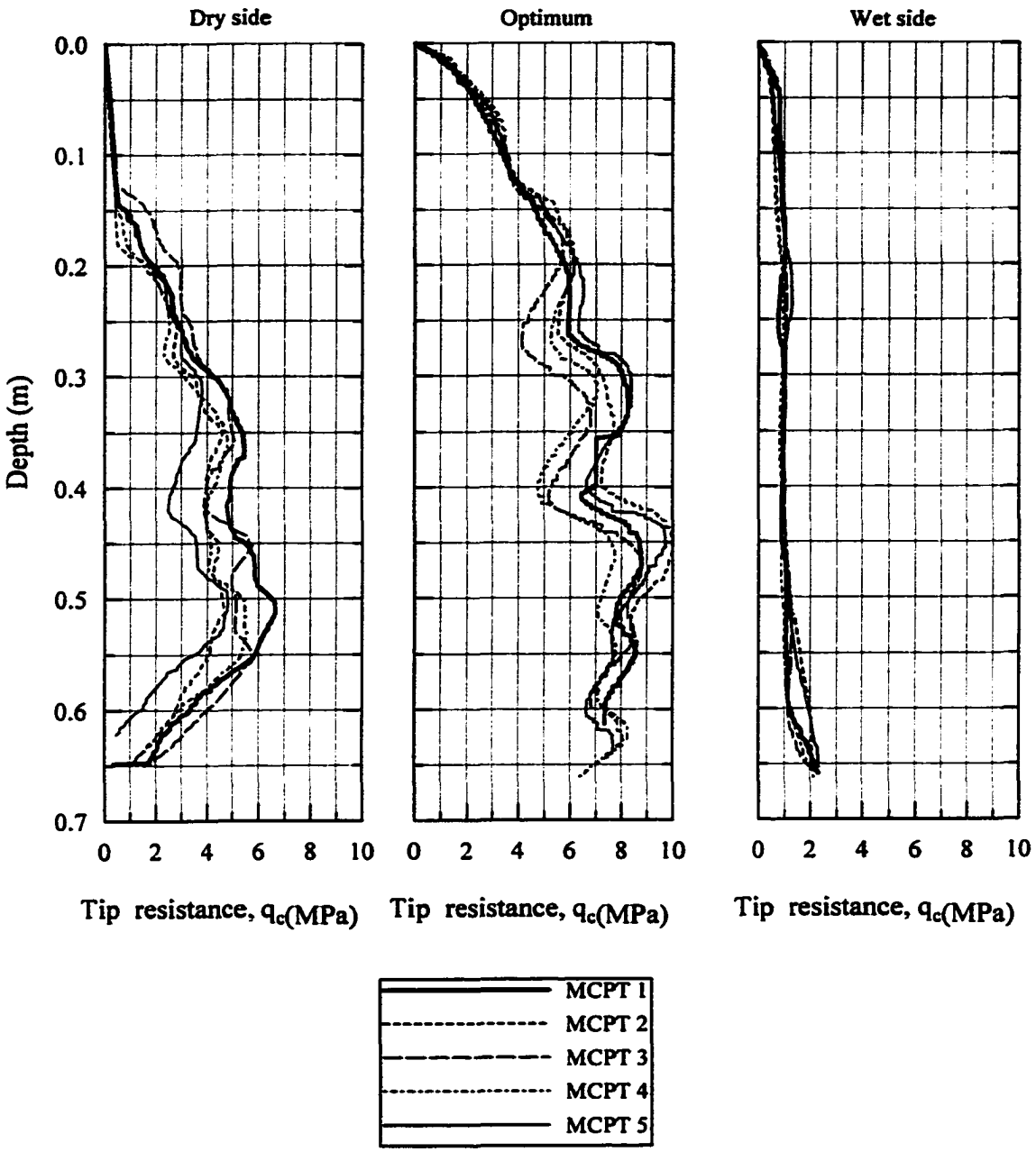

Figure 4.49 Laboratory cone penetration of silt

Cone test result for sand is depicted in Figure 4.50. The tip resistance of sand varies with the depth due to the effect of the layered compaction. For the range of data analysis, coefficient of variation of tip resistance for sand dry side, optimum, and wet side are 16 %, 9 %, and 11 % respectively.

4.5.4 Resilient Modulus

Figure 4.51 shows the resilient modulus test results for silty clay at dry side. A high resilient modulus for a subgrade soil is desirable to obtain a resistance to deformation due to traffic loading. As expected, the resilient modulus of silty clay decreases as deviator

stress increases. The resilient modulus of silty clay is higher than that of heavy clay. The cone tip resistance follows the same pattern. This is due to the higher stiffness in silty clay and soft nature in heavy clay. At optimum (Figure 4.52) the highest resilient modulus is observed. The highest soil stiffness at optimum may be a reason for this high resilient modulus. The resilient modulus of silty clay dry side is greater than that of wet side (Figures 4.51 and 4.53). This due to the high water content in the wet side.

Figures 4.54, 4.55, and 4.56 present the resilient modulus of heavy clay dry side, optimum, and wet side respectively. At optimum (Figure 4.55) the highest resilient modulus is observed. The resilient modulus of heavy clay dry side is greater than that of wet side (Figures 4.54 and 4.56). Figure 4.57 shows the resilient modulus test results for silt at dry side. As expected, the resilient modulus values of silt increases with bulk stresses. The resilient modulus at wet side is lower than that at dry side. A higher water content and lower stiffness result in lower resilient modulus. The highest resilient modulus occurs at optimum. This is due to the highest stiffness at optimum.

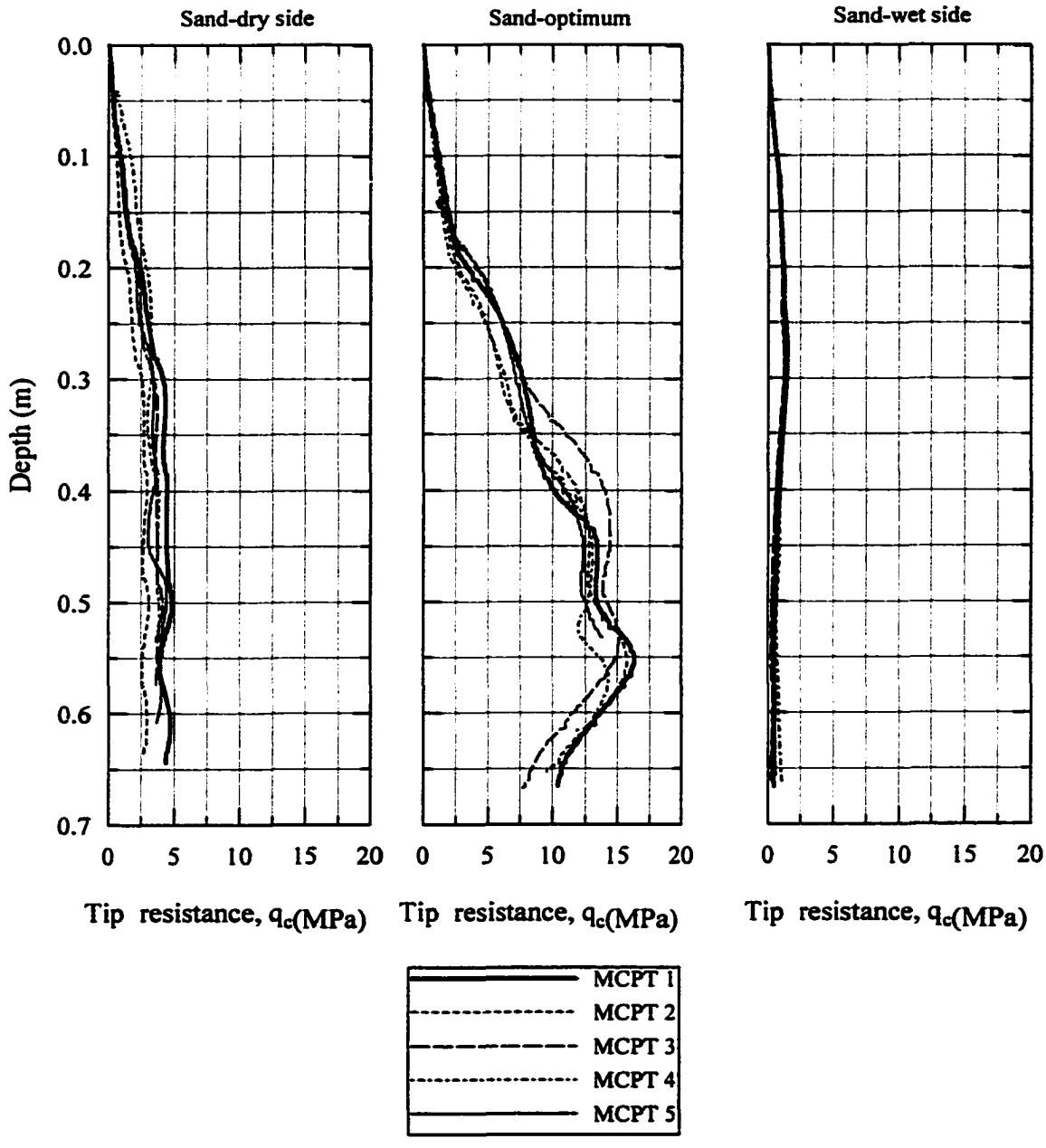

Figure 4.50 Laboratory cone penetration of sand

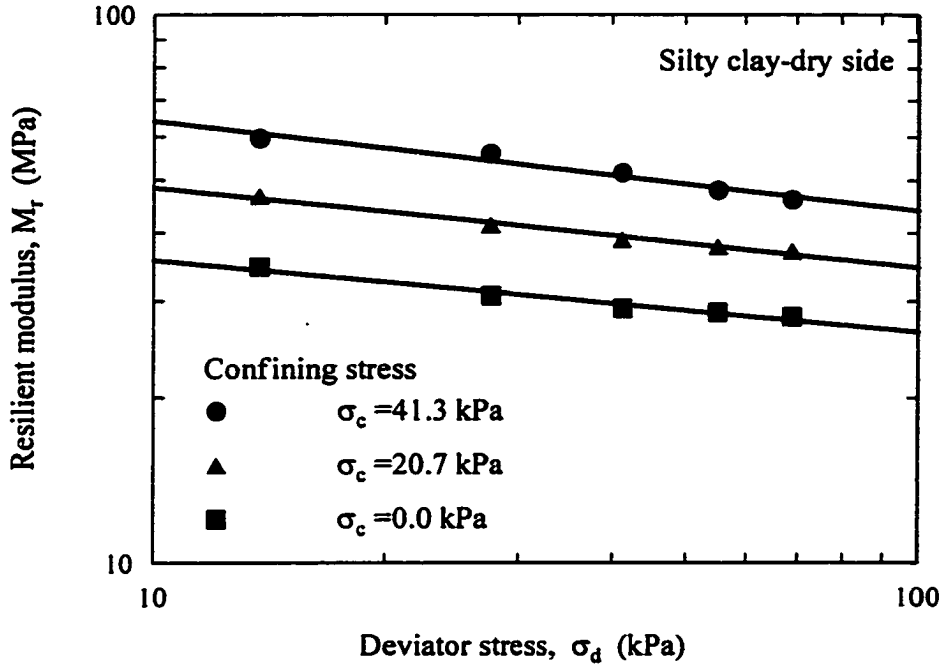

Figure 4.51 Resilient modulus of silty clay at dry side

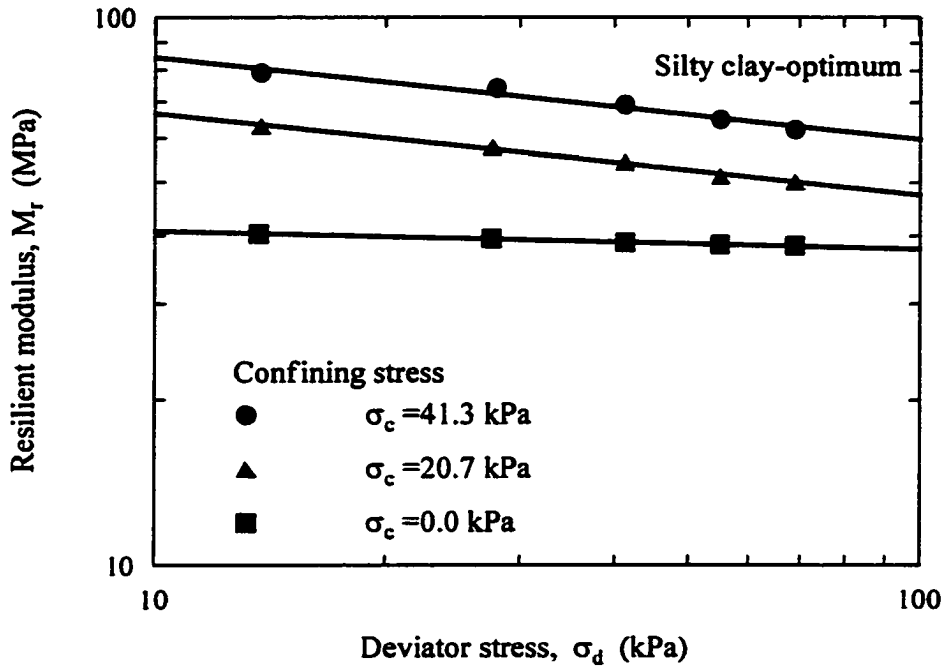

Figure 4.52 Resilient modulus of silty clay at optimum

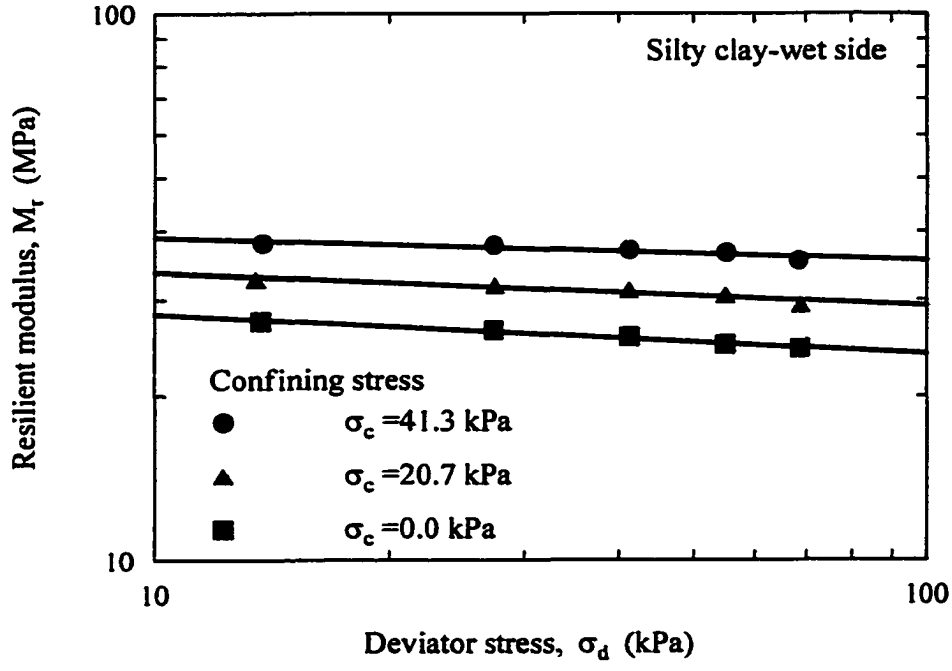

Figure 4.53 Resilient modulus of silty clay at wet side

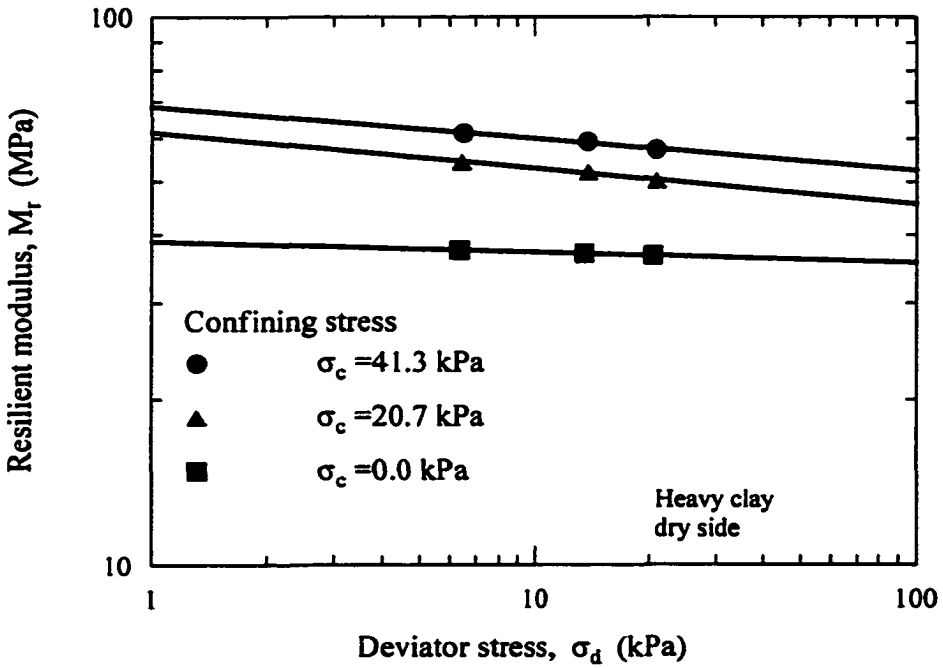

Figure 4.54 Resilient modulus of heavy clay at dry side

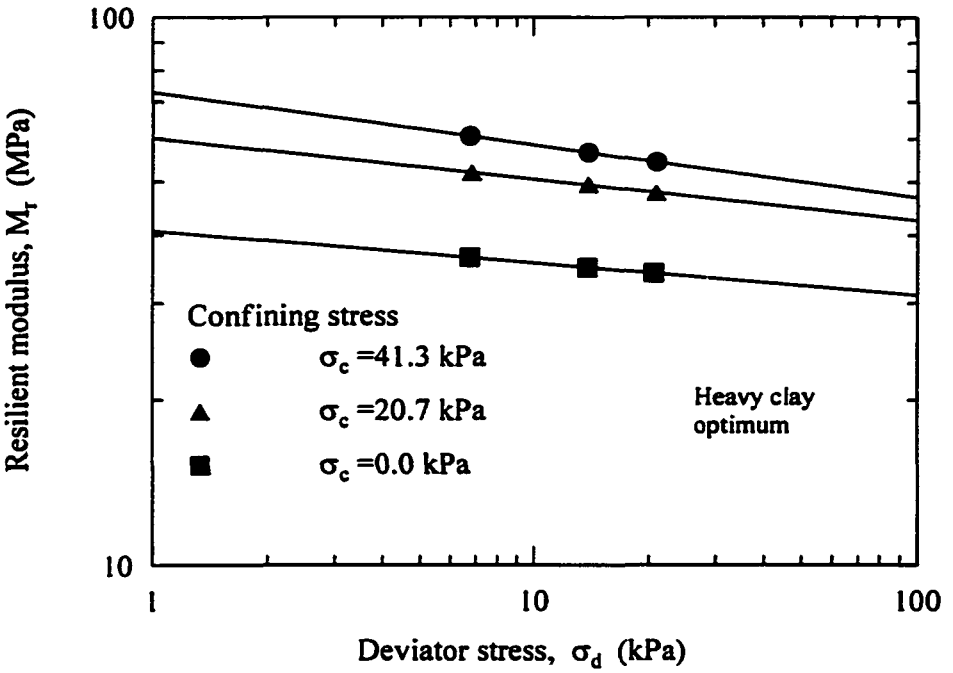

Figure 4.55 Resilient modulus of heavy clay at optimum

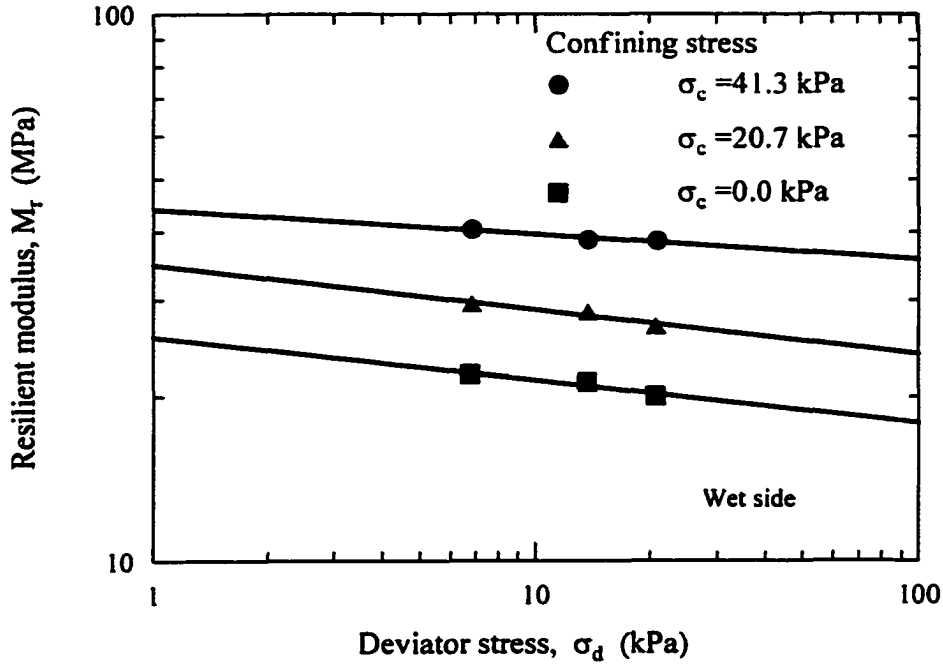

Figure 4.56 Resilient modulus of heavy clay at wet side

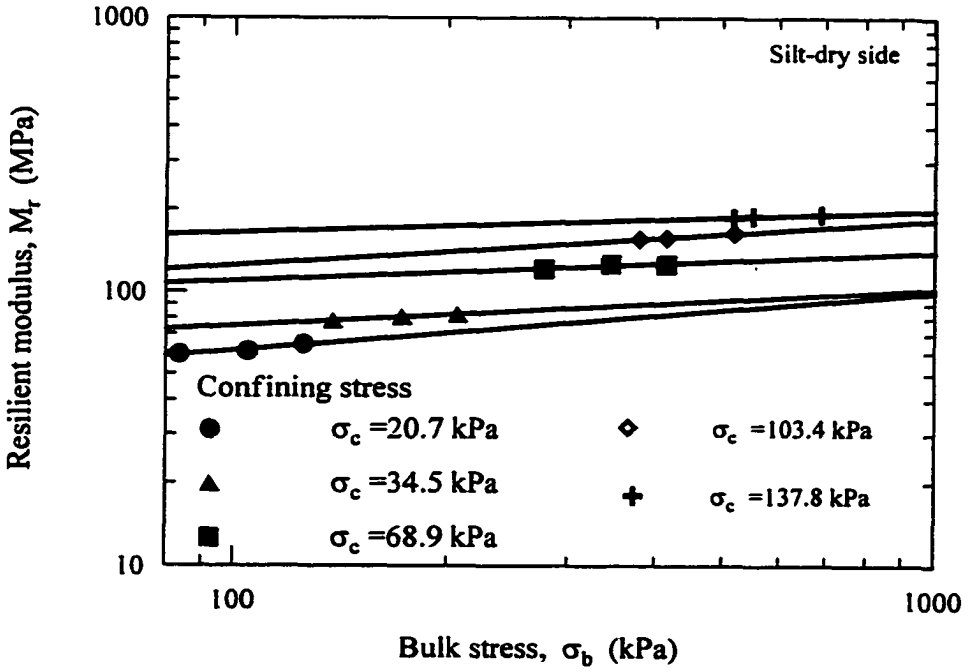

Figure 4.57 Resilient modulus of silt at dry side

Figure 4.58 presents the resilient modulus test results for sand at dry side. As expected, the resilient modulus of sand also increases with bulk stresses. The resilient modulus at wet side is lower than that at dry side due to the higher moisture content and lower stiffness at wet side. The highest resilient modulus occurs at optimum due to the highest stiffness at optimum.

4.5.5 Effect of Moisture Content and Unit Weight

After the cone penetration test, the soil sample was subjected to the moisture content and unit weight tests in different depths. For fine-grained soils and silt, unit weight was estimated by using the sand cone test (LADOTD TR 401-95). Along the depth of the soil sample, moisture contents were also obtained.

Moisture content, determined along the depth of soil sample of silty clay-dry side, showed an average value of 14.2 %, standard deviation of 0.3 %, and coefficient of variation of 1.8 % against the designed moisture content of 14.4 %. Coefficient of variation of moisture content for silty clay dry side, optimum, and wet side are 1.8 %, 1.7 %, and 1.5 %, respectively. Coefficient of variation of water content for heavy clay dry side, optimum, and wet side are 4.4 %, 2.2 %, and 1.3 % respectively. Coefficient of variation of water content for sand dry side, optimum, and wet side are 1.6 %, 3.7 %, and 5.8 %.

Dry unit weight determined along the soil sample depth of silty clay-dry side showed an average value of 15.9 kN/m^3, standard deviation of 0.2 kN/m^3, and coefficient of variation of 1.2 % against the designed unit weight 16.1 kN/m^3. Coefficient of variation of dry unit weight for silty clay dry side, optimum, and wet side are 1.2 %, 2.0 %, and 1.2 %, respectively. Coefficient of variation of dry unit weight for heavy clay

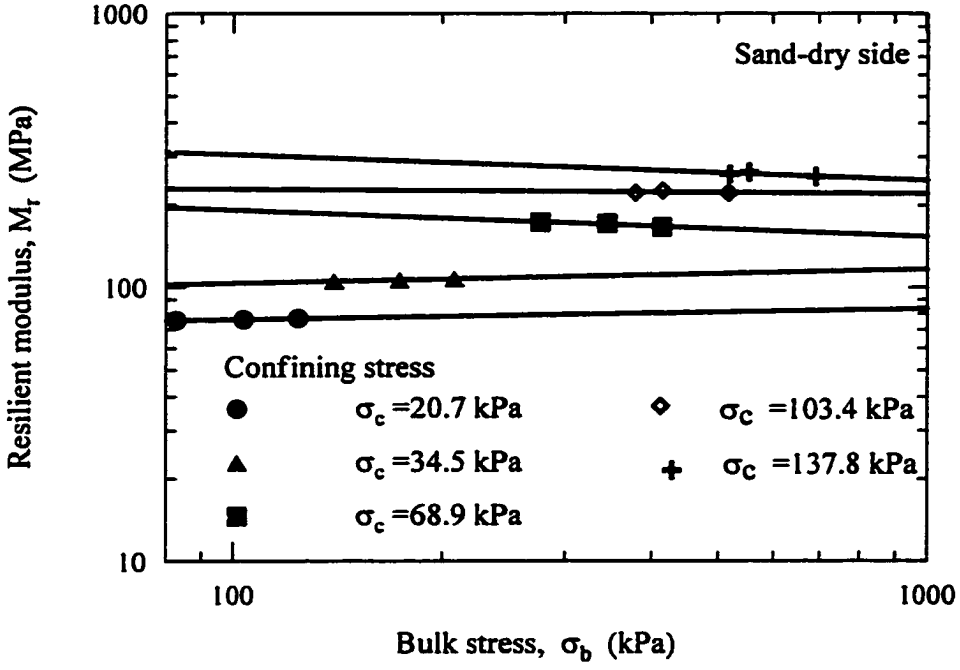

Figure 4.58 Resilient modulus of sand at dry side

dry side, optimum, and wet side are 5.0 %, 2.8 %, and 2.8 % respectively. Coefficient of variation of dry unit weight for silt dry side, optimum, and wet side are 2.4 %, 7.6 %, and 3.8 %. Coefficient of variation of dry unit weight for sand dry side, optimum, and wet side are 3.0 %, 6.2 %, and 2.2 %. This type of variation can be expected due to the layered compaction effects. Among the four soil types, the maximum coefficient of variation for tip resistance, water content, and dry unit weight are 25 %, 6 %, and 5 %, respectively.

Figures 4.59 and 4.60 depict the variation in the resilient modulus with the moisture content. In the wet side, as the moisture content increases effective deviator stress decreases and hence the resilient modulus decreases. In the wet side, soil fabric is dispersed whereas, in the dry side, soil is flocculated. Strength of the dispersed soil is less than that of flocculated soil. The resilient modulus is related to the strength of soil. In silty clay, the change in the resilient modulus in dry and wet sides was about 14 MPa for the change in moisture content of about 7 %. In heavy clay, the change in the resilient modulus in dry and wet sides was about 15 MPa for the change in moisture content of about 10 %. This may result in the change in the overlay thickness of a pavement significantly as explained in Section 4.6. Figures 4.61 and 4.62 indicate that as the unit weight increases the resilient modulus increases. But it decreases with the increasing moisture content. Figures 4.63 and 4.64 show the same behavior for the tip resistance. Therefore, the maximum resilient modulus and tip resistance occurred at the optimum.

4.5.6 Summary of the Laboratory Cone Testing

The laboratory cone test results were used to validate the proposed models, developed in the field testing program. The predicted and measured resilient modulus

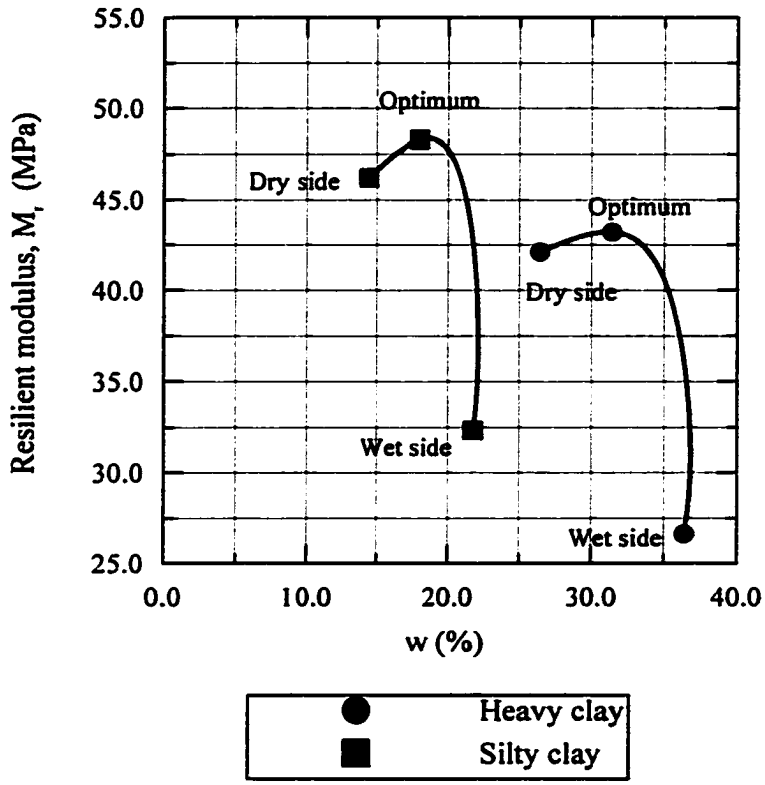

Figure 4.59 Variation in the resilient modulus with moisture content of fine-grained soil

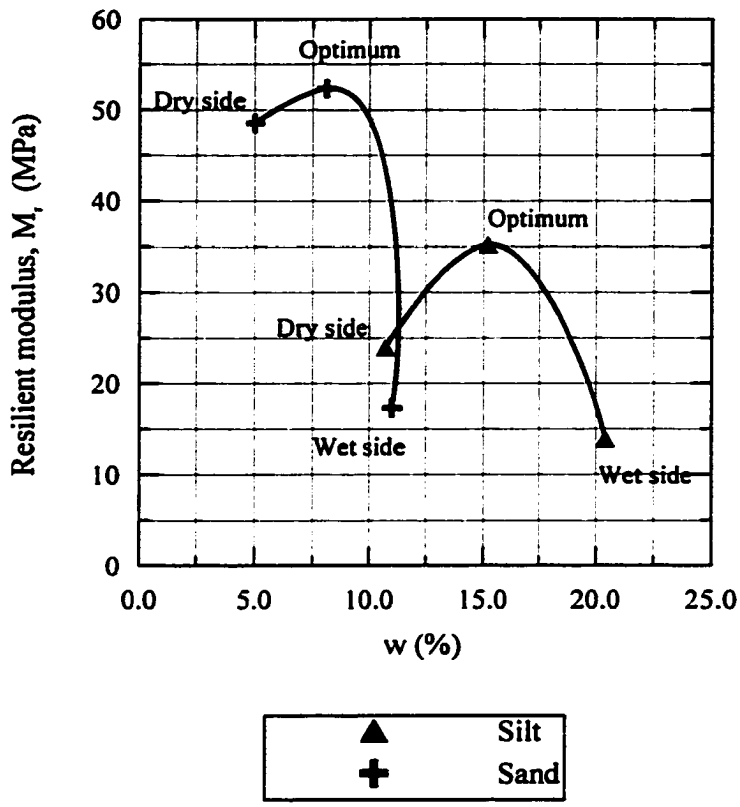

Figure 4.60 Variation in the resilient modulus with moisture content of coarse-grained soil

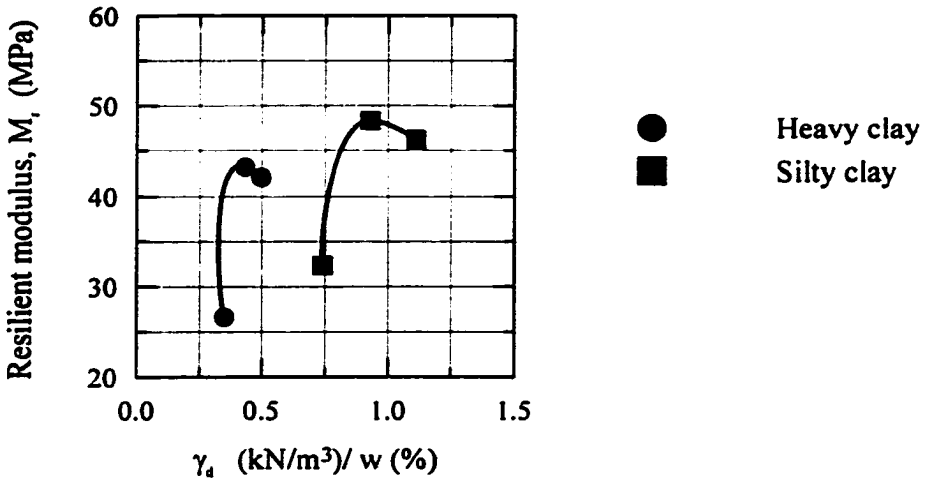

Figure 4.61 Variation of the moisture content, unit weight, and resilient modulus for fine-grained soil

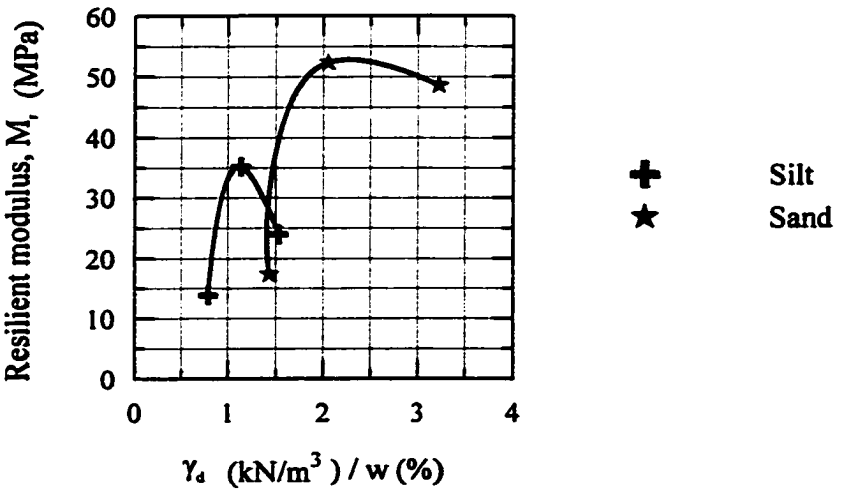

Figure 4.62 Variation of the moisture content, unit weight, and resilient modulus for coarse-grained soil

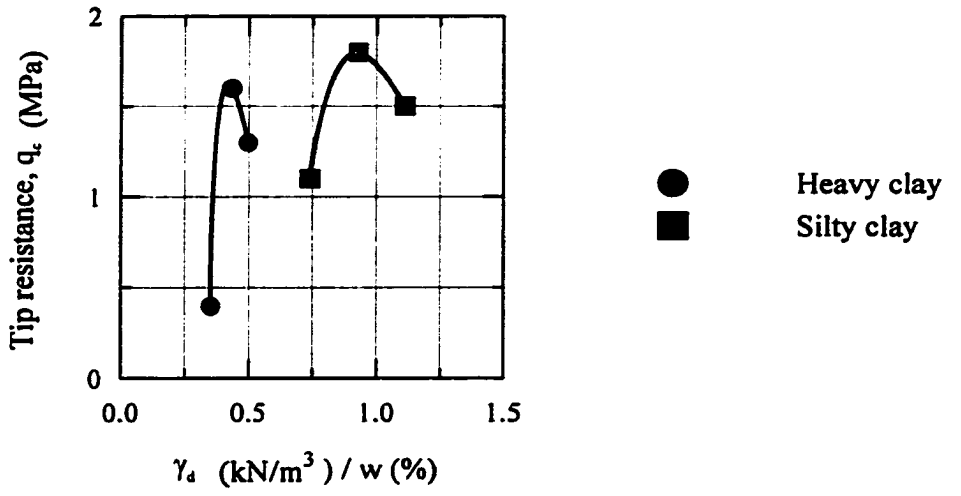

Figure 4.63 Variation of the moisture content, unit weight, and tip resistance for fine-grained soil

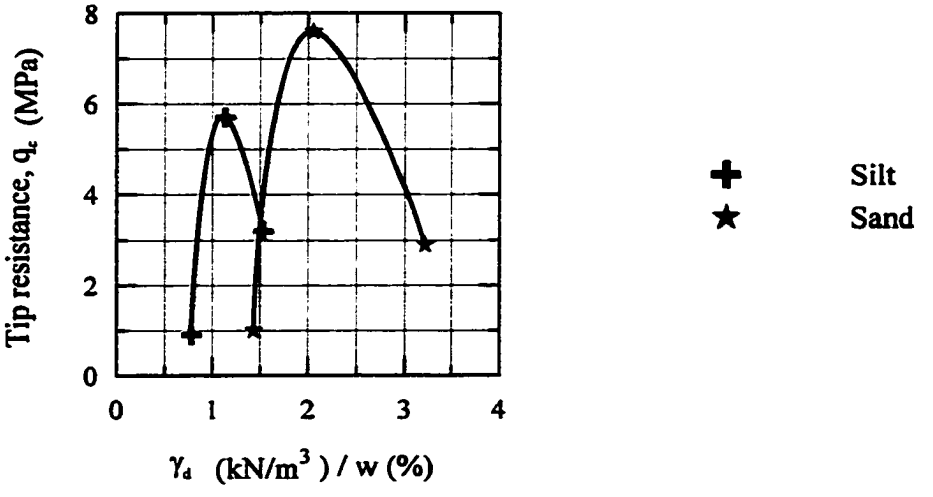

Figure 4.64 Variation of the moisture content, unit weight, and tip resistance for coarse-grained soil

values are presented in Figures 4.65 and 4.66. Most of the data fall close to the line of equality. The measured and predicted modulus values are not significantly different. Tables 4.9 and 4.10 present the result of the laboratory cone test.

Tables 4.5 and 4.11 present the elastic properties. The modulus of elasticity (E) were estimated from the laboratory repeated load triaxial testing. The Poisson's ratio (ν) was assumed.

4.5.7 Traffic Stress Analysis

The traffic stress models, given in equations (4.3) and (4.4), were applied to predict the resilient modulus of fine-grained soil using the laboratory cone test results. The predictions are presented in Figures 4.67 and 4.68. Most of the data fall close to the line of equality. The measured and predicted modulus values are not significantly different. The results of the stress analysis are presented in Table 4.10.

4.5.8 Preliminary Design Charts

From the laboratory resilient modulus and cone penetration test results, preliminary charts were developed to evaluate the resilient modulus from the cone penetration test parameters. But they were not verified due to lack of data. According to the type of soil, different resilient modulus and cone tip resistance can be obtained. The resilient modulus, moisture content, dry unit weight, and the cone tip resistance charts were prepared. Knowing the cone tip resistance, resilient modulus can be estimated from these charts. This may be useful in pavement designs as an estimation of the resilient modulus. Figures 4.69 to 4.76 present the simplified design charts for heavy clay, silty clay, silt, and sand respectively. As illustrated in Figure 4.69, when the soil type and the cone tip resistance are known, a chart for that soil type can be used for evaluating

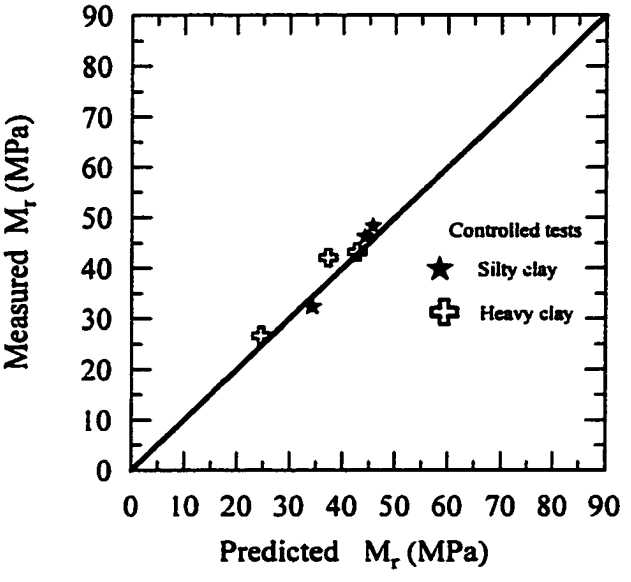

Figure 4.65 In-situ resilient modulus from the laboratory cone test for fine-grained soil

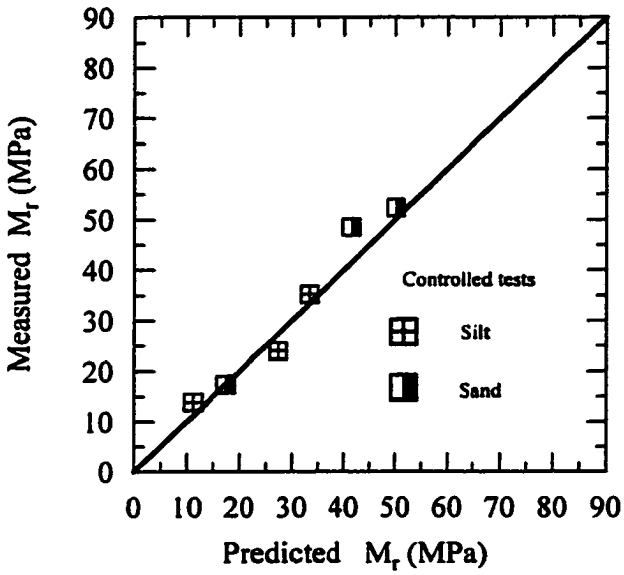

Figure 4.66 In-situ resilient modulus from the laboratory cone test for coarse-grained soil

Table 4.9 Summary of the laboratory cone test results

		Depth (m)	q_c (MPa)	f_s (MPa)	σ_c (kPa)	σ_v (kPa)	w (%)	γ_d (kN/m^3)
Silty clay	dry	0.31	1.5	0.0763	3.58	5.72	14.4	16.1
	opt.	0.31	1.8	0.0816	3.82	6.11	18.0	16.7
	wet	0.31	1.1	0.0705	3.80	6.08	21.8	16.1
Heavy clay	dry	0.31	1.3	0.0758	3.93	5.19	26.4	13.1
	opt.	0.31	1.6	0.1060	4.20	5.54	31.4	13.6
	wet	0.31	0.4	0.0965	4.09	5.40	36.4	12.8
Silt	dry	0.31	3.2	0.1622	3.03	5.72	10.7	16.4
	opt.	0.31	5.7	0.0032	3.28	6.17	15.2	17.2
	wet	0.31	0.9	0.0010	3.15	5.93	20.4	15.9
Sand	dry	0.31	2.9	0.0010	2.79	5.25	5.0	16.1
	opt.	0.31	7.6	0.0087	2.92	5.50	8.1	16.4
	wet	0.31	1.0	0.0300	2.86	5.39	11.0	15.7

Legend: M_r- resilient modulus, σ_c- confining (minor principal) stress, σ_v- vertical (major principal) stress, f_s- sleeve friction, w- water content, γ_d- dry unit weight, γ_w- unit weight of water, and q_c- cone resistance.

Table 4.10 Stress analysis for the laboratory cone tests

Soil type		Depth (m)	Controlled test-insitu			Controlled test-insitu & traffic		
			σ_c (kPa)	σ_d (kPa)	M_r (MPa)	σ_c (kPa)	σ_d (kPa)	M_r (MPa)
Silty clay	dry	0.31	3.58	2.14	46.20	7.88	11.30	39.36
	opt.	0.31	3.82	2.29	48.30	8.12	11.50	48.84
	wet	0.31	3.80	2.28	32.33	8.10	11.50	29.93
Heavy clay	dry	0.31	3.93	1.26	42.09	9.31	7.27	44.06
	opt.	0.31	4.20	1.34	43.20	9.62	7.37	42.67
	wet	0.31	4.09	1.31	26.63	9.43	7.43	25.08
Silt	dry	0.31	3.03	2.69	23.94	6.88	10.70	35.28
	opt.	0.31	3.28	2.89	35.18	7.15	10.90	40.21
	wet	0.31	3.15	2.78	13.85	7.04	10.80	18.00
Sand	dry	0.31	2.79	2.46	48.52	6.58	12.10	53.92
	opt.	0.31	2.92	2.58	52.35	6.63	12.10	57.84
	wet	0.31	2.86	2.53	17.27	6.49	12.00	23.31

Legend: σ_c - Confining stress , σ_d - Deviator stress, M_r - Resilient modulus

Table 4.11 Elastic properties of the soil

Elastic Property	*PRF*- Silt	Sand
E (MPa)	27.1	45.9
ν	0.35	0.35

Legend: E- Elastic modulus, ν- Possion's ratio

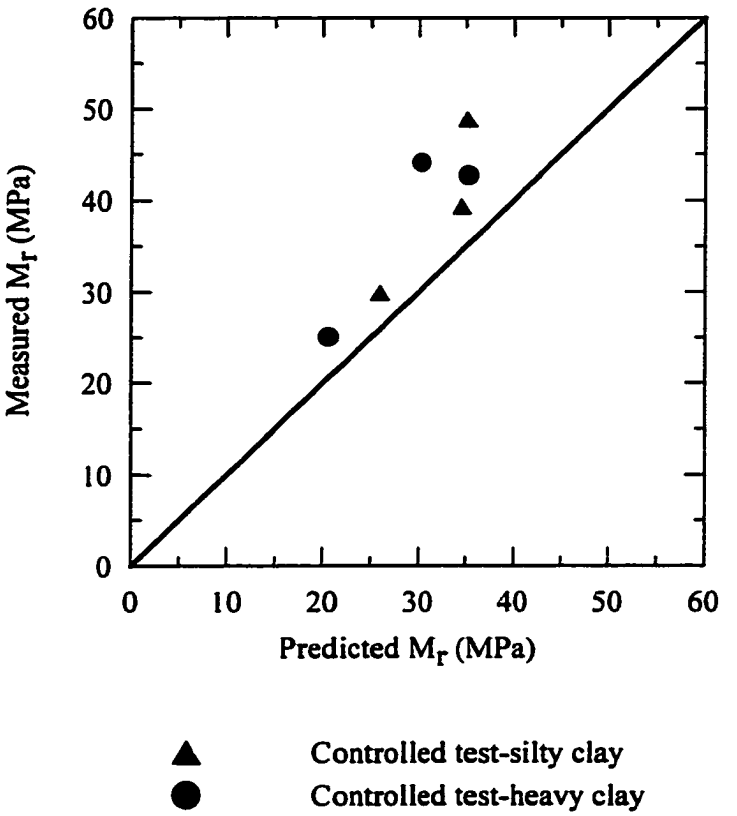

Figure 4.67 Prediction of resilient modulus from the traffic stress model for fine-grained soil

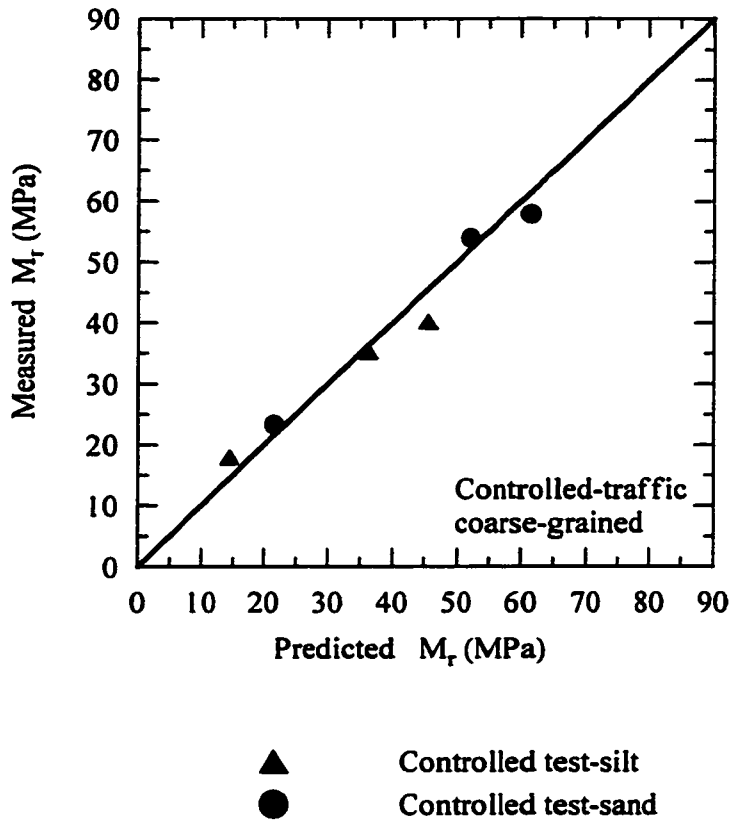

Figure 4.68 Prediction of resilient modulus from the traffic stress model for coarse-grained soil

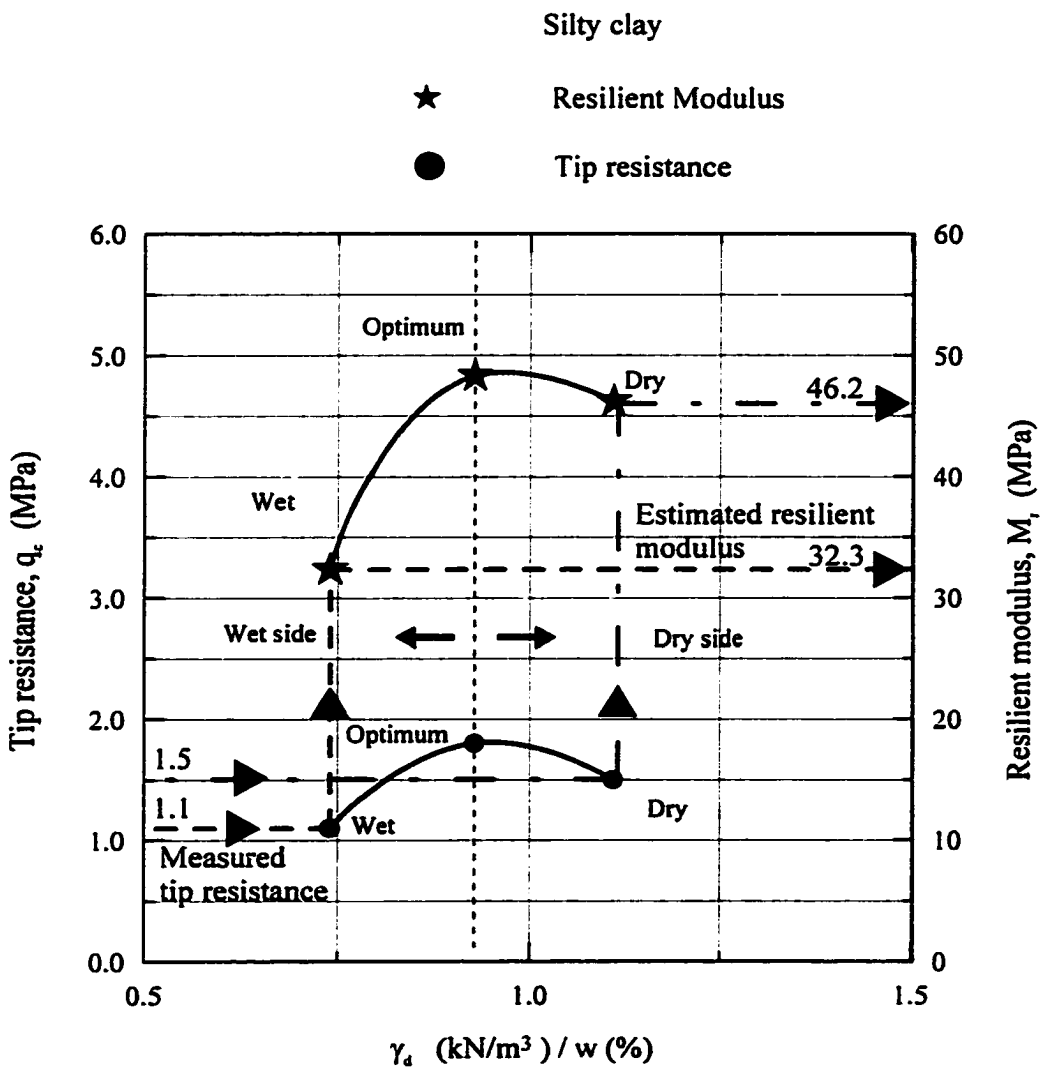

Figure 4.69 A chart for estimating in-situ resilient modulus of silty clay from cone penetration

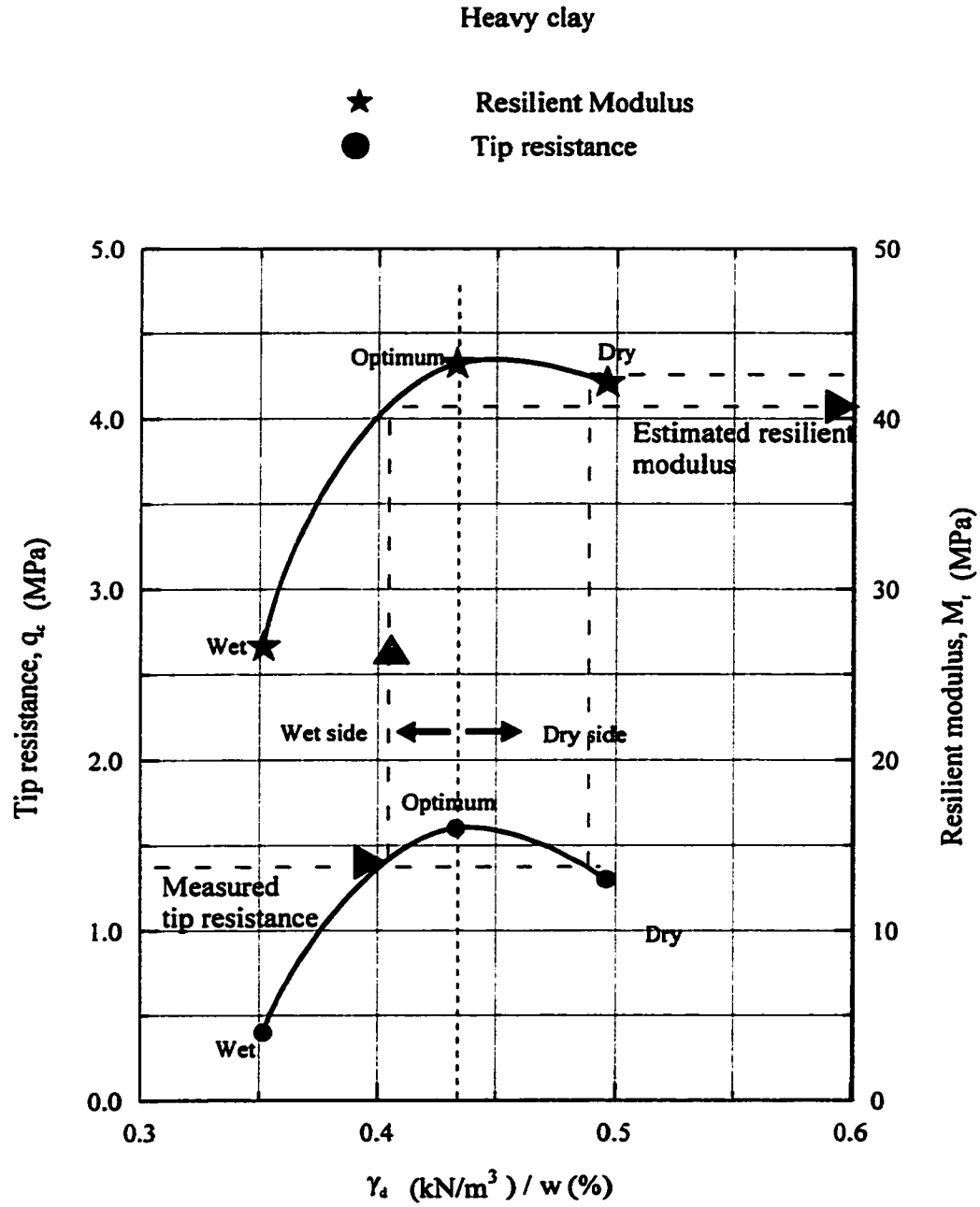

Figure 4.70 A chart for estimating in-situ resilient modulus of heavy clay from cone penetration

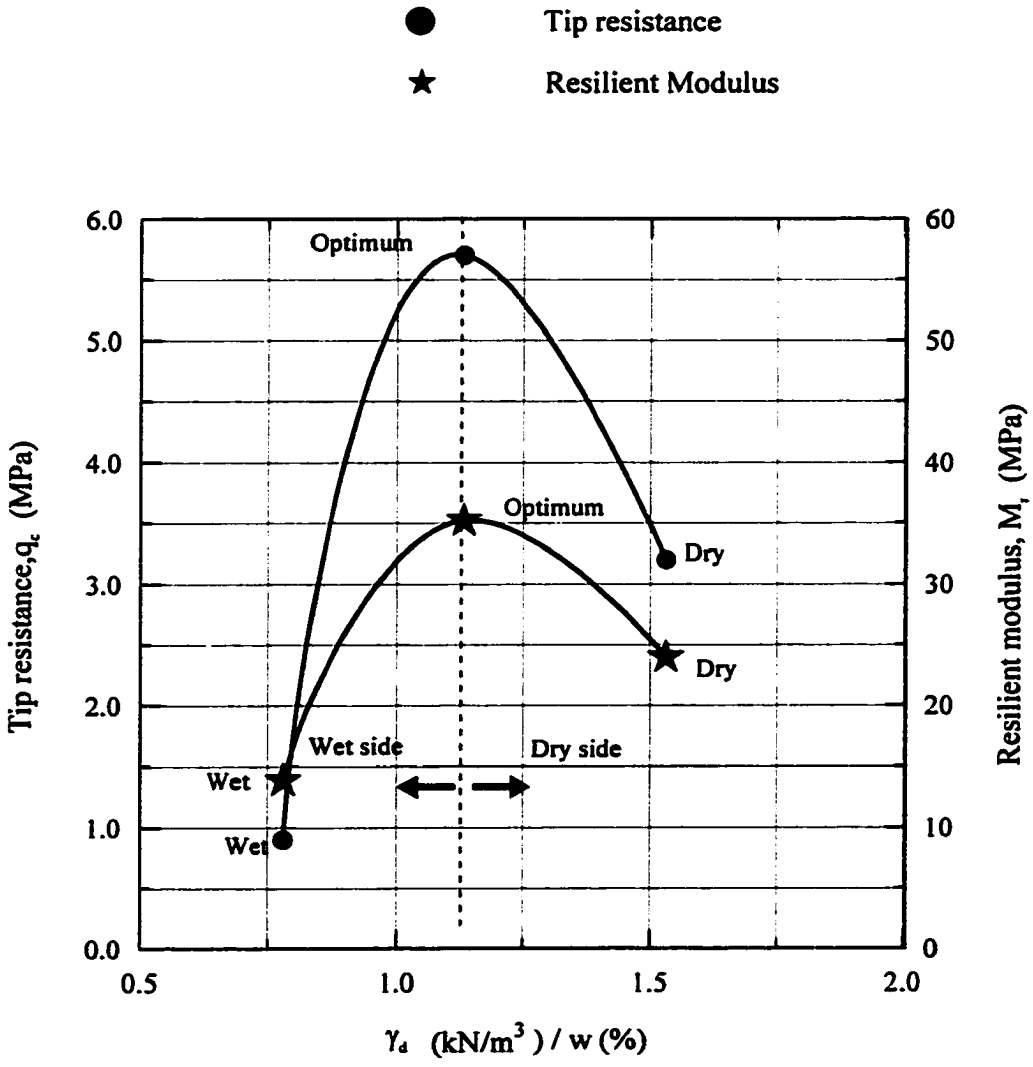

Figure 4.71 A chart for estimating in-situ resilient modulus of silt from cone penetration

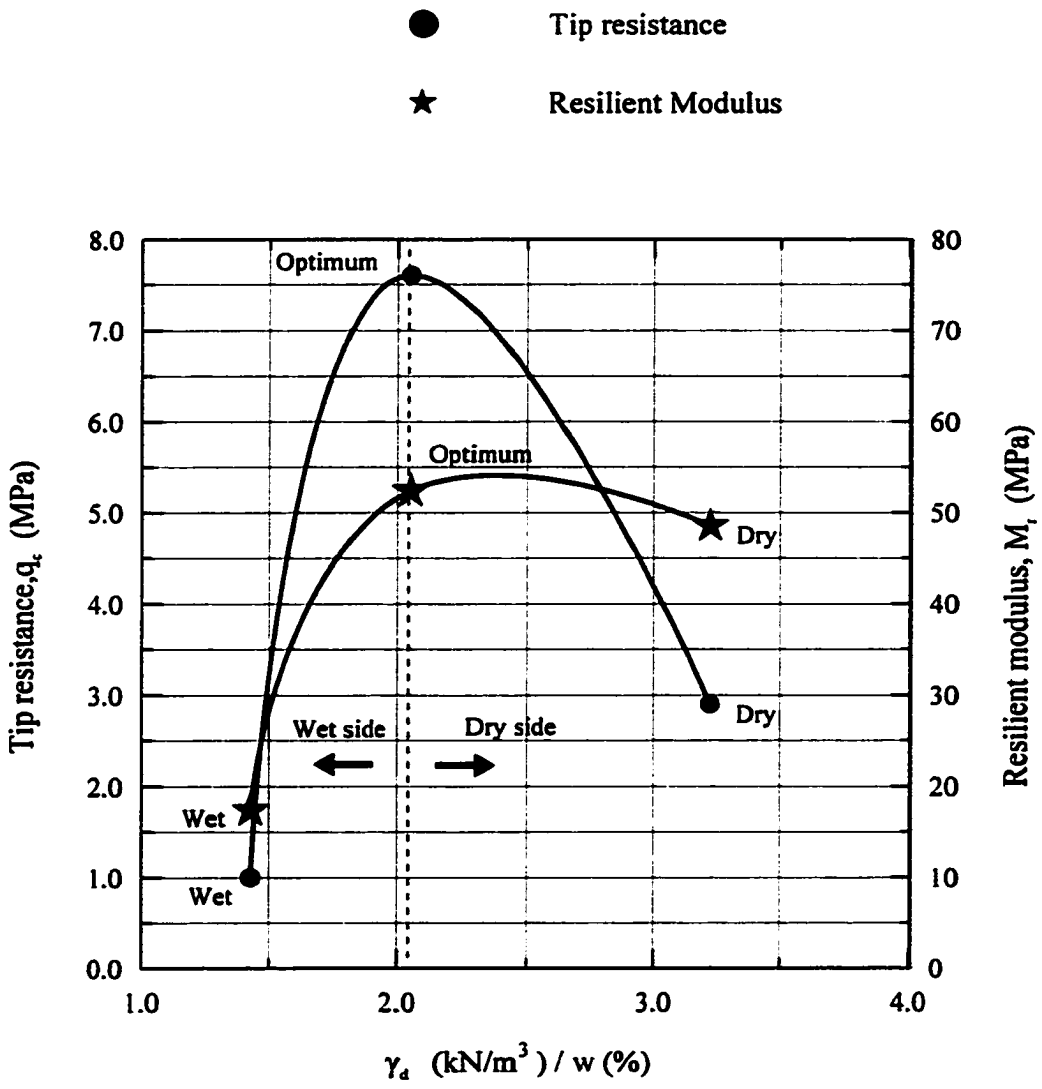

Figure 4.72 A chart for estimating in-situ resilient modulus of sand from cone penetration

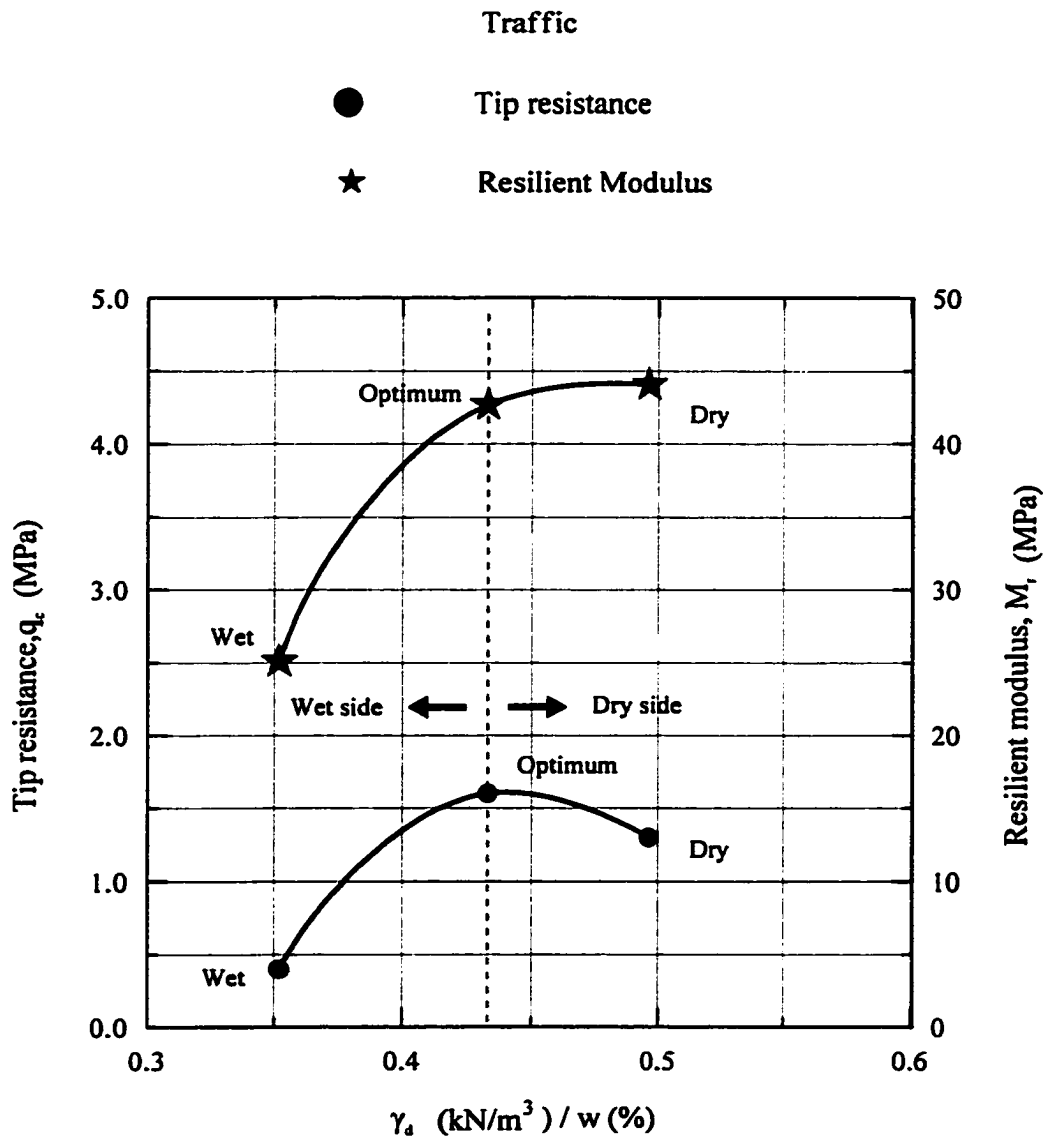

Figure 4.73 A chart for estimating resilient modulus of heavy clay from cone penetration under traffic stress

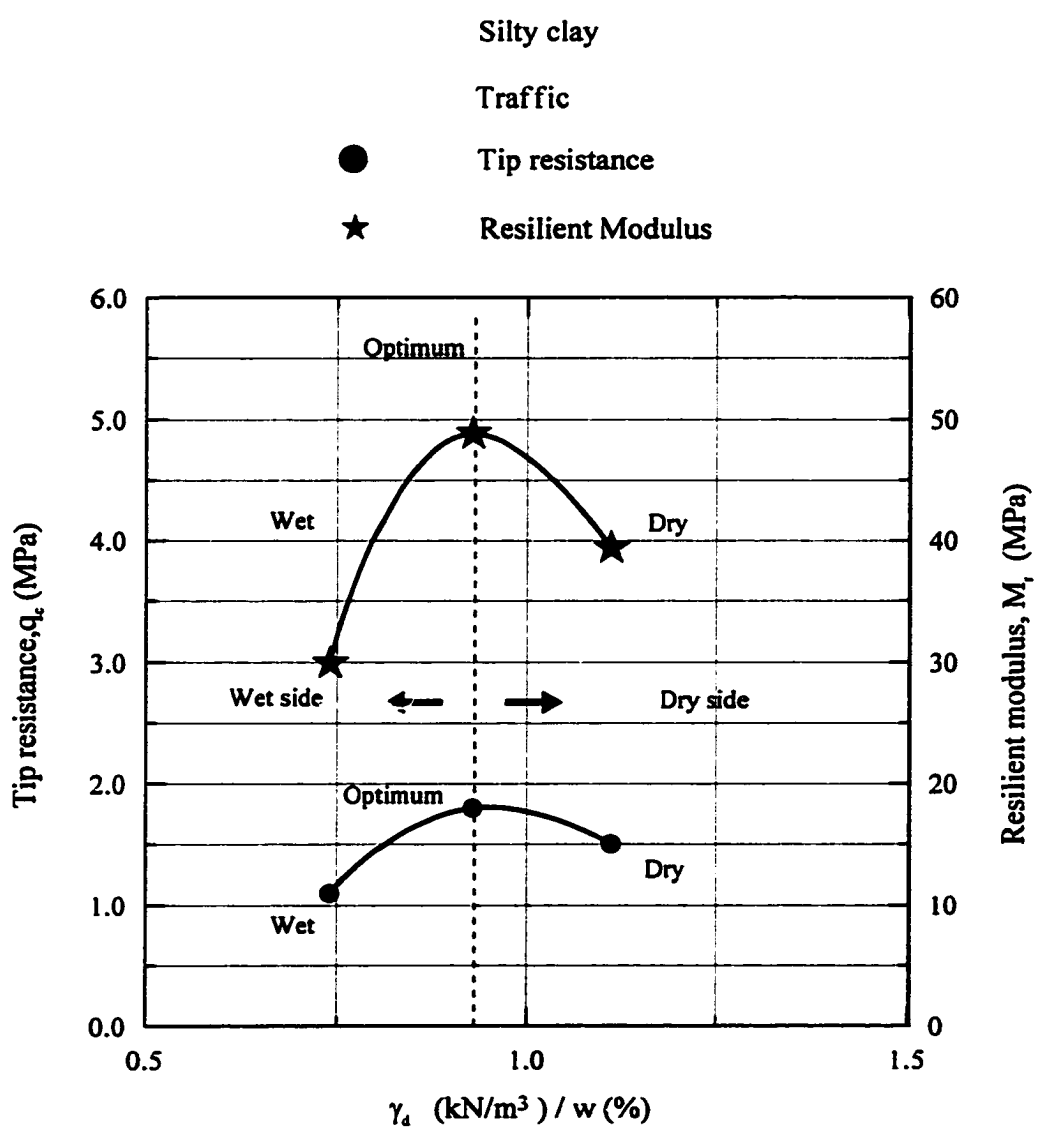

Figure 4.74 A chart for estimating resilient modulus of silty clay from cone penetration under traffic stress

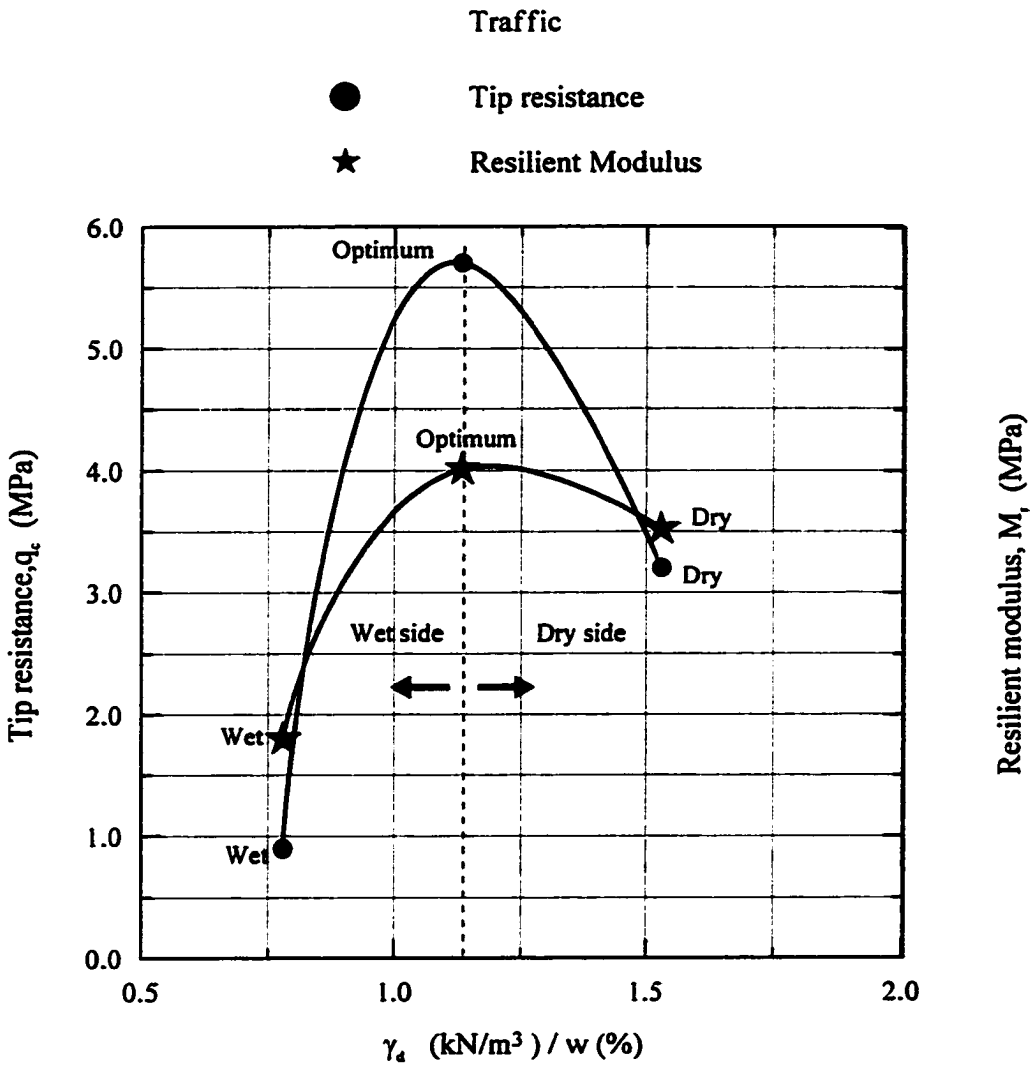

Figure 4.75 A chart for estimating resilient modulus of silt from cone penetration under traffic stress

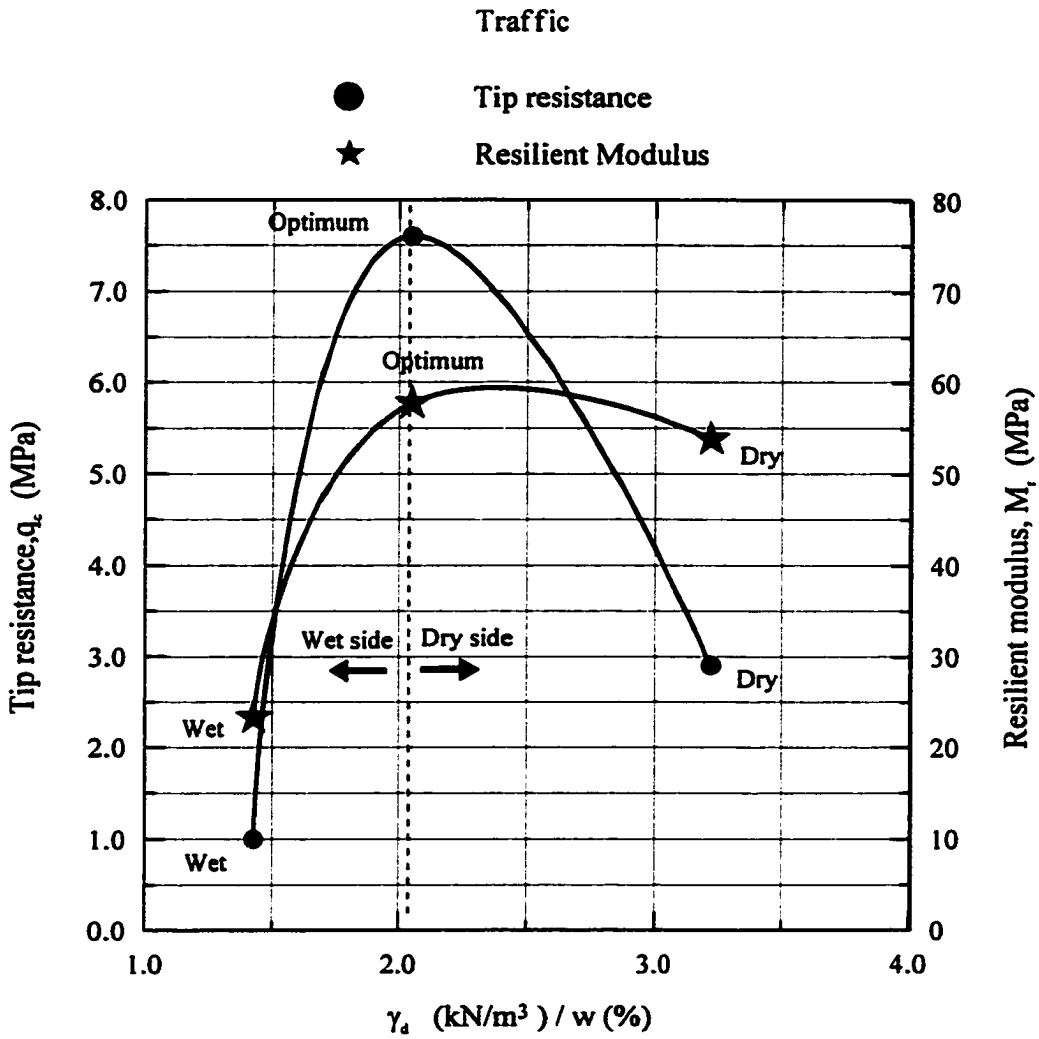

Figure 4.76 A chart for estimating resilient modulus of sand from cone penetration under traffic stress

the resilient modulus. In the absence of the moisture content and dry unit weight, these charts can still be used. But in this case, an approximate moisture content is to be guessed in order to assign the data point in the dry, optimum, or wet side in the moisture-unit weight curve. Otherwise, except at optimum, it is recommended that an average value of two resilient moduli be considered, corresponding to the dry and wet side. When the soil type is uncertain or unknown, a visual inspection or other engineering judgement is required to be classified as heavy clay, silty clay, silt, or sand.

How to use the chart (refer to Figures 4.69 to 4.76):

(1) Select the corresponding tip resistance from the field cone penetration test.

(2) To determine dry side or wet side, read the corresponding dry unit weight (kN/m^3) to moisture content (%) ratio from the chart of corresponding soil type.

(3) Read the corresponding resilient modulus from the chart.

(4) If the moisture content or dry unit weight is unknown, read the two resilient modulus values, except at the optimum, corresponding to the dry and wet side. Then take the average as the required value. This will provide a reasonable guess for the resilient modulus.

4.5.8.1 A Chart for Estimating Effective Subgrade Soil Resilient Modulus Using the Serviceability Criteria

The AASHTO guide for design of pavement structures (1993) stipulates analysis the subgrade soil for different moisture seasons in a year, such as dry and rainy, to estimate an effective resilient modulus for design purpose. Covering the primary moisture seasons, such as dry and rainy, the resilient modulus tests (AASHTO T- 294) should be performed on roadbed soil samples. By knowing the seasonal resilient moduli

of roadbed soil, the relative damage (U_r) of the pavement can be estimated. From the relative damage, an effective resilient modulus value for flexible pavements can be obtained by using the design charts and equations provided by the AASHTO guide for design of pavement structures. The same design charts were used while being modified the estimation of the resilient modulus from the cone penetration test results. This procedure consists of performing several cone penetration tests in different moisture seasons in a year, estimating corresponding moisture content, unit weight of soil, and soil stresses. Seasonal resilient modulus for each month can be evaluated by using a correlation or charts proposed in this study. The relative damage can be estimated by the equation (4.5), given in the AASHTO guide for design of pavement structures (1993). The effective design resilient modulus can be estimated from the average relative damage and the AASHTO equation. The effective roadbed resilient modulus, corresponding to the average relative damage, can be estimated.

Steps in this procedure:

1. As shown Figure 4.77, divide a year into one-month or one-half month seasons. All the seasons (time periods in the chart) in a year must be equal.

2. Allocate the seasonal tip resistance, sleeve friction, moisture content, dry unit weight, confining stress, and deviator stress in their respective time slots.

3. Compute the seasonal roadbed resilient modulus by using a correlation or charts proposed in this study.

4. Estimate the relative damage by using the charts or equations given in the AASHTO guide for design of pavement structures (1993).

5. Add the all relative damage values and compute an average relative damage value.

Month	q_c (MPa)	f_s (MPa)	w (%)	γ_d (kN/m^3)	σ_c (kPa)	σ_d (kPa)	M_r (psi)	U_r
Jan.								
Feb.								
March								
April								
May								
June								
July								
August								
Sept.								
Oct.								
Nov.								
Dec.								
Total								ΣU_r

Legend: U_r-relative damage, n - number of months, M_r- resilient modulus (*psi*)

Figure 4.77 A chart for estimating effective roadbed soil resilient modulus using the serviceability criteria

6. Estimate an effective resilient modulus, corresponding to the average relative damage, by using the charts or equations given in the AASHTO guide for design of pavement structures (1993).

In the case of rigid pavements, an effective modulus of subgrade reaction (k-value) must be calculated from the seasonal roadbed soil resilient modulus with the aid of the charts or equations given in the AASHTO guide for design of pavement structures.

Average relative damage $U_r = \frac{\sum U_r}{n}$ (4.5)

The AASHTO equation for relative damage,

$$U_r = 1.18x10^8 x M_r^{-2.32} \quad (4.6)$$

4.5.8.2 An Example for Using the Proposed Charts

The summary of the data for silty clay, used to characterize the subgrade soil resilient modulus, is presented in Table 4.12. A year is divided into 24 half-month seasons. The wet seasons are from mid-January to May and mid-September to mid-December. The dry seasons are from June to mid-September and mid-December to mid-January.

Table 4.12 Cone penetration and soil test data for silty clay

Test parameter	q_c (MPa)	f_s (MPa)	w (%)	γ_d (kN/m^3)	σ_c (kPa)	σ_d (kPa)
dry season	1.5	0.0763	14.4	16.1	3.58	2.14
wet season	1.1	0.0705	21.8	16.1	3.80	2.28

Legend: M_r- resilient modulus, σ_c- confining (minor principal) stress, σ_v- vertical (major principal) stress, f_s- sleeve friction, w- water content, γ_d- dry unit weight, γ_w- unit weight of water, and q_c- tip resistance

The resilient modulus values are estimated from the chart given in Figure 4.69 for silty clay for in-situ condition. The resilient modulus values are 46.2 MPa (6705 psi) and 32.3 MPa (4688 psi) for dry and wet seasons respectively.

From Figure 4.78, Average relative damage = $\frac{6.798}{24}$ = 0.28

Effective subgrade soil resilient modulus = 5200 (psi) = 35.8 (MPa)

4.6 Sensitivity of the AASHTO Flexible Pavement Design Equation

The effect of change in the subgrade soil resilient modulus on the AASHTO flexible pavement design equation is analyzed. The AASHTO design equation:

$$\log_{10} W_{18} = Z_R S_o + 9.36 \log_{10}(SN+1) - 0.20 + \frac{\log_{10}\left(\frac{\Delta PSI}{4.2-1.5}\right)}{0.40 + \frac{1094}{(SN+1)^{5.19}}} + 2.32 \log_{10} M_r - 8.07 \qquad (4.7)$$

(after AASHTO, 1993)

where,

W_{18}- predicted number of 18-kip equivalent single axle load (ESAL),

Z_R - standard deviation, SN- structural number,

R- reliability,

S_o- combined standard error of the traffic prediction and performance prediction,

M_r- effective resilient modulus of subgrade soil, and

ΔPSI- difference between the initial design serviceability index and the design terminal serviceability index.

The AASHTO design equation is iteratively evaluated for a typical pavement section, as shown in Figure 4.79, by varying the value of the overlay thickness while

Month	q_c (MPa)	f_s (MPa)	w (%)	γ_d (kN/m^3)	σ_c (kPa)	σ_d (kPa)	M_r (psi)	U_r
Jan.	1.5	0.0763	14.4	16.1	3.58	2.14	6705	0.157
	1.1	0.0705	21.8	16.1	3.80	2.28	4688	0.359
Feb.	1.1	0.0705	21.8	16.1	3.80	2.28	4688	0.359
	1.1	0.0705	21.8	16.1	3.80	2.28	4688	0.359
March	1.1	0.0705	21.8	16.1	3.80	2.28	4688	0.359
	1.1	0.0705	21.8	16.1	3.80	2.28	4688	0.359
April	1.1	0.0705	21.8	16.1	3.80	2.28	4688	0.359
	1.1	0.0705	21.8	16.1	3.80	2.28	4688	0.359
May	1.1	0.0705	21.8	16.1	3.80	2.28	4688	0.359
	1.1	0.0705	21.8	16.1	3.80	2.28	4688	0.359
June	1.5	0.0763	14.4	16.1	3.58	2.14	6705	0.157
	1.5	0.0763	14.4	16.1	3.58	2.14	6705	0.157
July	1.5	0.0763	14.4	16.1	3.58	2.14	6705	0.157
	1.5	0.0763	14.4	16.1	3.58	2.14	6705	0.157
Aug.	1.5	0.0763	14.4	16.1	3.58	2.14	6705	0.157
	1.5	0.0763	14.4	16.1	3.58	2.14	6705	0.157
Sept.	1.5	0.0763	14.4	16.1	3.58	2.14	6705	0.157
	1.1	0.0705	21.8	16.1	3.80	2.28	4688	0.359
Oct.	1.1	0.0705	21.8	16.1	3.80	2.28	4688	0.359
	1.1	0.0705	21.8	16.1	3.80	2.28	4688	0.359
Nov.	1.1	0.0705	21.8	16.1	3.80	2.28	4688	0.359
	1.1	0.0705	21.8	16.1	3.80	2.28	4688	0.359
Dec.	1.1	0.0705	21.8	16.1	3.80	2.28	4688	0.359
	1.5	0.0763	14.4	16.1	3.58	2.14	6705	0.157
Total								6.798

Figure 4.78 Estimation of the effective resilient modulus from the cone test parameters

keeping the design ESAL constant. The design variables are as follows. W_{18}= 5,000,000 ESALs, R= 95 %, S_o= 0.35, ΔPSI= 1.9, and design M_r= 34.5 MPa. This results in SN = 5. Layer coefficients are assumed as a_1= 0.42, a_2= 0.16 and a_3=0.10 for the surface course, base, and subbase respectively. The effect of variation in the resilient modulus on the overlay thickness is presented in Figure 4.80. According to Figure 4.80, variation in the resilient modulus may have a significant effect on the overlay thickness. Therefore selecting a correct design resilient modulus is desired in pavement design.

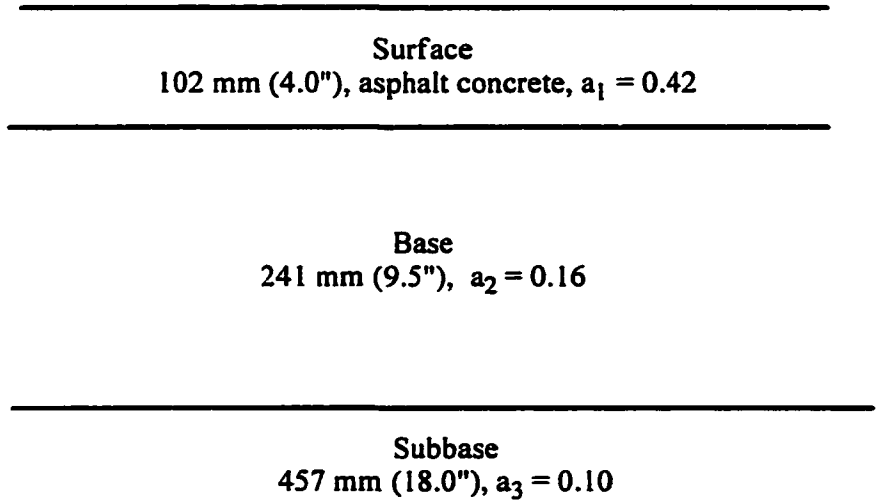

Figure 4.79 A typical pavement section

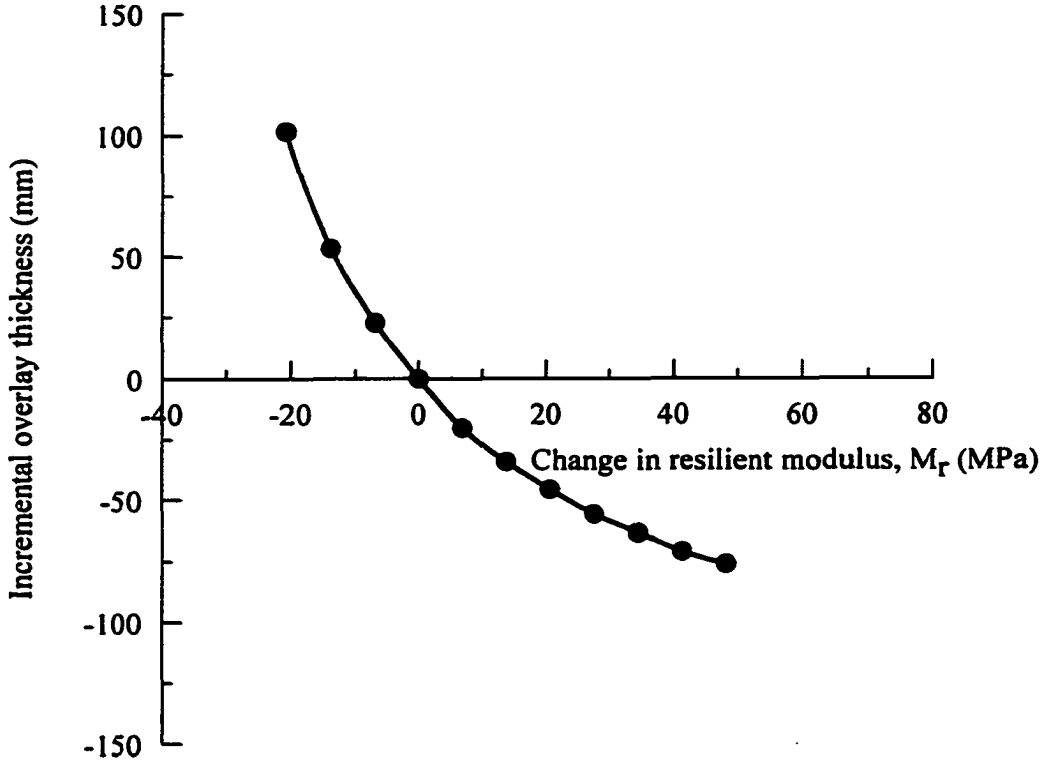

Figure 4.80 Variation in the overlay thickness with the resilient modulus

CHAPTER 5

FIELD APPLICATION OF THE PROPOSED MODELS

After development and verification of the proposed models, a successful attempt has been made to apply them in road rehabilitation projects in Louisiana with the support of Louisiana Department of Transportation and Development.

Resilient modulus is an input parameter for evaluating the structural number (SN) in flexible pavement designs. The CPT can also be used in a rehabilitation project of an existing pavement for evaluating the resilient modulus of subgrade soil. In this case, for the required traffic, reliability, initial serviceability, and terminal serviceability, a new structural number, based on the resilient modulus, can be estimated. By knowing the existing structural number, the difference in the structural numbers can be determined. Then required overlay thickness can be estimated.

For example, the developed correlations were applied in the road rehabilitation projects at Louisiana State Route LA-482, LA-513, and Henderson levee road. Several undisturbed soil samples were retrieved from the subgrade of these rehabilitation sites. These samples were tested for resilient modulus (AASHTO T- 294) and other soil properties in the laboratory according to the procedures described previously. The proposed correlations were also used to predict the resilient modulus. Then the measured and predicted resilient modulus were compared. Figures 5.1, 5.2, and 5.3 present the cone penetration test results of the LA-482 , LA-513, and Henderson levee road respectively. Figures 5.4, 5.5, and 5.6 show the resilient modulus test results of the LA-482 , LA-513, and Henderson levee road respectively. Figures 5.7 and 5.8 compare the measured and predicted resilient modulus under in-situ and traffic loading conditions

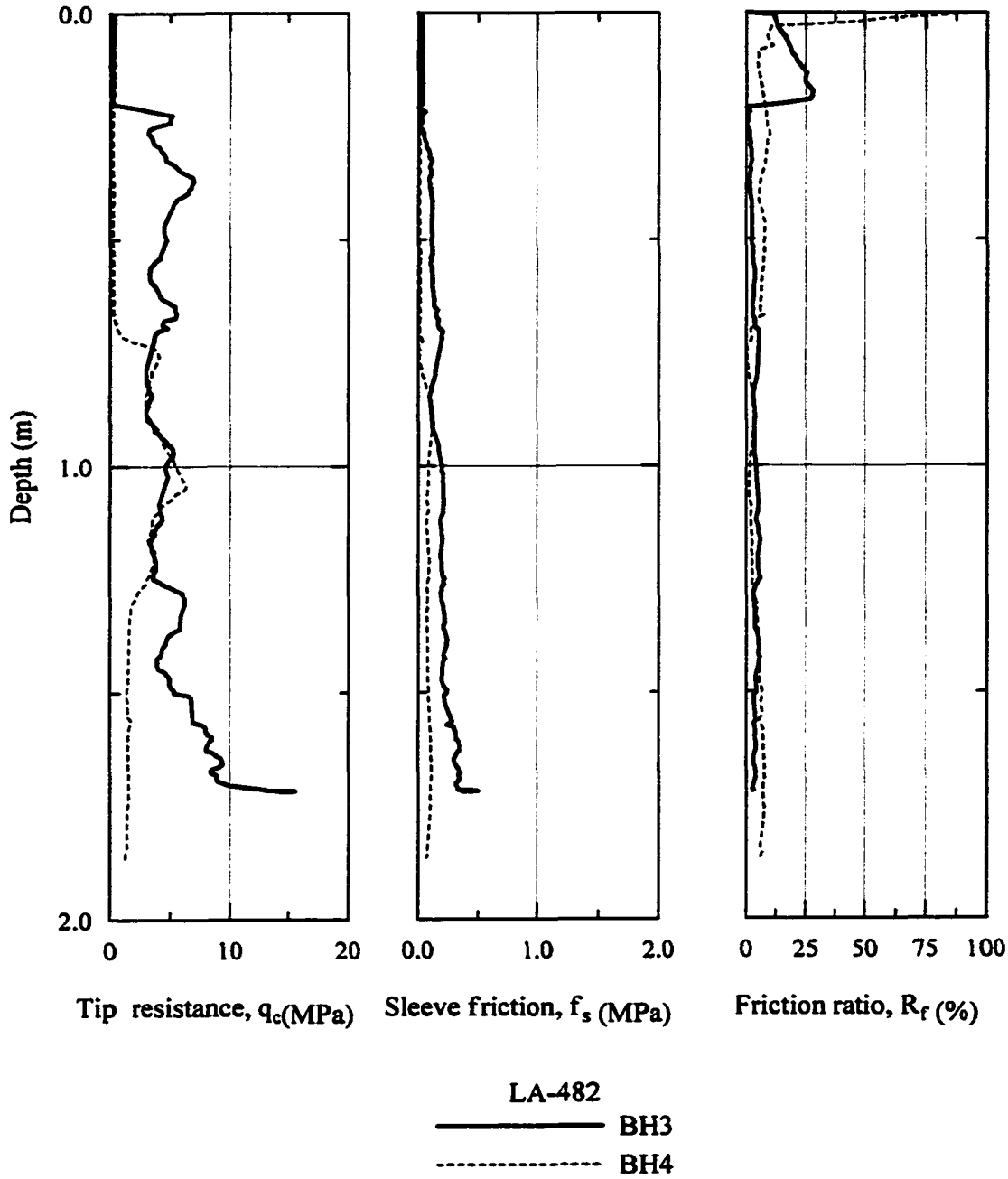

Figure 5.1 Cone penetration test results of the LA-482

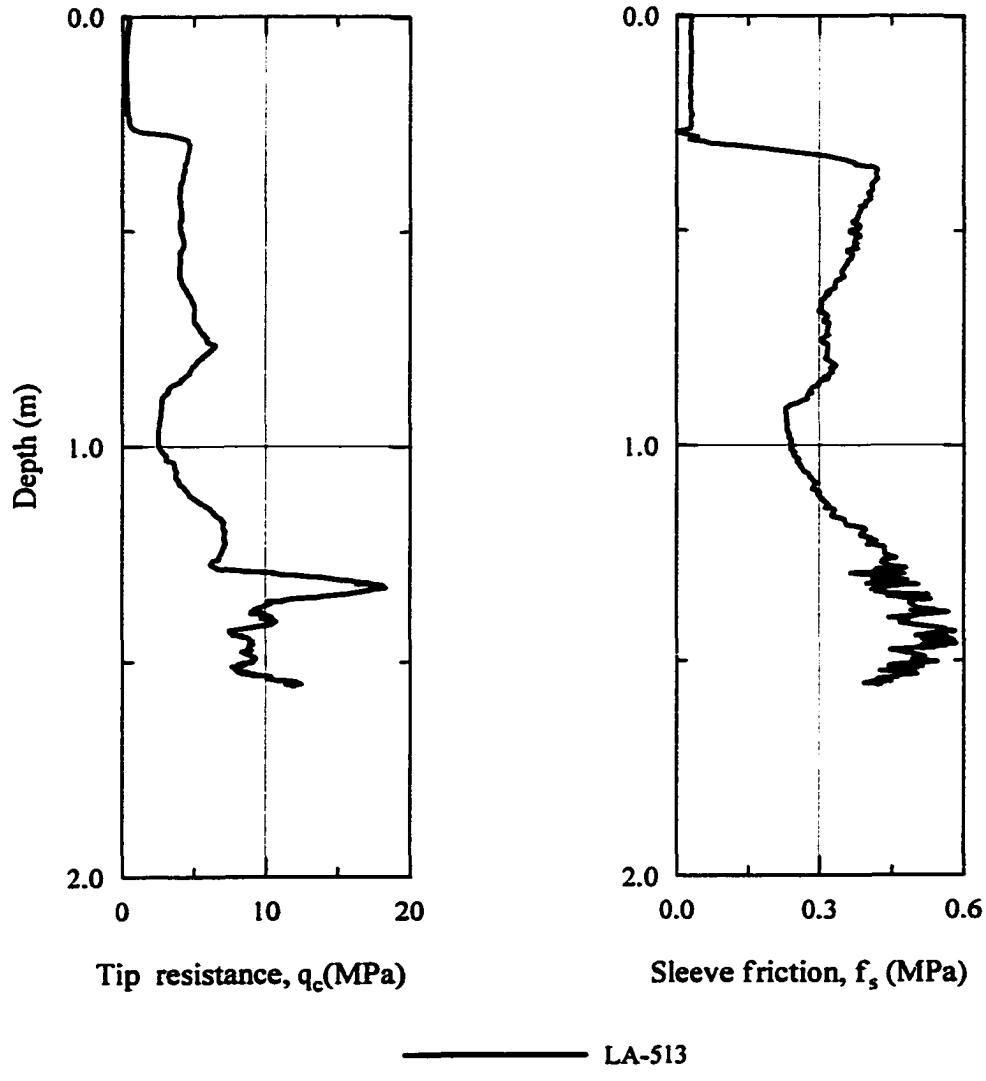

Figure 5.2 Cone penetration test results of the LA-513

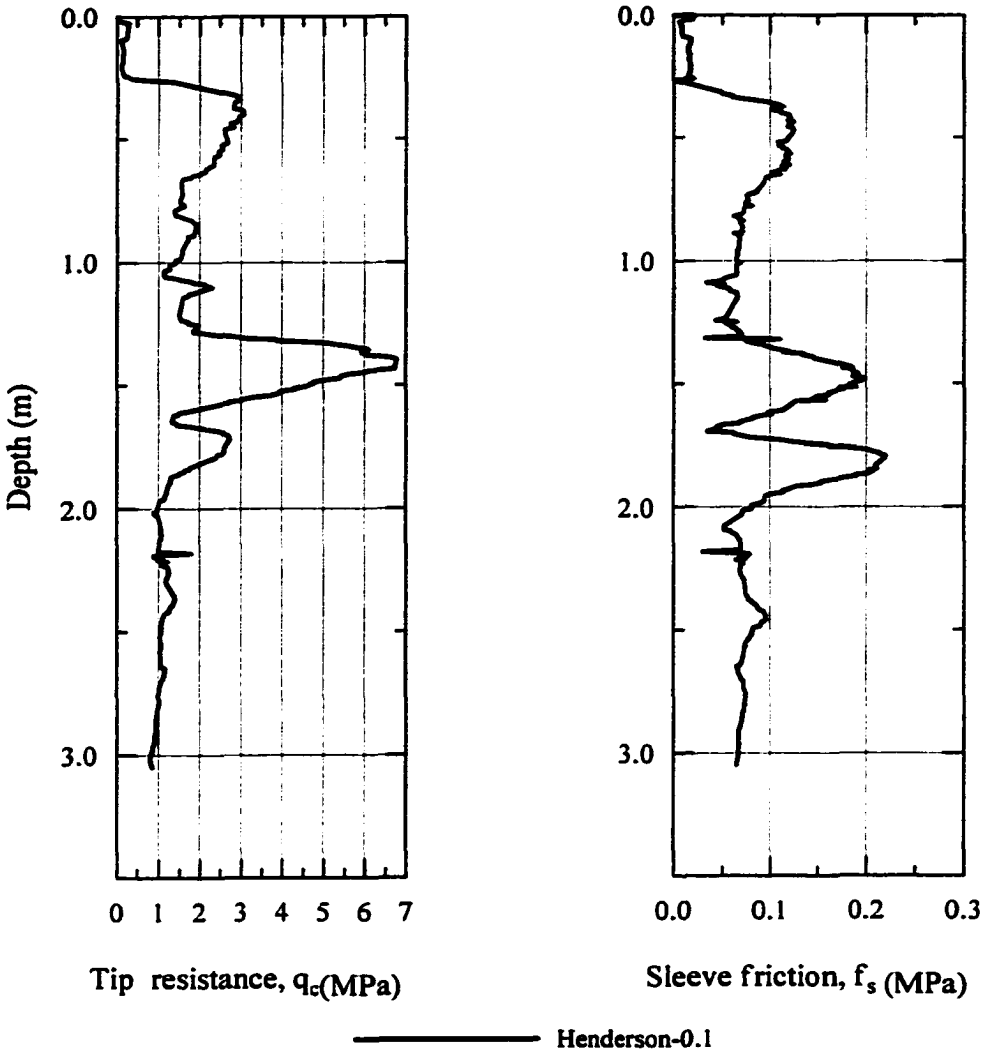

Figure 5.3 Cone penetration test results of the Henderson levee road

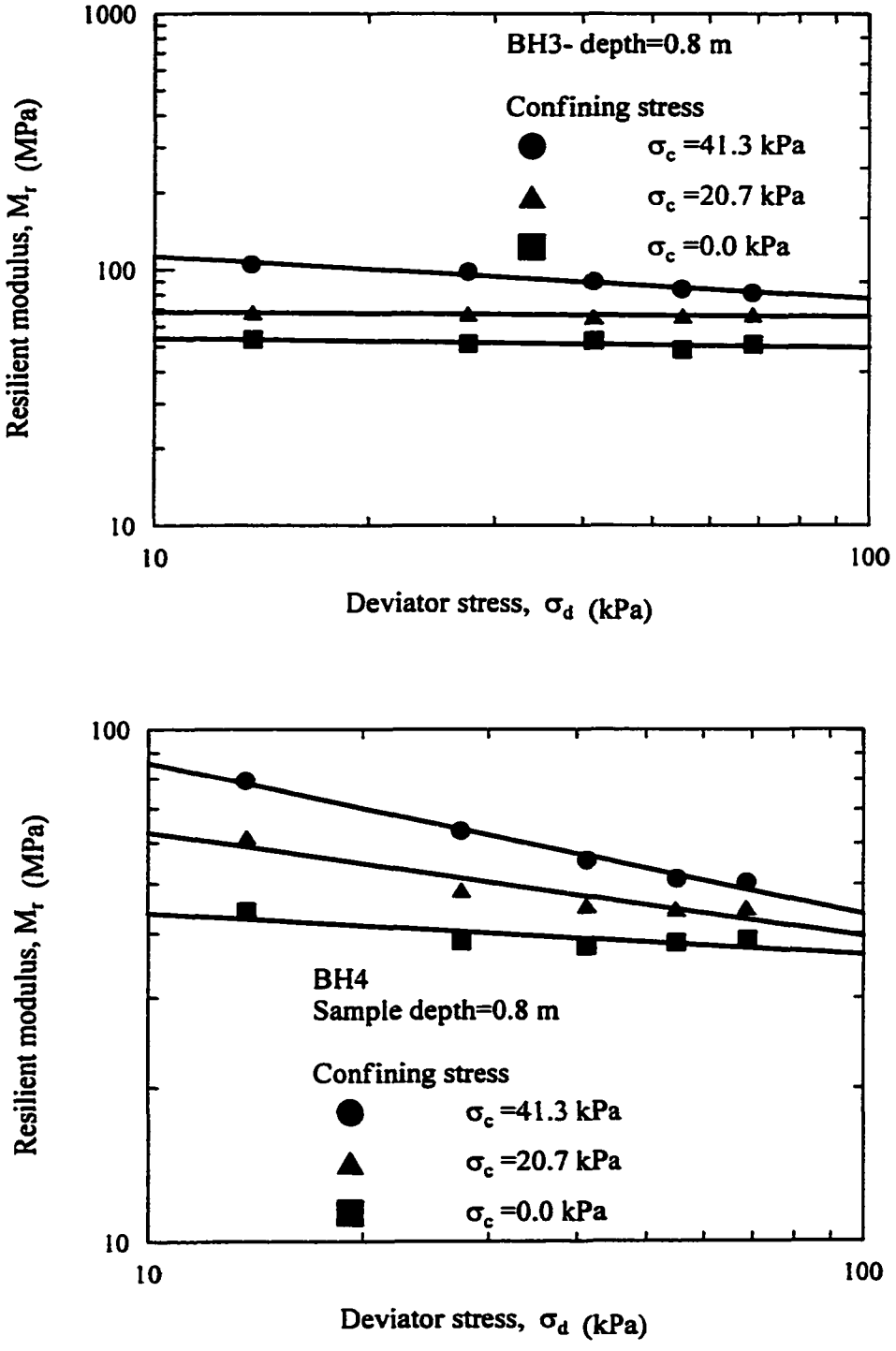

Figure 5.4 Resilient modulus test results of the LA-482

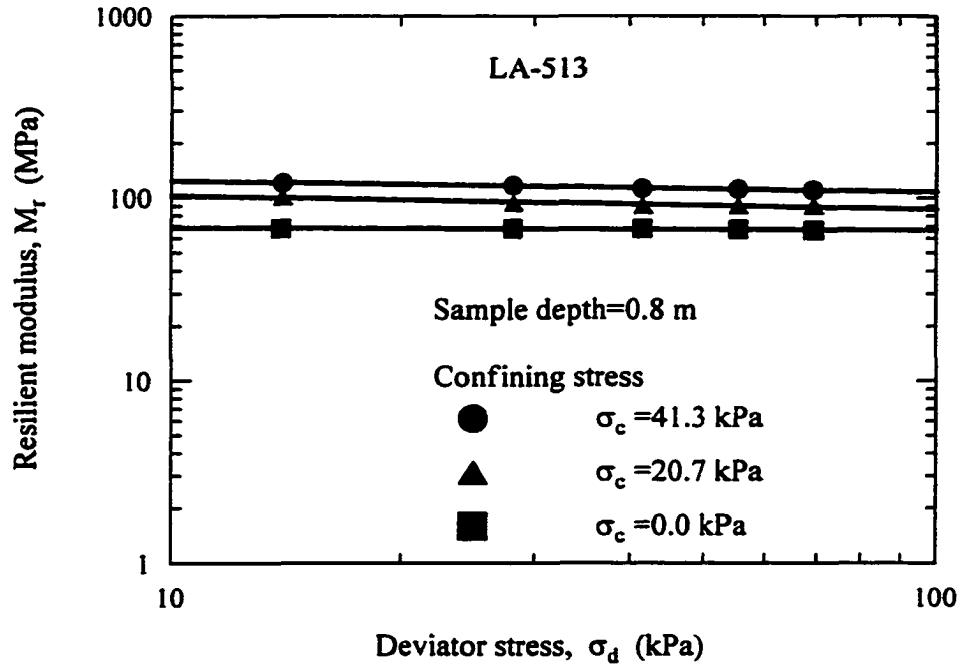

Figure 5.5 Resilient modulus test results of the LA-513

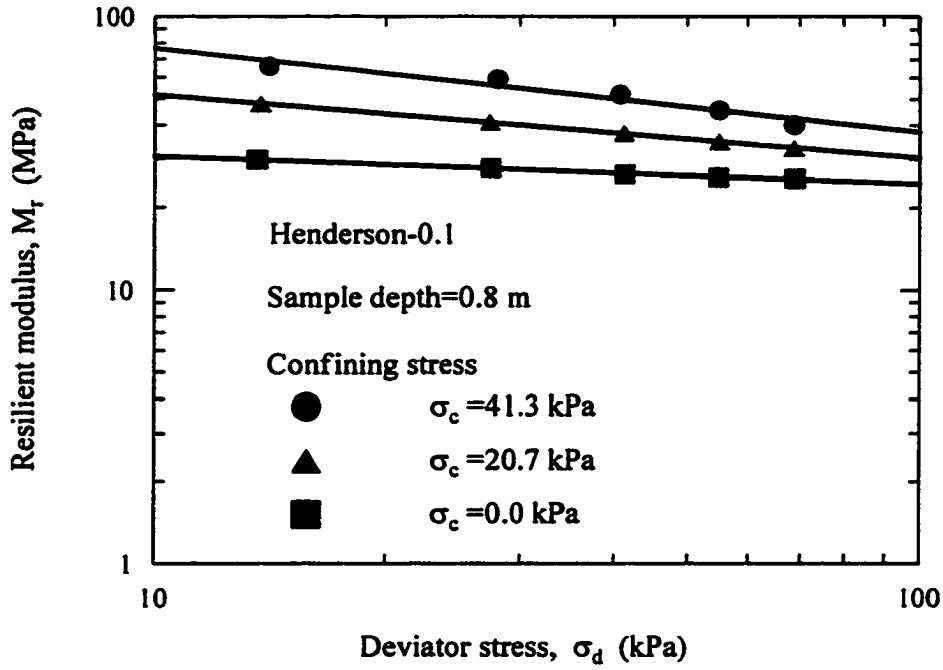

Figure 5.6 Resilient modulus test results of the Henderson levee road

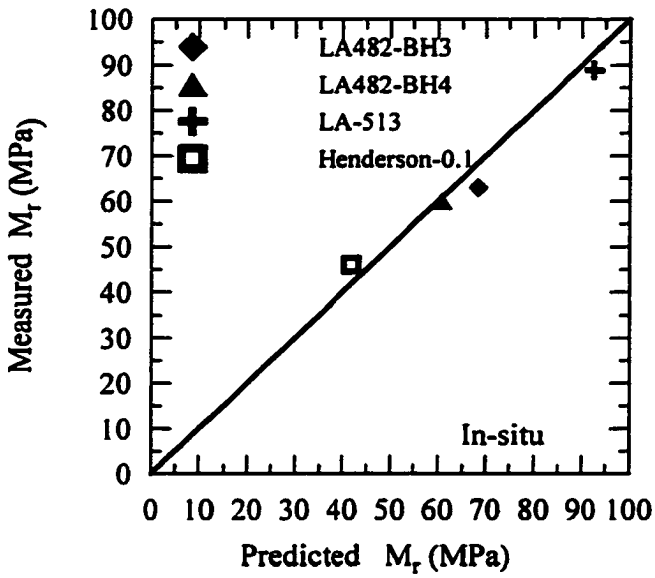

Figure 5.7 Prediction of resilient modulus under in-situ condition

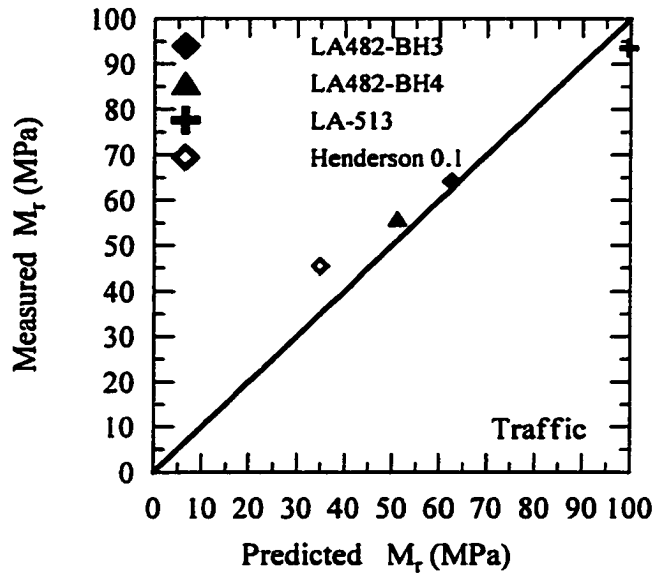

Figure 5.8 Prediction of resilient modulus under traffic loading

respectively. Most of the data fall close to the line of equality. The measured and predicted modulus values are not significantly different. Therefore, the proposed models are successful in predicting the resilient modulus in the rehabilitation projects. Tables 5.1 and 5.2 present the summary of test results.

Table 5.1 Summary of the test results

Borehole	Depth (m)	q_c (MPa)	f_s (MPa)	Water content(%)	Dry unit weight (kN/m^3)
LA-513	0.8	5.21	0.3163	21.3	16.9
Henderson 0.1	0.8	1.62	0.0718	23.3	15.4
LA-482-BH3	0.8	3.31	0.1349	17.0	18.6
LA-482-BH4	0.8	3.39	0.0686	18.0	17.9

Table 5.2 Summary of the stress analysis

	Depth (m)	In-situ				In-situ + traffic			
		σ_c (kPa)	σ_d (kPa)	Measured M_r (MPa)	Predicted M_r (MPa)	σ_c (kPa)	σ_d (kPa)	Measured M_r (MPa)	Predicted M_r (MPa)
LA-513	0.8	11.6	4.8	88.9	92.6	16.4	10.8	93.5	99.6
Hen.	0.8	10.7	4.4	46.0	42.0	15.5	9.8	45.4	35.0
BH3	0.8	12.3	5.1	62.9	68.4	15.9	11.9	64.1	62.4
BH4	0.8	12.0	4.9	59.9	60.7	15.6	11.7	55.9	51.1

Legend: M_r- resilient modulus (MPa), σ_c- confining (kPa), σ_d- deviator stress (kPa), f_s- sleeve friction (MPa), w (%)- water content, γ_d- dry unit weight (kN/m^3), γ_w- unit weight of water (kN/m^3), q_c- cone resistance(MPa), BH- borehole, and Hen- Henderson 0.1.

CHAPTER 6

SUMMARY AND CONCLUSIONS

This dissertation presented a study to assess the applicability of the intrusion technology for evaluating the resilient modulus of subgrade soil in pavements. The field and laboratory testing programs were performed at seven soil sites (eight soils), in Louisiana, to develop correlations between the resilient modulus and cone penetration parameters. The cone penetration tests were performed with the 2 cm^2 and 15 cm^2 miniature cones at the selected sites. The CPT tests were performed with a 15 cm^2 (44 mm in diameter) cone to verify the CIMCPT data. Undisturbed and disturbed soil samples were also retrieved from the field. Resilient modulus values were determined at the laboratory according to the AASHTO T-294 test method. The cone penetration and resilient modulus tests were performed at the same in-situ conditions to simulate the same field variation. In addition to the cone penetration and resilient modulus tests, several other soil tests, such as triaxial, hydrometer, soil classification, unit weight, standard proctor, specific gravity, Atterberg limit, and moisture content, were also performed. These tests were used to classify soil and determine strength parameters. The test results were analyzed and critically evaluated. Comparison of the test results showed that CIMCPT results follow the same patterns as those of the CPT.

Four statistical models, to predict the resilient modulus from the cone test parameters, were developed for fine-grained and coarse-grained soil with in-situ and traffic stress conditions. These models correlate the resilient modulus to the cone penetration parameters, resilient modulus, moisture content, dry unit weight, and stress levels. Both in-situ stresses and traffic stresses were considered. These models were

calibrated using the field test results of two soil types and used to predict the resilient modulus of different soil types. All of the models produced a high coefficient of multiple determination, 0.99. These models can be used to predict the resilient modulus of subgrade soil from the cone penetration test data. The parameters, such as confining stress, deviator stress, moisture content, dry unit weight, and the cone tip resistance, have a significant effect on the models between resilient modulus and cone penetration data. Since these models incorporate these parameters, they can be used to estimate the resilient modulus at any moisture-unit weight combination. This satisfies a requirement in the AASHTO pavement design procedure which stipulates to evaluate an effective subgrade resilient modulus by taking into account the subgrade moisture content variation throughout the year.

The laboratory cone penetration, resilient modulus, and soil property tests were also performed on the laboratory compacted soil samples to investigate the effects of the variation in the moisture content and unit weight on the resilient modulus as well as to validate the four models, developed in the field testing program. Also, from the laboratory cone penetration test data and resilient modulus test results, preliminary design charts were developed to evaluate the resilient modulus from the cone parameters. A designer can utilize these charts to estimate an effective subgrade soil resilient modulus. A successful application of the proposed models in predicting the resilient modulus at the rehabilitation projects was performed. In this case, the predicted and measured resilient modulus values were not significantly different. These results supported the validity of the proposed models in predicting resilient modulus of subgrade soil by the soil parameters and cone penetration test results. Therefore, the developed models in

predicting the resilient modulus of subgrade soil were successful. Major findings of this investigation are summarized below.

(1) Applicability of the cone penetration test to evaluate the resilient modulus of subgrade soil was demonstrated. Four models to predict the resilient modulus from the cone penetration parameters, two for fine-grained and two for coarse-grained soils with in-situ and traffic stress conditions, were developed. The coefficient of multiple determination was as high as 0.99 for all the models. The RMSE values were very low. These values indicate the high predictive capability of these models. These models were validated with the field and laboratory cone test results. The predicted and measured resilient modulus values from these models were not significantly different. The field applications of the models, in the road rehabilitation projects, were performed.

(2) Simplified design charts were developed to estimate an effective subgrade soil resilient modulus. Due to the lack of data, they were not verified.

(3) The higher the tip resistance, the higher the resilient modulus of subgrade soil.

(4) The parameters such as the cone tip resistance, confining stress, deviator stress, moisture content, and dry unit weight have a significant effect on the models between resilient modulus and cone penetration data. The resilient modulus increases with the unit weight and it decreases with the moisture content. There is a combined effect from the moisture content and unit weight on the resilient modulus of soil. The resilient modulus increases with the confining pressure. The resilient modulus increases with the bulk stress for coarse-grained soils. The resilient modulus decreases with the deviator stress for cohesive soils.

(5) The CIMCPT results are repeatable and reliable. The CIMCPT system is successful in shallow depth investigation in cohesive soils. The miniature cone penetrometer records a higher tip resistance and lower sleeve friction than the reference cone does. Coarse-grained soil exhibits higher tip resistance and lower sleeve friction than fine-grained soil does. In other words, fine-grained soil exhibits lower tip resistance and higher sleeve friction than coarse-grained soil does. The reference cone and miniature cone test results show the similar pattern along the depth while the magnitude is slightly different.

6.1 Future Recommendation

Implementation of the proposed models in the actual road designs and rehabilitation projects is important. Expanding the proposed design charts for more soil types is recommended. Future research should be aimed at developing a large data base that would be used for prediction of the resilient modulus of subgrade soil from the cone penetration test parameters.

REFERENCES

AASHTO Interim guide for Design of Pavement Structures, American Association of State Highway and Transportation Officials, 1986.

AASHTO T 294-92I, American Association of State Highway and Transportation Officials,"Resilient modulus of Unbound Base/Subbase Materials and Subgrade Soils-SHRP Protocol P46, AASHTO, T-294-92I, 1992, pp. 52-65.

AASHTO T 294-94, American Association of State Highway and Transportation Officials, "Resilient Modulus of Unbound Granular Base/Subbase Materials and Subgrade Soils-SHRP Protocol P46, AASHTO, T 294-94, 1995, pp. 794-807.

ASTM, American Society for Testing and Materials Annual book of ASTM Standards, Volume 4.03, Road and Paving Materials; Paving Management Technologies, 1993.

ASTM, American Society for Testing and Materials Annual book of ASTM Standards, Volume 14.02, 1990.

Alavilli, P., V., M., "Investigation of the use of resilient modulus for Louisiana soils in design of pavements," Master Thesis, Civil Engineering Dept., Louisiana State University, Baton Rouge, 1995.

Allen, A., J., "Development of a correlation between physical and fundamental properties of Louisiana soils," Master's Thesis, Dept. of Civil Engineering, LSU, 1996.

Allen, D., L., "M_r Testing in Kentucky," Workshop on Resilient Modulus Testing, Oregon State University, Corvallis, 1989.

Barksdale, R., D., Rix, G., J., Itani, S., Khosla, P., N., Kim, R., Lambe, C., and Rahman, M., S., "Laboratory Determination of Resilient Modulus for Flexible Pavement Design," Interim Report No.1-28, NCHRP, TRB, Geogia Institute of Technology, 1990.

Campanella, R.G., and Robertson, P.K., "Applied Cone Research," Symposium on Cone Penetration Testing and Experience, Geotechnical Engineering Division, ASCE, 1981, pp. 343-362.

Campanella, R., G. , Gillespie, D., and Robertson, P.,K., "Pore Pressures During Cone Penetration ", Proc., 2nd European Symposium on Penetration Testing, Amsterdam, Vol. 2, 1982, pp. 507-512.

Campanella, R., G. , Robertson, P.,K., and Gillespie, D., "Cone penetration testing in deltaic soils," Canadian Geotechnical Journal, Vol. 20, 1983, pp. 23-35.

Carmichael III, R., F., and Stuart, E., "Predicting Resilient Modulus: A study to determine the mechanical properties of subgrade soils," TRB, No. 1043, 1986.

Chen, B. S., and Mayne, P. W. , "Profiling the Over consolidation Ratio of Clay by Piezocone Tests," Report GIT-CEEGEO-94-1. Georgia Tech Research Corporation and Georgia Institute of Technology, School of Civil & Environmental Engineering, 1994.

Clark, J.I., and Meyerhof, G.G., "The Behavior of Piles Driven in Clay. I. An Investigation of Soil Stress and Pore Water Pressure as Related to Soil Properties," Canadian Geotechnical Journal, Vol. 9, 1972, pp. 351-373.

Das, B.M., "Advanced Soil Mechanics," Hemisphere publishing corporation, 1983, pp.406.

De Lima, D.C. and Tumay, M.T., "Scale Effects in Cone Penetration Tests," Special Publication No. 27, Proc. Geotechnical Engineering Congress, ASCE, Boulder, CO, 1991, pp. 38-51.

Drumm, E., C., Reeves, J., S., Madgett, M., R., and Trolinger, W., D., "Subgrade Resilient Modulus Correction for Saturation Effects," Journal of Geotechnical and Geoenvironmental Engineering, Vol. 123, No.7, July 1997, pp. 663-670.

ELSYM5, Developed by SRA Technologies, Inc., Under contract to Federal Highway Administration, October, 1985.

Fredlund, D., G., Bergan, A., T., and Wong, P., K., "Relation Between Resilient Modulus and Stress Conditions for Cohesive Subgrade Soils", Transportation Research Record, No. 642, 1977, pp. 73-81.

Holden, J.C., "Laboratory Research on Static Cone Penetrometrs," Internal Report CE-SM-71-1, Dept. Of Civil Engineering, University of Florida, 1971.

Kamal, M., A., et al., "Field and Laboratory Evaluation of the mechanical Behavior of Unbound Granular Materials in Pavements," Transportation Research Record, No. 1406, 1993, pp. 88-97.

Kim, D.,S., Stokoe, K., H., II, "Characterization of Resilient Modulus of Compacted Subgrade Soils Using Resonant Column and Torsional Shear Tests, Transportation Research Record, No. 1369, 1992, pp. 83-81.

Konard, J.M. and Roy, M., "Bearing Capacity of Friction Piles in Marine Clay," Geotechnique, Vol. 37, No. 2, 1987, pp.163-175.

Kurup, P.U., "Calibration Chamber Studies of Miniature Piezocone Penetration Tests in Cohesive Soil Specimens", Ph.D. Dissertation, Louisiana State University, 1990.

Kurup, P.U. and Tumay, M.T., "Continuous Intrusion Miniature Cone Penetration Test System for Transportation Applications," Seventh International Conference on Low-Volume Roads, TRB, No. 1652, Vol. 1, Baton Rouge, Louisiana, 1999, pp. 228-235.

Lee, K.W., Marcus, A.S. and Mao, H., "Determination of Effective Soil Resilient Modulus and Estimation of Layer Coefficients for Unbound Layers of Flexible Pavement in Rhode Island," Report No. URI-CVET-94-1 Res Rept No. 1, 1994 Sept. 30.

McGee, N., "Cold Region Facility- Subgrade Soils," Workshop on Resilient Modulus Testing, Oregon State University, Corvallis, 1989.

Mohammad, L.N., Huang, B., Puppala, A., and Alen, A., "A Regression Model for Resilient Modulus of Subgrade Soils," 78th Annual Meeting of the Transportion Research Board, Washington D.C., 1999.

Mohammad, L.N., Alavilli, P., Puppala, A.J., "Data Acquisition System for Determining the Resilient Modulus of Soils," ASCE Geotechnical special publication 37: Advances in Site Characterization: Data Acquisition, Management and Interpretation, 1993, Dallas,pp. 27-41.

Mohammad, L. N., Puppala, A. J., and Alavilli, P., "Influence of Testing Procedure and LVDT Location on Resilient Modulus of Soils", Transportation Research Record, No. 1462, 1994, pp. 91-101.

Mohammad, L. N., Puppala, A., and Alavilli, P., "Effect of Strain Measurements on Resilient Modulus of Granular Soils," Dynamic Geotechnical Testing: Second Volume, ASTM STP 1213, ASTM, 1994, pp.202-221.

Mohammad, L. N. and Puppala, A., "Resilient Properties of Laboratory Compacted Subgrade Soils," National Academy of Science, Transportation Research Record, No. 1504, 1995, pp. 87-102.

Mohammad, L.N., Titi, H.H., and Herath Ananda, "Evaluation of Resilient Modulus of Subgrade Soil by Cone Penetration Test Results," Seventh International Conference on Low-Volume Roads, Transportation Research Records, No. 1652, Vol. 1, Baton Rouge, Louisiana, May 1999, pp. 236 to 245.

Mohammad, L.N., Titi, H.H., and Herath Ananda, "Intrusion Technology: An Innovative Approach to Evaluate Resilient Modulus of Subgrade Soil," Application of Geotechnical Principles in Pavement Engineering, ASCE, Geotechnical Special Publication Number 85, Geo Congress'98, Boston, Massachusetts, 1998, pp. 39-58.

Mohammad, L.N., Titi, H.H., and Herath Ananda, "Investigation of the Applicability of Intrusion Technology to Estimate the Resilient Modulus of Subgrade Soil," Final Report, Louisiana Transportation and Research Center project No. 98-6GT, April 2000.

Monismith, C., L., "M_r testing- Interpretation of Laboratory Results for Design Purposes," Workshop on Resilient Modulus Testing, Oregon State University, Corvallis, 1989.

Nataatmadja, A. and Parkin, A., "Characterization of Granular Materials for Pavements," Canadian Geotechnical Journal, Vol.26, No.4, 1989, pp. 725-730.

Nazarian, S. and Feliberti, M., "Methodology for Resilient Modulus Testing of Cohesionless Subgrades," Transportation Research Record, No. 1406, 1993, pp. 108-115.

Parkin, A.K. and Lune, T., 1982, "Boundary Effects in the Laboratory Calibration of a Cone Penetrometer for Sand," Proceedings of the European Symposium on Penetration testing, Vol.2, Amsterdam, pp. 761-768.

Pezo, R. and Hudson, W.R., " Prediction Models of Resilient Modulus for Nongranular Materials", Geotechnical Testing Journal, Vol.17, No.3, 1994, pp.349-355.

Puppala, A.J., Acar, Y.B., and Tumay, M.T., "Cone Penetration in Very Weakly Cemented Sands," ASCE, Journal of Geotechnical Engineering, Vol 121, No. 8, 1995, pp.589-600.

Puppala, A., Mohammad, L.N., Allen, Aaron, "Engineering Behavior of Lime Treated Subgrade Soils," National Academy of Science, Transportation Research Record, No. 1546, Issues in Geotechnical Engineering Research, 1996, pp. 24-31.

Puppala, A., Mohammad, L.N., Allen, A., "Rutting Potential of Subgrade Soils from Repeated Load Triaxial Resilient Modulus Test," ASCE Journal of Materials in Civil Engineering, Vol. 11, No. 4, 1999, pp. 274-282.

Rada, G. and Witczak, M., W., " Comprehensive Evaluation of Laboratory Resilient Moduli Results for Granular Material ," Transportation Research Record, No. 810, 1981, pp. 23-33.

Robertson, P.,K., and Campanella, R., G., "Interpretation of Cone Penetration Tests-Part I: Sand," Canadian Geotechnical Journal, Vol.20, No.4, 1983, pp. 724-733.

Robertson, P.,K., and Campanella, R., G., "Interpretation of Cone Penetration Tests-Part II: Clay," Canadian Geotechnical Journal, Vol.20, No.4, 1983, pp. 734-745.

Schmertmann, J.H., "Guidelines for Cone Penetration Test: Performance and Design", Report No. FHWA-TS-78-209, FHWA, Washington, D.C., 1978, pp. 145.

Sebaaly, P.E., Tabatabaee, N. and Scullion, T., "Comparison of Backcalculated Moduli from Falling Weight Deflectometer and Truck Loading," TRB No. 1377, 1992, pp. 88-98.

Strategic Highway Research Program, "Resilient Modulus of Unbound Granular Base, Subbase Materials and Subgrade Soils," SHRP Protocol P-46, UG07, SS07, 1989.

Titi, H.H., Mohammad, L.N., and Tumay, M.T., "Miniature Cone Penetration Tests in Soft and Stiff Clays," Geotechnical Testing Journal, ASTM, Vol. 23, No.4, December 2000, pp.432-443.

Tumay, M., T., Boggess, R.L., and Acar, Y, "Subsurface Investigation with Piezocone penetrometer," Proceedings, ASCE National Convention, St. Louis, 1981, pp. 325-342.

Tumay, M.T. and de Lima, D.C., "Calibration and Implementation of Miniature Electric Cone Penetrometr and Development, fabrication and Verification of the LSU In-situ Testing Calibration Chamber (LSU/CALCHAS)," LTRC/FHWA Report No. GE-92/08, 1992, pp. 240.

Tumay, M.T., and Kurupp, P.U., and Boggess, R.L., "A continuous intrusion electronic miniature cone penetration test system for site characterization," Geotechnical Site Characterization, Proc. 1st International Conf. On site characterization-ISC'98, Atlanta, Vol. 1, 1998, pp. 1183-1188.

Tumay, M.T., and Kurup, P.U., , "Calibration and Implementation of Miniature Electric Cone Penetrometers for Road and Highway Design and Construction Control," LTRC State Project No. 736-13-0036, 1997.

Tumay, M.T., "Implementation of Louisiana Electric Cone Penetrometer System (LECOPS) for Design of Transportation Facilities, Executive Summary, FHWA/LA, Report No. LA-94/280 A&B, 1994.

Tumay, M., T., Acar, Y., B., "Piezocone Penetration Testing in Soft Cohesive Soils," Strength Testing of marine Sediments: Laboratory and In-Situ Measurements, ASTM, STP 883, ASTM, Philadelphia, PA, 1985, pp. 72-83.

Ullidtz, P., "Pavement Analysis," Elsevier Publications, New York, 1987.

Uzan, J., "Charaterization of Granular Materials", Transportation Research Record, No. 1022, TRB, 1985, pp. 52-59.

Wissa, A., E., Martin, R.T., and Garlanger, J.E., "The Piezometer Probe", Proc., ASCE Conference on In-situ Measurement of Soil Properties, Raleigh, NC, Vol. 1, 1975, pp. 536-545.

APPENDIX A

RESILIENT MODULUS TEST RESULTS

Table A.1 Resilient modulus test results for silty clay at controlled test

σ_c (kPa)	σ_d (kPa)	M_r (Mpa) dry side	COV (%)	M_r (Mpa) optimum	COV (%)	M_r (Mpa) wet side	COV (%)
41	14	59.57	4.1	79.09	2.0	38.01	3.4
41	28	55.84	5.5	74.10	1.9	37.69	4.6
41	41	51.54	5.2	69.07	1.7	36.91	4.6
41	55	47.87	2.1	64.92	4.8	36.47	7.6
41	69	45.96	7.5	62.18	2.7	35.28	8.3
21	14	46.70	5.2	63.18	5.5	32.69	2.4
21	28	41.28	7.4	57.82	2.1	31.89	3.6
21	41	38.81	7.3	54.28	4.3	31.21	6.1
21	55	37.72	3.2	51.18	5.4	30.56	7.7
21	69	36.99	5.6	49.99	3.9	29.37	6.7
0	14	34.66	7.6	40.27	4.2	27.43	9.9
0	28	30.67	9.3	39.44	2.3	26.44	9.4
0	41	29.08	9.2	38.77	3.5	25.65	8.1
0	55	28.57	9.3	38.42	5.5	24.86	9.7
0	69	28.06	7.6	38.23	8.7	24.43	9.2

Table A.2 Resilient modulus test results for heavy clay at controlled test

σ_c (kPa)	σ_d (kPa)	M_r (Mpa) dry side	COV (%)	M_r (Mpa) optimum	COV (%)	M_r (Mpa) wet side	COV (%)
41	7	61.29	2.8	60.69	2.4	40.38	4.3
41	14	59.11	1.8	56.55	3.8	38.60	3.2
41	21	57.11	2.1	54.34	1.5	38.43	4.9
21	7	54.27	2.7	51.92	4.0	29.51	5.8
21	14	52.03	2.0	49.42	6.1	28.51	6.3
21	21	50.11	2.1	47.69	2.7	26.85	8.5
0	7	37.43	5.8	36.34	5.0	21.94	9.4
0	14	36.90	5.4	34.78	2.9	20.76	8.0
0	21	36.57	3.3	34.05	3.8	20.04	9.8

Table A.3 Resilient modulus test results for silt at controlled test

σ_c (kPa)	σ_d (kPa)	M_r (Mpa) dry side	COV (%)	M_r (Mpa) optimum	COV (%)	M_r (Mpa) wet side	COV (%)
21	21	58.94	4.1	56.25	5.3	33.94	9.5
21	41	60.51	3.2	56.82	5.6	34.80	7.2
21	62	64.27	4.6	57.39	9.0	35.42	4.7
34	34	78.03	2.9	76.98	4.3	60.82	4.2
34	69	80.81	3.0	77.62	3.6	61.92	4.2
34	103	82.37	4.6	78.39	4.6	63.27	5.0
69	69	121.33	3.3	110.21	2.8	103.52	2.5
69	138	126.62	4.3	111.23	3.6	104.70	2.8
69	207	126.45	3.0	113.71	3.2	105.12	3.1
103	69	155.98	3.1	135.29	2.4	146.27	1.7
103	103	157.93	2.0	136.35	2.5	148.48	2.3
103	207	164.00	1.6	137.40	3.4	151.41	1.7
138	103	187.01	1.5	165.13	2.0	180.67	1.7
138	138	189.94	1.8	167.21	1.7	182.84	2.3
138	276	191.98	1.8	167.90	2.8	184.16	1.9

Table A.4 Resilient modulus test results for sand at controlled test

σ_c (kPa)	σ_d (kPa)	M_r (Mpa) dry side	COV (%)	M_r (Mpa) optimum	COV (%)	M_r (Mpa) wet side	COV (%)
21	21	75.51	2.2	79.17	3.1	42.92	7.6
21	41	75.97	2.1	79.79	4.2	43.74	3.0
21	62	76.71	2.3	80.49	3.8	45.04	3.3
34	34	105.00	2.0	107.68	3.0	70.20	3.7
34	69	106.00	2.1	108.39	3.2	70.75	5.5
34	103	107.15	1.9	110.00	2.3	72.06	4.6
69	69	172.58	1.3	174.07	1.4	143.99	2.7
69	138	171.05	1.4	174.76	1.8	144.17	2.7
69	207	165.74	1.5	171.34	1.3	146.58	1.5
103	69	220.66	1.0	234.07	1.9	213.99	1.6
103	103	225.22	0.9	237.06	1.1	217.50	1.6
103	207	220.71	0.8	234.30	1.3	214.19	1.5
138	103	257.80	0.9	271.46	1.4	251.97	1.8
138	138	262.22	0.8	276.17	1.5	255.39	1.2
138	276	252.64	1.1	271.56	0.9	246.28	1.0

APPENDIX B

PROCEDURE FOR MODEL DEVELOPMENT

B.1 The Procedure for Model Development

The development of the proposed model for fine-grained soils under in-situ condition is described in this appendix. The data for the model development are given in Tables 4.3 and 4.4 of Chapter 4. The results of silty clay and heavy clay were selected for the fine-grained (in-situ) model development. The steps of the model development are presented below.

Step 1: From Tables 4.3 and 4.4 of Chapter 4, input the variables, M_r- resilient modulus (MPa), σ_c- confining (minor principal) stress (kPa), σ_d- deviator stress (kPa), σ_v– vertical stress (kPa), q_c- tip resistance (MPa), f_s- sleeve friction (MPa), w- water content (as a decimal), γ_d- dry unit weight (kN/m^3), and γ_w- unit weight of water (kN/m^3).

Step 2: The variables were arranged according to the required physical conditions, described in Section 4.4, Chapter 4, as in the nondimensional forms. Several trials of regression analysis were performed with different ratio values of the resilient modulus to power terms of confining stress ($M_r/\sigma_c^{0.45}$, $M_r/\sigma_c^{0.50}$, and $M_r/\sigma_c^{0.55}$). Among all these, the model with $M_r/\sigma_c^{0.55}$ yielded the highest R^2 and the lowest RMSE value. By increasing the power term of the confining stress above 0.55 creates impractical resilient modulus values in the model prediction. Therefore, the power term for the confining stress was selected as 0.55.

Step 3: The model can parametrically be described as,

$$\frac{M_r}{\sigma_c^{0.55}} = \frac{1}{\sigma_v}\left(\beta_1 q_c + \beta_2 \frac{f_s}{w}\right) + \beta_3 \frac{\gamma_d}{\gamma_w} \qquad \text{(B.1)}$$

where, β_1, β_2, and β_3 are regression coefficients. As a first order approximation, the dependent variable ($M_r/ \sigma_c^{0.55}$) varies linearly with the independent variables. A linear multiple regression analysis was performed by the Statistical Analysis System (SAS) program (Table B.1). If the regression coefficients are positive in the regression analysis, the physical conditions are satisfied. For example, if β_2 in equation (B.1) is positive, as the moisture content increases the resilient modulus decreases.

Step 4: Table B.2 shows the results of the regression analysis for fine-grained soil (in-situ). Four models were developed, two for fine-grained and two for coarse-grained soil with in-situ and traffic stress conditions.

Table B.1 The SAS program for the model development

```
dm 'output;log;clear;'log;
options ps=60 ls=72 pageno=1;
data one;
infile 'd:\ananda\In-situ analysis\insitu-fine.dat';
input Mr qc fs w γd σc σd;
run;
data two;
input Mr qc fs w γd σc σd;
cards;
. 2.1  0.1042  0.21   16.9  8.6  7.8
;
data three;
set one two;
gw=γd/9.81;
σv=σd+σc;
fr=fs/σv;
c1=σc**0.55;
mc=Mr/(c1);
qv=qc/σv;
qg=gw;
fg=fr/w;
keep qc qv Mr mc fs fr qg fg w γd gw σv  σd  c1 σc;
proc reg data=three;
model mc=qv fg qg/clm cli noint;
id m;
run;
quit;
```

Table B.2 The results of the regression analysis

Dependent Variable: MC

Analysis of Variance

Source	DF	Sum of Squares	Mean Square	F Value	Prob>F
Model	3	1038.17090	346.05697	185.331	0.0001
Error	8	14.93788	1.86724		
U Total	11	1053.10878			

Root MSE	1.36647	R-square	0.9858
Dep Mean	8.82070	Adj R-sq	0.9805
C.V.	15.49160		

Parameter Estimates

Variable	DF	Parameter Estimate	Standard Error	T for H0: Parameter=0	Prob > |T|
QV	1	31.789744	23.18114903	1.371	0.2075
FG	1	74.807433	162.25682949	0.461	0.6570
QG	1	4.079008	0.73730501	5.532	0.0006

Obs	M	Dep Var MC	Predict Value	Std Err Predict	Lower95% Mean	Upper95% Mean
1	48.4	12.1189	12.4691	0.723	10.8020	14.1363
2	50.4	11.0837	12.8038	0.872	10.7926	14.8151
3	54.1	13.5461	13.9794	1.200	11.2120	16.7468
4	63.34	15.8597	13.7399	0.736	12.0426	15.4372
5	60.74	13.3576	13.3514	0.672	11.8021	14.9007
6	14.3	3.6558	4.9715	0.561	3.6778	6.2652
7	14.6	3.3020	4.8562	0.584	3.5104	6.2021
8	24.68	6.3095	5.2058	0.565	3.9029	6.5087
9	26.2	5.9255	5.0916	0.542	3.8410	6.3423
10	24.76	6.3299	5.3600	0.532	4.1323	6.5877
11	24.49	5.5388	5.1217	0.577	3.7912	6.4521
12	.	.	13.3610	2.460	7.6882	19.0338

Obs	M	Lower95% Predict	Upper95% Predict	Residual
1	48.4	8.9042	16.0341	-0.3502
2	50.4	9.0656	16.5421	-1.7201
3	54.1	9.7856	18.1732	-0.4332
4	63.34	10.1608	17.3190	2.1198
5	60.74	9.8401	16.8627	0.00624
6	14.3	1.5652	8.3778	-1.3157
7	14.6	1.4298	8.2827	-1.5542
8	24.68	1.7960	8.6156	1.1037
9	26.2	1.7015	8.4818	0.8339
10	24.76	1.9782	8.7418	0.9699
11	24.49	1.7012	8.5421	0.4172

Obs	M	Lower95% Predict	Upper95% Predict	Residual
12	.	6.8718	19.8503	.

Sum of Residuals	0.077195
Sum of Squared Residuals	14.9379
Predicted Resid SS (Press)	31.6035

VITA

Ananda Herath was born in Sri Lanka. He received his bachelor of science degree in engineering (first class (honors) from the University of Peradeniya, Sri Lanka, in 1983 December. He worked for the University of Peradeniya as an instructor from 1984 January to 1984 August. He was a project engineer in the Mahaweli Engineering and Construction Agency (MECA), Sri Lanka, from 1984 August to 1984 October. He also worked for the University of Peradeniya as an assistant lecturer from 1984 November to 1986 September. He was a master's student at the University of Tokyo from 1986 October to 1988 September. He received his master's degree in civil engineering (structural engineering) in 1988 September from the University of Tokyo. Then he was a consulting engineer in Japan from 1988 October to 1995 September. He gained in experience in design of bridges, pile foundations, culverts, retaining walls, and other structural designs in Japan. He has been a doctoral student at the Louisiana State University since 1996 January. He is also a Professional Engineer (P.E.) in Louisiana, U.S.A. He will receive his doctoral degree in civil engineering (transportation engineering) in August, 2001.

DOCTORAL EXAMINATION AND DISSERTATION REPORT

Candidate: Ananada H.M.P.J. Hearth

Major Field: Civil Engineering

Title of Dissertation: A Study of the Applicability of Intrusion Technology for Evaluating Resilient Modulus of Subgrade Soil

Approved:

Major Professor and Chairman

Dean of the Graduate School

EXAMINING COMMITTEE:

Date of Examination:

June 7, 2001